Studies on the influence of processing techniques and their parameters on the characteristics of Cu/CNT composites having different CNT size and its concentration for steel industries

A thesis
submitted in partial fulfillment of the requirements
for the award of the degree of

DOCTOR OF PHILOSOPHY

by

R. VIGNESH BABU
(Roll No. 136103035)

DEPARTMENT OF MECHANICAL ENGINEERING
INDIAN INSTITIUTE OF TECHNOLOGY GUWAHATI
GUWAHATI – 781039
INDIA

July 2019

Department of Mechanical Engineering

Indian Institute of Technology Guwahati

Guwahati-781039, Assam, India

CERTIFICATE

It is certified that the work contained in the thesis entitled "**Studies on the influence of processing techniques and their parameters on the characteristics of Cu/CNT composites having different CNT size and its concentration for steel industries**" submitted by **Mr. R. VIGNESH BABU** to the Indian Institute of Technology Guwahati, Guwahati, India for the award of degree of Doctor of Philosophy has been carried out under our supervision in the department of Mechanical Engineering, Indian Institute of Technology Guwahati. This work has not been submitted elsewhere for the award of any other degree or diploma.

Dr. S. KANAGARAJ

Professor

Department of Mechanical Engineering

Indian Institute of Technology Guwahati

Assam, India

Dedicated to

My parents Mr. N. B. N. Rajendren and

Mrs. R. Mekala

And

My Grandparents (Late) Mr. B. Neelamegam

and (Late) Mrs. N. Kaveriammal

ACKNOWLEDGEMENT

I would like to express my sincere gratitude to my thesis supervisor and my well-wisher, Prof. S. Kanagaraj for his valuable guidance and constant encouragement throughout my Ph.D. work. His cognizance, enormous goodwill and unruffled patience made me work at ease and kept me highly motivated throughout my journey along with him. His innovative ideas and consistent support by extending all the necessary facilities, which are helpful in successful completion of my research work. I have immensely benefited from each and every moment of my association with him.

I would like to express gratitude towards my Doctoral committee members Prof. S. Senthilvelan, Dr. Swarup Bag and and Dr. R. Prasanna Venkatesh for continually reviewing the progress of our research with valuable suggestions and constructive criticism to improve the quality of the thesis.

I am grateful to Prof. Gautam Biswas, Director, IIT Guwahati and Prof. Anoop K. Dass (former head) and Prof. Santosha K. Dwivedy, Head, Department of Mechanical Engineering, IIT Guwahati for providing the facilities during the research work.

I, sincerely thank Ministry of steel, India and Tata steel, India for funding the entire research work.

I would like to thank Department of Mechanical Engineering officers, Mr. Saifuddin Ahmed, Materials Science laboratory, Mr. Sanjib Sarma, Strength of Materials Laboratory, Mr. Jiten Basumatary, Advanced Manufacturing Laboratory and Mr. N. K. Das and his associates, Central workshop for their support during my experimentation, testing and fabrication throughout the research work and staffs Mr. Nabajyoti Dutta and Mr. Raju Talukdar for helping me in the academic and administration works.

I, sincerely acknowledge Prof. Bharat B. Panigrahi, Department of Materials Science and Metallurgical Engineering, IIT Hyderabad, and Dr. P. Sudharshan Phani, and Mr. Naveen Manhar Chavan, ARCI, Hyderabad for providing facilities. I also thank Mr. P. K. Kannan, Dr. Raj Kumar and Dr. Bolla Reddy accompanying me during the experimentation work.

I extend my heartfelt thanks to the project members Mr. Kunwar Avanish Verma, and Mr. M. Charan for their strong support during the formation of the research. I am very much grateful to Materials Science laboratory, and Biomedical Devices and Biomaterials laboratory colleagues Dr. S. Arun, Dr. N. Shanmuga Priya, Mr. Sridhar, Dr. Susanta, Mr.

Devarshi, and Mr. Ashirbad for their valuable support during my thesis work and the support received from Mr. Kishore Kumar, Mrs. Nandhani Rai, Mr. Vaibhav, Mr. Raagdeep, Dr. Aparna and other associates at different phases of research work.

I would like to specially thank Dr. V. Satheesh Kumar and Dr. A. Johnney Mertens for the encouragement, knowledge and timely support during the research work.

It has been a pleasure to work with my colleagues Dr. Kodesswaran, Dr. Muthu Raja, Dr. Hakeem Niyas, Dr. Gururaj, Mr. Rashmi, Dr. Prakash, Dr. Sumit, Mr. Anupam, Mr, Kamal, Dr. Soumya, Mr. Sibanandha, Mr. Debabrata, Mr. Manish, Mr. Shahnawaz, and Mr. Tinu Saju and I am also thankful to my department colleagues, who helped me directly and indirectly at various stages of my work.

I am hearty grateful to my friends Mr. S. Narendren and Mr. M. Vijay for their care and support during the characterization of my thesis work.

My sincere thanks to Central Instruments Facility, IIT Guwahati, for giving permission to utilize the facilities throughout the thesis work.

I also thank my friends Mr. P. Vivek Selvan, Mr. N. BalaSubramani, Mr. R. Someshwaran, Dr. Balaji, Dr. Monisha, Mrs. G. Padmavathi, Ms. G. Janani, Ms. Sumitha Banu, Mr. M. Dhanasingh, Mr. Philip, Mr. Siddarth and Mr. Karthik Pandian, who held my hand and supported me during my stay at IIT Guwahati.

I would like to sincerely thank my Professors, lectures and teachers Dr. R. Mohan Kumar, Dr. V. Mohan Siva Kumar, Dr. R. Ganeshamoorthy Mr. N. Sankareswaran, Mr. Madan Manohar, Mr. M. Subramanian, Mr. S. Ravindran, Mr. Ravichandran, and Mr. S. Gopal, who encouraged and guided me at every single stage of my life.

I express my gratitude to my friends Mr. S. Venkatesh, Mr. S. Lakshmanan Prasad, Mr. K. Venkat Raman, Mr. R. Pandia Rajan, Mr. T. Amal Seba Thomas, and Mr. B. Santhana Kumar, who always supported me on both morally and professionally at every stages of my life.

I extend my hearty gratitude to my parents Mr. N. B. N. Rajendren and Mrs. R. Mekala for their unconditional love and moral strength throughout these years, who taught me the essence of hard work, patience, belief and dedication of what I do.

I am thankful to the Supreme energy for all this raising step towards the successful life, opportunity and good health to serve for the nation and earth.

(**R. VIGNESH BABU**)

ABSTRACT

In current era, there is a high demand for energy efficient materials and processes in order to reduce their impact in our environment, natural resources and carbon foot print. Due to stringent requirements, steel industries are looking for improving the efficiency of a plant using different approaches including energy efficient-thermal management systems and materials e. g. staves in a blast furnace and heat transfer tubes in heat exchangers. The requirements of improving the relevant characteristics of conventional monolithic materials lead to utilize different types of metal matrix composites. The main objective of the present work is to develop Cu/CNT composite materials and characterize them in order to explore the same for potential industrial applications in general and steel industries in particular. In this work, the molecular level mixing (MLM) technique is followed to synthesize the Cu/CNT composite powder. The sintering behaviour of the copper and composite powder is studied and the sintering parameters to have complete diffusion of grain boundaries are obtained, which are followed to get the test samples. The Cu/CNT composite powder is compacted using uniaxial compaction (UA) at 800 MPa followed by either conventional (CS) or microwave sintering (MW) technique to obtain the final sintered test samples. In addition, the Cu/CNT composite powder is also consolidated through cold isostatic press (CIP) at 300 MPa followed by microwave sintering. The sintered samples and the synthesized powder are characterized using suitable techniques. The composite powder obtained through MLM technique is observed to have a good encapsulation of CNT by copper and homogeneous dispersion of CNT in copper. The sintering duration of composites is greatly reduced by the synergic effect of CNT and temperature and it is reduced by 37%, when the sintering temperature is increased from 600 to 900 °C for 20-40 nm diameter CNT reinforced composites. The relative density (RD), microstructure, hardness, electrical conductivity and thermal conductivity of the sintered products are studied against different CNT size (10-20 nm, 20-40 nm and 40-60 nm diameter), CNT concentration (0.25, 0.5, 0.75 and 1wt.%), sintering duration (60, 75 and 90 min.), and processing technique such as UA-CS, UA-MW and CIP-MW. The maximum RD of 93.8% is observed at 0.25wt.% of 20-40 nm diameter CNT, CIP-MW processed composites sintered at 600 °C for 75 min. in comparison to that of pure copper. In addition, the RD of the composites is found to be increased in the order of UA-CS, UA-MW and CIP-MW processing technique. The grain

size of the composites is increased with CNT size, its concentration and sintering duration. The hardness of the composites is observed to be 88.8 ± 2.5 VHN at 0.25wt.% of 40-60 nm diameter CNT composites sintered at 600 °C for 75 min. irrespective of processing technique and the diameter of CNT is dominated only at 0.25wt.%. The maximum electrical and thermal conductivity of composites are observed to be 50.4 ± 0.2 MS/m and 372.8 W/mK at 93.8% RD for the 0.25wt.% of 20-40 nm diameter CNT composites sintered at 600 °C for 75 min. and processed through CIP-MW technique, which is about 20% higher than that of pure copper obtained by the same technique. The trend noticed on the electrical and thermal conductivity of the composites is observed to follow the same pattern of RD of composites. The thermal conductivity of the composites obtained by the CIP-MW processing technique is found to be superior in comparison that of other techniques and the results are found to be at par with that of the results obtained from the spark plasma sintering technique. Thus, the best characteristics of thermal conductivity, hardness and RD of Cu/CNT composites obtained from the present study can be explored for possible applications in steel industries.

LIST OF CONTENTS

Page No.

LIST OF FIGURES

Page No.

LIST OF TABLES

Page No.

LIST OF NOMENCLATURE

Symbol		Description
b	-	Oil impregnated sample mass, g.
d	-	Diagonal, μm
f	-	Oil impregnated sample immersed in water mass, g
k	-	Thermal conductivity of test material, W/mK
t	-	Thickness, mm
A	-	Mass of sample in air, g.
D	-	Diameter, mm
F	-	Force, gf
HV	-	Vickers hardness, VHN
L	-	Lorenz number of Copper 2.44×10^{-8} Ω W/K^2 at 30 °C
T	-	Temperature, K
β	-	Full width at half maximum, radian
θ	-	Diffracted angle of X-ray beam with the lattice plane, theta
ρ_s	-	Sintered density, g/cc
ρ_w	-	Density of water, g/cc.
ρ	-	Theoretical density, g/cc
W_f	-	Weight of reinforcement, g
ρ_f	-	Density of reinforcement, g/cc
W_m	-	Weight of matrix, g
ρ_m	-	Density of matrix, g/cc

CHAPTER 1

INTRODUCTION

1.1 Introduction

In current era, there is a high demand for energy efficient materials and processes since the relatively older systems and technologies of energy management are causing serious environmental problems and large consumption of natural resources. These energy-related problems need to be addressed to minimise the carbon footprint and judiciously utilise the naturally available resources. One of the major energy consuming giants is the steel industry, which utilises 25 % of total energy consumption of India's energy resources, Ministry of steel, India [2018]. The heat exchangers used in different processes such as various furnaces, steel rolling unit, ore purification plant, thermomechanical treatment, and other minor processes are expected to consume 300 million m^3 of water resources as a heat transfer medium, Ministry of steel, India [2012], which becomes scarce with each passing day. The overall consumption of water per tonne of steel production is 3.3 m^3, Colla *et al.* [2017]. In addition, the maintenance of water cooling plant is expensive and storage area required for the same is large. The complicated cooling system forced the industries to look for alternative viable solutions. The conventional methods of exploiting energy are under serious scrutiny, which demands the more energy efficient thermal management systems and materials. In 2017, India produced 101.4 million tonne (MT) of steel, and it is ranked third largest steel producer in the world having the growth rate of 6.2% to sustain its economic development, Ministry of steel, India [2018]. Now, India has fixed ambitious target of 300 MT steel production by 2030, Ministry of steel, India [2018]. At present, the steel consumption per capita is 65.2 kg against the world average of 214.5 kg, Steel (2018). The energy consumption in India integrated with steel is high and varied in the range of 6.5 GCal/tcs (giga calories per tonne of crude steel), as compared to 4.5 GCal/tcs in benchmark companies abroad, Iron & Steel sec [2013]. The Green House Gas (GHG) emission of steel industries in India is 1.5 times higher than their counterparts in abroad, as per the Ministry of Steel. Considering the fact of industrial revolution 4.0, the steel industries are motivated

to enhance the performance of production of steel by improving the efficiency of a plant using all possible approaches.

Scientists from different domains have been forced to think of materials with superior characteristics based on the recent advances in aerospace, automobile and space engineering, which could be potentially explored for industries to improve their productivity, efficiency, cost reduction of products. As it is very difficult to get all the desired properties from a monolithic material to explore the same for a specific application, researchers started to combine different materials to achieve desired extraordinary characteristics. The resulting material in combination is called as a composite. Composite materials are the amalgamation of two or more different constituent materials leading to obtain the desired properties such as low weight, high stiffness and strength, which are all not possible to be derived from the monolithic materials. Composite materials are majorly classified into three categories, which are all discussed below in detail.

1.1.1 Polymer matrix composites

The polymer matrix composites (PMC) are having the following advantages: easy to process, low operating temperature, light weight and desirable mechanical properties and others. There are two types of polymers: (i) thermoset plastics: a three-dimensional bonding is attained after curing; it is flexible; it is mostly suitable as a matrix for advanced fiber reinforced composites; (ii) thermoplastics: one or two-dimensional structure, desired melting point, softening temperature, and different attractive characteristics against heating and cooling, which give desired characteristics close to isotropic properties. The reinforcing materials in PMC majorly are fiber glass, carbon fiber, Kevlar etc., and the reinforcement can be arranged in the form of unidirection, random orientation or continuous and the properties of composites depend on matrix, reinforcement and its concentration. The heat resistance and mechanical properties of thermoplastics are increased by selecting a suitable filler/reinforcement in the desired matrix. The major limitations of PMC are the high coefficient of thermal expansion and low thermal resistance. The PMC is used in automotive, biomedical and military applications like Kevlar jackets, biomedical implants and electrical housing etc.,

1.1.2 Ceramic matrix composites

Ceramic matrix composites (CMC) are generally described as solid materials, typically crystalline in nature, which exhibit strong ionic bonding and / or covalent bonding.

The conventional ceramic materials have high modulus, high compressive strength, high temperature capability, high wear resistance and hardness, low thermal conductivity and chemically inert, which are prominent factors for their usage at high temperature applications. However, the low fracture toughness of ceramic materials limited their usage in structural applications. In order to enhance their desired properties, different reinforcements like particles, whiskers, chopped fiber or continuous fibers, glass-ceramics and oxides are being used as reinforcements to develop the composites, where the matrix provides desired orientation and acts as a load transfer medium. The addition of reinforcement in ceramic materials enhances their different characteristics. The CMC can be prepared through conventional or customized techniques. The major advantages of CMC are as follows: excellent wear and corrosion resistance and stable at higher temperature; its limitations are as follows: processing at higher temperature, brittleness, high coefficient of thermal expansion, and high thermal residual stresses. A few applications of CMC are gas turbine components, hot gas ducts, and brake disks.

1.1.3 Metal matrix composites

The metal matrix composites (MMC) are primarily developed for military and space applications. A matrix with one or more physically distributed phases namely reinforcements or fillers, enhances the properties of a matrix over conventional materials to the desired level. In addition, recent demand for advanced materials having specified functional properties led to their broad applications in transportation, automotive applications, chemical, electronics and telecommunication industries. MMC has the ability to withstand corrosive environment even at elevated temperature. The reinforcement like continuous fiber has most effective in a given direction and the processing technique for particulate reinforcement is found to be similar to that of monolithic materials. The major advantages of MMC are as follows: desired magnetic and structural properties, low temperature creep resistance, and enhanced electrical and thermal conductivity. The applications of MMC are light weight components in aviation industry, axle tubes in automotive industries, and particle-strengthened brakes in locomotives etc.,

1.2 CNT reinforced metal matrix composites (CNT-MMC)

The requirement of light weight and high strength materials in different industries has received special attention, where the strength and stiffness of material are increased and the density of material is reduced while retaining its load bearing characteristics. It led to

utilize the MMC in aerospace and automobile applications, where improving the payload and enhancing the fuel efficiency are focussed. The inherent limitations on the characteristics of metals and alloys led to explore on the need of metal matrix composites, where thermal expansion, electrical conductivity and thermal conductivity of them assist their potential applications in electrical and electronics industries. The materials required in space shuttle, defense vehicles, sports goods, low temperature applications, and super conductors are synthesised by selecting a suitable reinforcement and matrix materials.

After the successful identification of carbon nanotube (CNT) by Iijima [1991], a lot of research have been carried out to use it as a reinforcement in a matrix. The stiffness, strength and thermal conductivity of CNT are reported to be 1000 GPa, 150 GPa and 3000-6000 W/mK, Bhat *et al*. [2011], respectively, which are expected to serve the current requirements in all aspects due to its attractive and desirable characteristics. There are several advantages of incorporating CNT in a metal matrix to prepare MMC having increased surface area, reduced density, and enhanced strength and thus, it can be explored for thermal management systems. However, there are many technical challenges, which are required to be addressed to prepare the MMC with CNT as a reinforcement and these are given below: the homogenous dispersion and distribution of CNT in the matrix; formation of cluster of CNT due to its Van der Waals attractive forces; non-wetting characteristics of CNT; retaining the characteristics of structural and chemical stability. The clustering or agglomeration of CNT in the matrix is expected to significantly reduce the strength and increase the porosity of the composites, which will not fulfill the requirements under the servicing conditions. As CNT composites are processed at high temperature and high pressure, it is expected to influence their characteristics. In order to overcome the above discussed limitations, various processing techniques are proposed to make CNT reinforced metal matrix composites, which are listed in **Figure 1.1**.

1.3 Various processing techniques to synthesize Cu/CNT composites

The Cu/CNT composites are majorly synthesized through five different techniques, which are briefly discussed below.

1.3.1 Powder metallurgy route

Powder metallurgy is one of the most popular techniques used for the preparation of metal matrix composites, Pham *et al*. [2011]. During the process, the powder is pressed at a desired pressure in the die in order to obtain the required shape. The powder is either

compacted by cold compaction followed by conventional sintering or hot compaction, where compaction and sintering process are simultaneously occurring. During sintering, the sample is heated to a temperature lower than that of its melting point. The sintering can be done through conventional sintering, hot pressing, hot isostatic pressing, spark plasma sintering and deformation process.

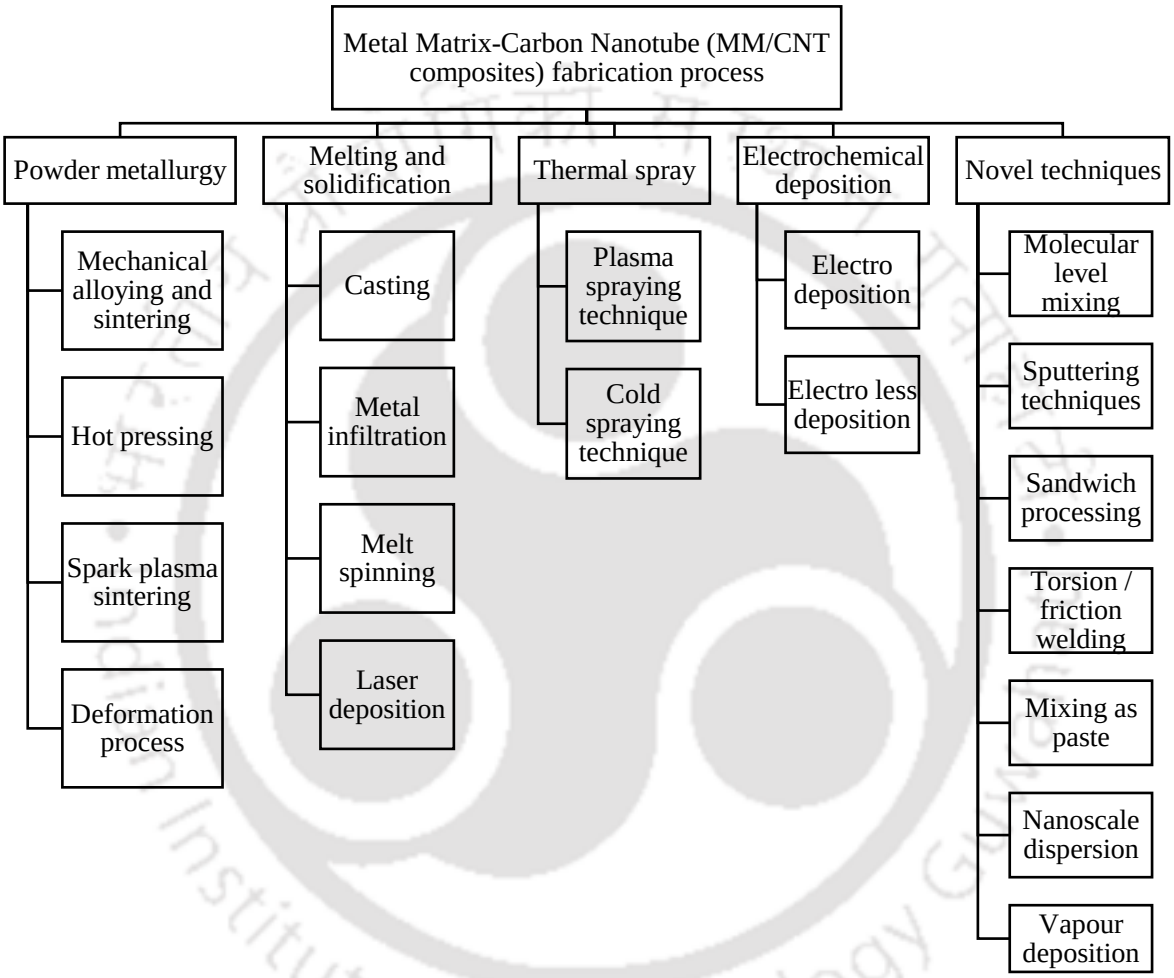

Figure 1.1 Different processing techniques to prepare metal matrix – CNT reinforced composites

1.3.2 Melting and solidification

Melt processing is the most primitive form of fabrication of metallic compound, where the composite is heated up to its melting point and then solidified, Zhou *et al*. [2007]. In this method, four different techniques namely casting, metal infiltration, melt spinning and laser deposition are used. In general, the low melting point materials are fabricated using this technique. Metal infiltration is mainly used for the fabrication of porous structures,

where the CNT is dispersed and the liquid metal is infiltrated into pores and then solidified. Melt spinning contains molten alloy, which is poured continuously on a rotating wheel. The precipitations are converted into ribbons, which become amorphous due to their high cooling rate. Laser deposition technique is very much limited due to its high processing temperature, where increase in defect density and the graphitization of CNT are reported.

1.3.3 Thermal spraying

It is an industrial scale processing technique, Laha *et al*. [2009], which can be used to produce a coating or free-standing structure. This technique involves a process, where the material to be sprayed is fed into the heat source in the form of powder or wire, which is converted into molten or semi-molten state accelerated by a carrier gas and impinged on the substrate. It can be achieved by two processing techniques: plasma spraying, where the plasma is created by ionization of an inert gas by an arc and it is struck between a tungsten cathode and concentric copper anode; cold spraying, where the substrate is targeted by the particles at very high velocity. Due to such an impact, substrate undergoes plastic deformation and glued with particles.

1.3.4 Electro chemical route

A typical galvanic cell under electrochemical process consists of two metals, eg. zinc and copper, Zhang *et al*. [2013]. Both are immersed in a solution containing dissolved salts corresponding to the metal. Two solutions are separated by a porous barrier that prevents them from rapidly mixing but allows ions to diffuse through. This technique mostly used for producing 1-D composites and the major applications are focused in nano-sensors, magnetic recorder and electrodes etc.,

1.3.5 Novel techniques

In addition to the above, a few novel techniques namely vapour deposition, nano-scale dispersion, molecular level mixing (MLM), sputtering techniques, torsion/friction welding, mixing as paste and sandwich processing are also proposed by Zhang *et al*. [2000], Noguchi *et al*. [2004], Cha *et al*. [2005b], Ci *et al*. [2006], Lim *et al*. [2009], Arribas *et al*. [2006] and Lahiri *et al*. [2009], respectively to develop metal matrix composites.

The vapour deposition process is carried under vacuum, where W-filament and CNT containing crucible are heated and hydrogen gas is blown to CNT with specific flow rate for certain period leading to obtain a grey layer on CNT. It is suitable for processing a 1-D or particulate type of CNT-MMC. In a nano-scale dispersion (NSD) technique, a preform of

CNT in rubber, CNT and metal in rubber are stacked alternatively compressed and heated. In order to further improve the characteristics of MMC, spark plasma sintering and hot extrusion are followed. In a molecular level mixing (MLM) technique, the solvent is mixed with CNT and sonicated, where the precursor is added and further sonicated. The composite powder is obtained after the calcination and reduction process. In case of torsion/friction welding (TW) process, the CNT is kept on a groove on a metal alloy block, where friction stirring process is done to produce a composite. It provides a reduction in grain size and distribution of CNT along the direction of tool movement. The sandwich process (SP) involves by spraying a dispersed solution of CNT in acetone over the several thin metallic films followed by applying the required pressure to develop the sandwich composites.

The advantages and limitations of each processing techniques as discussed above are summarised in **Table 1.1.**

1.4 Selection of a matrix material

Among the available conventional materials, copper is one of the materials, which has an excellent electrical and thermal conductivity in addition to good ductile characteristics. At present, copper is being used in industrial and engineering applications, building and construction, transport, coinage, ordnance, wrought alloys, compounds, and heat exchangers. Since it has a good thermal conductivity, there is a scope for further improvement in heat transfer applications using copper based MMC, which plays a major role in removal of heat in a shorter period of time. The composite is expected to be used in different applications like blast furnace, steel rolling operation, electric furnace, plate making operation and others. The conventional cooling systems used in those applications contain large storage tanks and cooling towers to dissipate the heat, which increase the operating cost and maintenance cost. In addition, the conventional metals are expected to corrode during the usage period at the working conditions and degrade in a period of time due to ageing process.

Table 1.1 Advantages and limitations of different processing techniques to synthesize / develop CNT-MMC

Sl. No.	Processing techniques	Advantages	Limitations
1.	Mechanical alloying	• Physical blending • Easy to fabricate • Traditional process and economic	• Agglomeration of CNT occurs due to the absence of chemical bonding between the CNT and matrix • It damages the structure of reinforcement during the ball milling process
2	Melting and solidification	• Processing of low melting material like Magnesium	• Formation of cluster due to surface tension and difficult to maintain dispersion of CNT in melt pool.
3	Thermal spray	• Faster rate of fabrication of components and saving machining costs	• It requires sophisticated facility and rigid support structure during the impact of reinforcement.
4	Electrochemical deposition	• Simple technique to fabricate, applicable for electronic applications, and 1-D structures	• Limitation of coating thickness and not suitable for bulk composite structure, difficult in CNT dispersion

Table 1.1 continued

Sl. No.	Processing techniques	Advantages	Limitations
5	Novel techniques 1. Molecular Level Mixing	• Homogenous dispersion of CNT, structural and chemical stability of CNT in matrix can be achieved	• Not yet explored for industrial applications
	2. Sandwich processing	• Achieve directional properties by several layer of matrix and reinforcement	• Severe damage on CNT during consolidation
	3. Vapour deposition	• Suitable for 1-D coating • Coating without any structural stress	• Non-uniform coating and not suitable for bulk production of MM-CNT composites
	4. Nano scale dispersion	• Dispersion of CNT is achieved	• Requires high end consolidation techniques
	5. Torsion welding	• Increase of mechanical properties and embedded CNT in matrix	• Dispersion of CNT is reduced with travel speed of tool

1.5 Motivation of the present work

Among the available technology for the production of steel, a blast furnace contributes to 46% of total production in India against the world average of 70%, Ministry of steel, India [2018]. The working life of a blast furnace is very much affected by the thickness and properties of refractory lining materials, where the thickness of a furnace is found to be reduced due to the erosion during the operating life. It is also noted that the life of a furnace mainly depends on the effective cooling of refractory lining or maintaining the lowest possible temperature in order to avoid inbuilt thermal stress over the period of time. The lining of cooling stave is one of the results of such research endeavours. A stave is conventionally made of cast iron and a cooling part having one or more channel is introduced in the stave towards inward surface of a blast furnace. Recently, copper staves are also used due to its attractive thermal characteristics. The excess heat of stave is removed with water in order to keep the lining in an intact condition and reduce the significant residual thermal stresses developed due to temperature gradient.

A schematic diagram of a stave cooler and its arrangement in a blast furnace are shown in **Figure 1.2,** Mohanty *et al*. [2016]. In general, the normal service life of lining brick of belly zone is shorter than the other zone. The damages on cooling staves generally require costly maintenance and redesign of a total system. The intensity of heat load inside the blast furnace is high at the lower stave area, where the smelting process occurs. The major maintenance cost of blast furnace depends on the how best is the cooling staves, which limit the operating life of the blast furnace. The cast steel staves are still in use due to its specific elongation, tensile strength and melting temperature. However, its limitations lie in low thermal conductivity, thermal stress and phase transformation at high temperature, and fatigue crack, which led to expose the cooling pipe to furnace heat. Under such conditions, the efficiency of blast furnace is compromised and it ends up with repairing the current facilities. In order to overcome the above-said limitations, the composite materials are suggested to be suitable alternatives to enhance the heat dissipation, which has the cascading effect on emission, efficient utilisation of water, and reduce the energy consumption in place of monolithic materials used in the system.

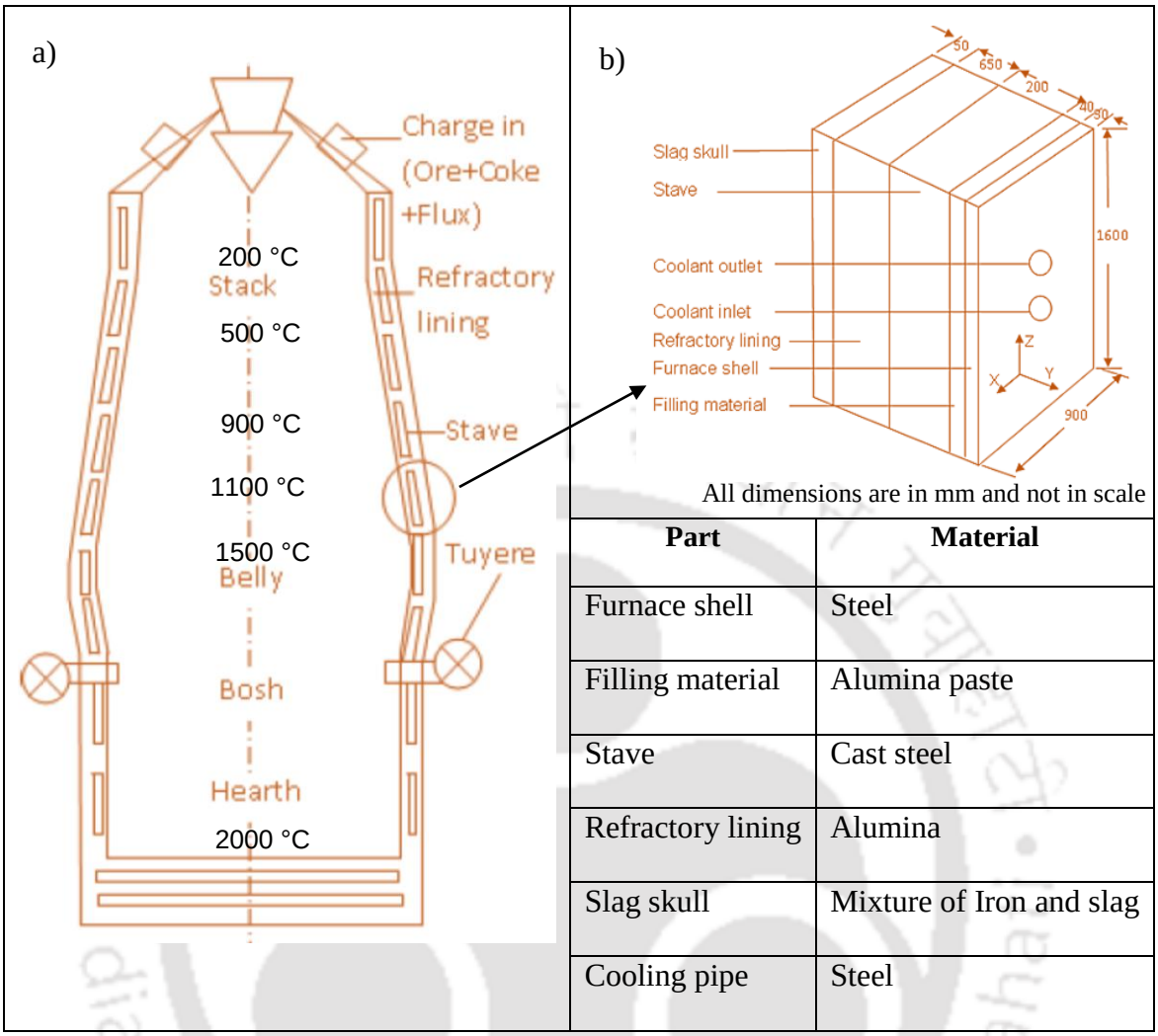

All dimensions are in mm and not in scale

Part	Material
Furnace shell	Steel
Filling material	Alumina paste
Stave	Cast steel
Refractory lining	Alumina
Slag skull	Mixture of Iron and slag
Cooling pipe	Steel

Figure 1.2 a) Schematic representation of a blast furnace and b) Cooling stave arrangement and types of materials used [Mohanty et al. [2016]]

1.6 Organization of thesis

This thesis contains 5 chapters. **Chapter 1** discusses about the requirement of novel materials based on the current scenario in steel industries, different types of composites including CNT-MMC and their processing techniques. The advantages and limitations of all the manufacturing techniques of composites are also highlighted. Later, the motivation behind the present work and the need of composite materials in place of monolithic materials in steel industries are also highlighted. The importance of using an alternate material for a stave in a blast furnace is also discussed, whose performance has direct influence on increasing the efficiency of the furnace.

Chapter 2 deals with the earlier work done on the Cu/CNT composites based on the published literature, which gives the vast information on synthesis of Cu/CNT composite

powder, experimental details, processing techniques, characterization of composite powder and synthesized sample. It also discusses about the properties of composites, where use of different reinforcement is explored in copper. Based on these studies, it reports on the different technical gaps noticed from the available literature and accordingly, the objectives of the proposed thesis work are framed.

Chapter 3 gives the detailed description of raw materials used in the present study, chemical treatment of CNT, synthesizing techniques used to prepare the composite powder, sintering of Cu/CNT composites and different characterization techniques used for the Cu/CNT composites. The procedure followed in the present study at different stages is explained with the help of schematic flowcharts and pictorial representations, wherever it is desired.

Chapter 4 involves with the results and discussion of Cu/CNT composites characterized through qualitative and quantitative analysis. The relative density of the composites and the influence of CNT concentration on the same are reported in detail. The enhancement of hardness, electrical conductivity and thermal conductivity of the composites is explained in detail. The influence of CNT and its concentration on the properties of composites are explained with the help of physical and structural properties. In addition, the influence of different compaction and sintering techniques on the composites are studied in detail and the trend noticed on the characteristics of composites is discussed in detail. The superior characteristics of hardness, relative density, electrical conductivity and thermal conductivity of the composites obtained from the present study are compared in order to understand the influence of compaction technique, sintering technique, CNT diameter and its concentration.

Chapter 5 summarizes the overall work done and important findings of the present thesis work. Major conclusions and future scope of the work are reported here.

CHAPTER 2

LITERATURE REVIEW

2.1 Introduction

The copper / carbon nanotubes (Cu/CNT) composites are being explored in many industrial applications such as steel making, electrical industry, electronics and sensors due to their attractive thermal properties. However, the processing of CNT in metal matrix to prepare MMC is still in a critical stage and requires a special attention. In order to understand the synthesizing and processing difficulties to develop Cu/CNT composites and their influence on the characterization of composites, the existing literature in this domain on the mechanical, electrical and thermal properties of Cu/CNT composites are elaborately studied and reported. Based on the detailed studies, the technical gaps noticed from the available literature are summarised and the objectives of the proposed thesis work are framed.

2.2 Studies on the different compaction pressure on copper powder

Sun and Kim [1997] performed the compaction of copper through simulation using different plastic deformation models and compared with that of experimental results. They reported that the green density of copper is observed to be 87% at 300 MPa compaction pressure and the Cam-Clay model is observed to predict the exact value of relative density (RD) in comparison to that of experimental results. Eksi *et al*. [2004] compacted the copper powder through uniaxial compaction (UA) and cold isostatic press (CIP) at 800 and 500 MPa, respectively, and the RD of about 94% is observed in both the techniques. In order to get the desired RD through UA, it is required to have about 60% higher compaction pressure in comparison to that of CIP. He *et al*. [2008] fabricated the copper and nanodiamond (Cu/ND) composite through co-deposition process and mechanical mixing, where the composite powder is consolidated at 300 MPa and 1000 °C. The sintered samples are repressed at 100 MPa in order to improve its RD. It is reported that the maximum RD and hardness of Cu and Cu- 3wt.% ND composites are noted to be 95.6% and 86 HV, and 96.3% and 116 HV, respectively.

Table 2.1 Comparison of different parameters of copper based composites against compaction pressure

	Compaction pressure (MPa)	**Dimension of the sample (D × t) (mm)**	**Green density (g/cc)**	**Sintered density (g/cc)**	**Relative density of specimen**	**Hardness (VHN)**	**Analysis type***
Sun and Kim [1997]	300	14 × 14					M
Eksi *et al*. [2004]	800 (UA) 500 (CIP)	10 × 5			94	118	E
He *et al*. [2008]	1000	12			95.6	86	E
Goudah *et al*. [2010]	600	13 × 3	8.906	8.911	98		E
Raza and Khalid [2014]	500	16			92		E
Ayyappadas *et al*. [2017]	600	16 × 5	7.43	7.71	86	43± 2.6	E

* M- Modelling data; E- Experimental data

Goudah *et al*. [2010] prepared the Cu/CNT composites through ball milling process and consolidated using UA at 600 MPa followed by conventional sintering at 900 °C, where the RD of Cu and Cu- 1wt.% CNT composites is found to be 98 and 97%, respectively. Raza and Khalid [2014] studied the sintering parameter of Cu and copper/Diamond (Cu/D) composites. They reported that the copper and Cu- 5vol.% D composites obtained through uniaxial compaction followed by conventional sintering showed the RD of 92 and 91.5%, respectively, and their corresponding processing conditions are 500 MPa and 925 °C, and 525 MPa and 900 °C. Ayyappadas *et al*. [2017] fabricated the copper and graphene (Cu/G) composites, where the compaction pressure is kept at 600 MPa and sintering is done through different techniques. It is observed that the relative density of Cu and Cu/G composites sintered at 900 °C is noted to be 86 and 88%, respectively, by conventional sintering and the corresponding values are increased to 88 and 92% for microwave sintered samples.

Table 2.1 shows the summary of results obtained from the above discussion on the copper based composite samples synthesized through different compaction techniques at varying pressure starting from 300 MPa to 1000 MPa. It is observed that the RD of sintered specimen is found to vary in the range of 86 - 98%. It is inferred from the above studies that there is a scope for improving the RD of copper based composites by varying different processing parameters and methodology. As it is noticed from the above observation, the uniaxial compaction pressure at 800 MPa is observed to give the RD in the range of about 95%, and thus, the same is chosen in the present study. In case of CIP, the maximum compaction pressure is maintained at 300 MPa due to the capacity limit of isostatic press.

2.3 Mechanical properties of Cu/CNT composites obtained through different techniques

2.3.1 Molecular level mixing technique

Cha *et al*. [2005] fabricated the Cu/CNT composites by molecular level mixing (MLM) technique followed by the Spark plasma sintering (SPS). They reported that (i) synthesis technique followed by them produced the homogeneous dispersion of CNT in the Cu matrix; (ii) the morphology of Cu/CNT and CuO/CNT composites is observed to be same. They also reported that the composite having 5 and 10 vol.% of CNT showed the yield strength of 360 and 455 MPa, respectively, which are correspondingly 2.3 and 3 times higher than that of Cu. Kim *et al*. [2006] studied the tensile behaviour of Cu/CNT composites prepared by MLM technique followed by SPS and cold rolling. It is observed that the

agglomeration of CNT in copper is reduced by the above mentioned processing techniques. The relative density of Cu/CNT composites is observed to be 98.5%, which is further increased to 99% by cold rolling and annealing process. The tensile strength and yield strength of Cu- 10 vol.% CNT composites are noted to be 281 and 137 MPa, respectively, and the corresponding enhancement is found to be 1.6 and 2 times in comparison to that of copper. Kim *et al*. [2007] processed the material by MLM technique and consolidated the same by SPS, and it is reported that the consolidated Cu/CNT composites having 5 vol.% are found to have homogeneous dispersion of CNT and 3D network within copper. The Cu/CNT composite having 10 vol.% reinforcement showed the hardness of 1.1 GPa, which is 1.8 times higher than that of Cu. Kim *et al*. [2008] synthesized the Cu/CNT composite through MLM followed by SPS, where the homogenous dispersion of CNT is confirmed for 5 vol.% CNT concentration. It is found that the average grain size of Cu and Cu/CNT is reported to be approximately 1.5 μm in size, where the yield strength of composites, Cu and their enhancement of CNT embedded copper composite are reported to be 460 MPa, 190 MPa and 27%, respectively at 5 vol.% of CNT. Xu *et al*. [2011] prepared the composites through MLM technique followed by hot pressing and hot rolling. It is reported that the hardness of composites is observed to be 124 HV and it is 1.8 times higher in comparison to that of Cu. Lim *et al*. [2012] synthesized the Cu/CNT powder by MLM technique and sintered using SPS. They investigated their suitability in multifunctional applications and filling with SiC/W (silicon carbide/tungsten) nanowires. They reported that the MLM technique provided the homogenous dispersion of CNT in matrix and chemical bonding between CNT and metal ions. It is noted that the yield strength of Cu/CNT composites is observed to be 360 and 485 MPa for 5 and 10 vol.%, respectively. It is found that the hardness of Cu- 10 vol.% CNT is observed to be 110 HV, which is 1.8 times more than that of pure copper.

Xue *et al*. [2012] fabricated the Cu/CNT composites by MLM process followed by SPS and hot rolled up to 50% thickness reduction. The tensile strength and yield strength of Cu- 5vol.% CNT composites are reported to be about 2 and 2.5 times higher than that of pure copper, respectively. It is also reported that the CNT exposed on the surface of tensile fracture confirmed to have the weak interfacial bonding between the reinforcement and matrix due to its low wettability. Lal *et al*. [2013] fabricated the Cu/CNT composites by combining the MLM technique and high energy ball milling process to ensure the homogeneous dispersion of the CNT in the matrix. The aqueous medium of sodium

borohydride mixed with edetic acid is used as an oxidation control agent followed by the cold pressing and consolidated at 900 °C for 4 hr in vacuum environment. The maximum hardness of the composites having 1.5wt.% CNT is observed to be 127 HV. Tsai and Jeng [2013] investigated the Cu/CNT composites, where the sample is prepared by MLM technique followed by high pressure torsion (HPT) at 2.5 GPa. The mechanical properties of the composites are studied by nanoindentation technique. The strength and stiffness of Cu/CNT composites having shorter CNT are observed to be significant in comparison to that of large CNT, which is also supported by their molecular dynamics simulation. The Young's modulus and hardness of Cu/CNT composites are observed to be 8.98 GPa and 85.21 MPa, and 10.17 GPa and 96.26 MPa for larger diameter and smaller diameter, respectively at 5vol.% CNT concentration.

2.3.2 Electrochemical deposition technique

Daoush *et al*. [2009] reported that the hardness and Young's modulus of Cu/CNT composites at 20 vol.% are observed to be 1.4 GPa and 105.9 GPa, respectively, and the yield strength is noted to be the maximum of 341.2 MPa at 15 vol.% of CNT, which is 2.85 times more in comparison to that of Cu. Peng and Chen [2009] fabricated the Cu/CNT composite nanowire using ultrasonic-assisted electroless copper plating method. They reported that the ultrasonic technique is found to be an effective tool for the dispersion and de-agglomeration of reinforcement in Cu/CNT composite. Rajkumar and Aravindan [2011] studied the characteristics of microwave sintered Cu/CNT composites prepared through electroless two-step techniques: sensitization and activation method, where the concentration of reinforcement is in the range of 5-20 vol.%, and the CNT is not found to be broken due to the compaction process and intact within the matrix material. The maximum hardness of the composites is obtained at 15 vol.%, which is 126 HV and 22% higher than that of Cu. Long *et al*. [2015] studied the strengthening mechanisms of Cu/CNT composites through electrochemical co-deposition route. The experimental results are compared with that of theoretical model, where the CNT affected the plastic flow of Cu and the strength is found to be increased due to Orowan effect, which depends on the outer diameter of CNT. The yield strength and ultimate tensile strength of composites are observed to be 420 and 710 MPa, respectively, at 4vol.%, which are 3 times more than that of pure copper. Wang *et al*. [2017] processed the Cu/CNT composites by electroless deposition and SPS. The presence of chemical groups in the CNT assisted to have its homogeneous dispersion and

strong chemical bonding with the matrix. The obtained results are 1.3 GPa and 142.2 MPa for Vickers hardness and yield strength, respectively, at 0.5 vol.% CNT concentration. Wang *et al*. [2018] fabricated the composites through electroless deposition followed by SPS and then hot rolling. The yield strength and high plasticity are reported to be 264 MPa and 29%, respectively, at 1 vol.% CNT concentration. Wang *et al*. [2018a] synthesized the Cu/CNT composites through electroless deposition technique and consolidated through hot pressing technique followed by cold rolling with 65% thickness reduction. It is found that the CNT is dispersed homogeneously and chemical bonding is observed with the Cu matrix and the tensile strength of Cu/CNT composite having 0.99 vol.% is reported to be 418 MPa.

2.3.3 Ball milling process

Uddin *et al*. [2010] studied the effect of size and shape of metal particles to improve the mechanical and electrical properties of Cu/CNT composites, where the composites are fabricated through ball milling process followed by hot pressing. It is reported that the relative density of sintered sample prepared with spherical Cu particles is noted to be significantly high in comparison to that of a sample prepared with dendritic shaped Cu particles and the reduced particle size is observed to improve the CNT dispersion in the matrix. It is reported that the hardness of Cu- 0.1wt.% CNT composites having the particle size of 3 μm is improved by 47% in comparison to that of Cu. Goudah *et al*. [2010] fabricated the Cu/CNT composites by uniaxial compaction and conventional sintering process. The sample sintered at 900°C for 90 min. showed the good diffusion of Cu particles, where the difference between experimental and theoretical density is noted to be within 1%. Shukla *et al*. [2013a] processed the Cu/CNT composites by high energy ball milling process and studied the effect of particle size, type, and concentration of reinforcement. The samples are observed at every 5 hr of milling interval to confirm the effect of same using Raman spectroscopy, where the cold welding and fracture of grain are observed to be influenced by the concentration and types of CNT. The cold welding process led to agglomeration of grain, which increased the particle size, whereas the fracture phenomena led to the breakage of the powder particle and hence decreased the particle size. The type of CNT and its concentration influenced the cold welding process leading to have increased particle size with respect to milling time. Shukla *et al*. [2013b] processed the Cu/CNT composites via milling and hot pressing. It is reported that the hardness of copper/single walled carbon nanotube (Cu/SWCNT) is observed to be about 105 BHN and it is reduced to 65 BHN at 5 vol.% for

the multi walled CNT reinforced composites. It is reported that the SWCNT and multi walled CNT based composites having 5 vol.% are getting delaminated during sintering at the middle of cross section. The compressive strength of SWCNT and multi walled CNT composite is reported to be 330 MPa and 170 MPa, respectively, at 5 vol.%. Madavali *et al*. [2014] investigated the effect of atmosphere and milling time of copper powder. It is reported that the powder size is observed to be increased with milling time irrespective of environment. Deng *et al*. [2017] prepared the Cu/CNT composites through ball milling and SPS. The Cu/CNT composites having 0.5 vol.% showed the maximum relative density of 98.1% and the ultimate tensile strength of 307 MPa. Yang *et al*. [2018] prepared the Cu/CNT composites by wet mixing and ball milling followed by SPS. The tensile strength and elongation of Cu- 2.5 vol.% CNT composites are observed to be 280 MPa and 41.7%, respectively, which is 2 times more than that of Cu.

2.3.4 Other synthesis techniques to prepare Cu/CNT composites

Chu *et al*. [2010b] synthesized the Cu/CNT composites by blending the powder under the high speed of air followed by SPS. It is reported that the distribution of CNT, porosity and kinks are observed to influence the sintering phenomenon and the thermal conductivity of the sintered product. It is reported that the homogenous dispersion of CNT and dense composites are noted upto 10 vol.% CNT concentration. It is also reported the spherical powder provided the good dispersion of CNT and better flowability of powder during the sintering process. Guiderdoni *et al*. [2011] prepared the Cu/CNT composite by rapid route involving freeze-drying method without any oxidative acidic treatment or ball milling. It is reported that the XRD pattern of Cu/CNT composite powder showed only Cu peaks up to 16 vol.% of CNT concentration. They also reported the behaviour of low temperature sintering of Cu, and it is observed at 230 and 260 °C for pure Cu and Cu- 5 vol.% CNT composites, respectively. The hardness of the composites is observed to be around 103 HV, which is about 2 times higher in comparison to that of Cu. Jenei *et al*. [2011] investigated the Cu/CNT composites consolidated through powder blend followed by high pressure torsion (HPT) at room temperature and 373 K. It is observed that the hardness at the centre of the sample is noted to be less due to low strain induced during the HPT process compared to the region along the radial direction of the disc. Jenei *et al*. [2013] studied the ultrafine grained microstructure of copper and Cu/CNT composites processed by HPT process. The

hardness of Cu/CNT composites is observed to be 1.8 and 1.5 GPa at 200 and 600 K, respectively, and the copper is noted to have the hardness of 1.7 GPa.

Bittencourt *et al*. [2012] studied the interaction between Cu and CNT, where the CNT is pre-treated with oxygen plasma. It is observed that the copper atom is thermally evaporated and diffused on the surface of CNT, and formed a discrete crystalline facetted particles. It is reported that the presence of oxygen atom over CNT is induced to have the formation Cu-O bond in the Cu/CNT interface. Cho *et al*. [2012] fabricated the Cu/CNT composite by cold spraying process on the Al substrate at low pressure. It is reported that the Cu and CNT is mixed using ball milling process leading to have structural defects and shortened length of CNT. Hippmann *et al*. [2013] followed the melt stirring technique, where the pre-dispersed mixture of matrix and reinforcement at high melting temperature is poured into the graphite mould, where some kind of non-homogeneous is observed in the composites. It is concluded that the 0.1wt.% CNT concentration has significant influence on the compressive strength of pre-dispersed CNT composites. Pialago and Park [2014] fabricated the Cu/CNT composite through mechanical alloying and cold gas dynamic spray (CGDS) process. The deposition efficiency of Cu/CNT powder in CGDS process is observed to be decreased with an increase of CNT concentration. The XRD results showed the micro strain on the coated composite powder. Sule *et al*. [2014] studied the effect of consolidation of SPS for Cu/CNT composites, where the Cu and CNT are blended using wet mixing technique. The maximum hardness of the composites is reported to be 1.30 and 1.12 GPa at 650 and 700 °C, respectively. The presence of CNT in the Cu matrix increased the hardness of the composites and reduced the porosity. Sule *et al*. [2015] prepared Cu/CNT composites through mechanical stirring followed by SPS, where the hardness of 1 vol.% CNT composites is observed to be 140 HV.

Huang *et al*. [2015] sintered the copper powder under electric field. It is reported that the copper grains, which are in contact with neighbouring grains, are observed to be sintered even at low sintering temperature (200°C), and it is due to localised induced field at particle contact area. Later, grain boundary diffusion is also found to be predominated. In addition, the electric field generated a faster diffusion, new grain formation and grain refinement in the copper samples. Jafari *et al*. [2015] developed the Cu/CNT composites through friction stir processing. The hardness of composites is enhanced by 65 and 105% for one pass and three passes, respectively, and corresponding weight loss is observed to be 31 and 68% in comparison to that of pure copper. Arnaud *et al*. [2016] prepared the Cu/DWCNT composite

powder through chemical reaction. It is followed by SPS and then wire drawn process at room temperature. It is reported that the ultimate strength of composites is increased to 710 MPa with 10% enhancement. Huang *et al*. [2017] studied the hardness and tensile strength of Cu/CNT composites, where the CNT is aligned in the composites through die stretching process. The maximum hardness and tensile strength of the composites are noted to be 174 HV and 371.9 MPa, respectively at 5 vol.% along the stretching direction.

2.4 Electrical and thermal conductivity of Cu/CNT composites

Daoush [2008] studied the electrical resistivity of Cu/CNT composites using four-probe technique, where the sample is prepared by electroless copper deposition technique followed by SPS, and it is observed to be 6.9 μΩ.cm at 97.9% RD and 13.5 μΩ.cm at 96% RD for 10 and 40 vol.% of CNT in Cu matrix, respectively. Daoush *et al*. [2009] studied the properties of Cu/CNT composites having different concentration of reinforcement in the range of 5-20 vol.%. It is reported that the electrical resistivity of composites at 15 vol.% of CNT is observed to be 50% of IACS (International Annealed Copper Standard) at 96.5% RD. Uddin *et al*. [2010] fabricated the Cu/CNT composites through ball milling followed by hot pressing, where the electrical conductivity of the composites having Cu- 0.1wt.% CNT composites is noted to be about 50 MS/m and the same is found to be decreased with CNT concentration. Chu *et al*. [2010b] reported that the thermal conductivity of copper obtained through powder metallurgy technique is observed to be 331 W/mK, whereas the single crystal copper showed the value of 400 W/mK. It is observed that the sample obtained at 50 MPa compaction pressure and sintered at 600 °C showed the maximum thermal conductivity of 320 W/mK at 98.4% RD for Cu- 5 vol.% CNT composites. Cho *et al*. [2010] prepared the composites by wet mixing process, where the Cu powder and CNT is mixed in ethanol and sonicated. They reported the influence of CNT in the matrix to obtain the desired thermal conductivity of the composites, where the maximum value of thermal conductivity is noted to be 359.2 W/mK at 1 vol.% of CNT in Cu matrix composite having 98% RD. In addition, the grain size of the matrix is not changed significantly.

Chu *et al*. [2010a] fabricated the Cu/CNT composites by mixing the powder under the high stream of air and consolidated by SPS. It is found that the maximum thermal conductivity of composites is observed to be 328 W/mK at 99% RD and 327 W/mK at 98.8 % RD for 5 and 10 vol.%, respectively, whereas, the same for pure copper is noted to be 331 W/mK at 99% RD. It is suggested that the effect of higher sintering temperature, CNT

content and segregation are required to be examined with appropriate microscopic technique. Chai and Chen [2010] fabricated the Cu/CNT composites using a novel electrochemical co-deposition route, where the thermal conductivity of Cu/CNT composites is observed to be about 700 W/mK and it is 180% higher than that of pure copper, which is noted to be 339 W/mK. Xu *et al*. [2011] synthesized the Cu/CNT composites, and the thermal conductivity of same is reported to be 205.7 W/mK. It is reported that the thermal conductivity is observed to be decreased with an increase of CNT concentration. Kim *et al*. [2011] studied the thermal properties of Cu/CNT composites, where the sample is processed through MLM technique and consolidated by SPS. It is reported that the thermal conductivity of 5 and 10 vol.% of composites is observed to be 250 and 200 W/mK, respectively. Khaleghi *et al*. [2012] synthesized Cu/CNT composites using electroless plating, freeze drying and SPS. The sample is kept under the influence of magnetic field to align the CNT to enhance the thermal conductivity of the Cu/CNT composites. The freeze drying is carried at 77 K and the magnetic field of 0.5 T (Tesla) is used to align the CNT in the axial direction, which provides the anisotropic thermal conductivity of the composites. It is reported that the 10 vol.% aligned CNT by the magnetic field showed about 70.01 W/mK, which is 3.8 times more in comparison to that of randomly oriented CNT composites. Jenei *et al*. [2013] confirmed that the thermal stability of copper is found to be increased with CNT concentration, where the recrystallization of composite is not observed at 1000 K in contrary to that of pure Cu samples.

Subramaniam *et al*. [2013] studied the electrical conductivity of Cu/CNT composites by two-probe and four-probe methods, where the sample is fabricated through electrodeposition process. It is found that the Cu/CNT composites exhibited the current carrying density of 6×10^8 A/cm^2, which is 100 times higher than that of copper. Koppad *et al*. [2013] investigated the thermal and electrical properties of Cu/CNT composites by laser flash technique at 473 K, where the sample is prepared by powder metallurgy technique followed by hot forging process. They reported that the thermal and electrical conductivity of the composite having 1wt.% CNT are observed to be 300 W/mK and 80 IACS, respectively, and the corresponding value of pure Cu is reported to be 390 W/mK and 98% IACS. Subramaniam *et al*. [2014] reported the thermal conductivity of 395 W/mK for 45 vol.% Cu/CNT composites. Sule *et al*. [2014] reported that the thermal conductivity of Cu is observed to be 395 W/mK at 98.5% RD, which is reduced to 273 W/mK at 96% RD for 1 vol.% CNT reinforced composites. Sule *et al*. [2015] reported that the thermal conductivity

of the composites having 1 vol.% CNT is found to be 327 W/mK at 98.28% RD. Wang et al. [2017] reported that the electrical conductivity of 0.5 vol.% CNT composites is observed to be 90.9% IACS, where the sample is obtained through electroless deposition technique. Chen *et al*. [2017] studied the microstructure and thermal conductivity of Cu/CNT composites, which are prepared using electroless plating technique followed by hot pressing, and the thermal conductivity of Cu/CNT composite having 1 vol.% is observed to be 420 W/mK at 98.2% RD. It is noted from different published literature that the electrical conductivity of 0.99, 1 and 2.5 vol.% Cu/CNT composites is observed to be 90% IACS at 98.7% RD (Wang *et al*. [2018a]), 96.6% IACS (Wang *et al*. [2018]) and 91.6% IACS (Yang *et al*. [2018]), respectively.

2.5 Different properties of multiphase Cu/CNT composites

Nam *et al*. [2012] studied the effect of precipitation hardening behaviour of Al-Cu/CNT composites fabricated through molecular level mixing followed by high energy ball milling, and then consolidated by SPS. The strengthening mechanism of Al-Cu/CNT composites is found to be influenced by the aspect ratio of CNT. It is also reported that the grain refinement of the composites is observed to be increased by the reinforcement of CNT. The acid treated CNT is observed to be well dispersed in the matrix in comparison to that of PVA (Poly-vinyl alcohol) coated CNT. It is also reported that the combination of molecular level mixing and high energy ball milling led to have the ultimate tensile strength, Young's modulus and hardness of 601 MPa, 450 MPa and 193 HV, respectively, at 4 vol.% concentration of CNT. Gill and Munroe [2012] studied the properties of Cu/Cr-CNT composite prepared through powder metallurgy route, where the composites are sintered at 750, 900 and 1050 °C. They reported that the formation of carboxyl and carbonyl groups on the CNT caused its partial oxidation due to the presence of entrapped air within the CNT. It is also reported that there is a significant peak shift in Raman spectrum of CNT, which confirmed its damage during milling and the compaction process. Gao *et al*. [2016] fabricated the Cu/G (Copper/Graphene) composites through wet mixing and hot pressing technique. The ultimate tensile strength of the composites having 0.3 wt.% is observed to be 210 MPa. Cheng *et al*. [2017] fabricated the Cu/CNT composites, where 1wt.% titanium is mixed with copper through ball milling and CNT is dispersed in Cu-Ti powder using wet mixing technique followed by the consolidation through SPS. The ultimate strength and tensile elongation of Cu-Ti- 0.4wt.% of CNT are observed to be 355 MPa and 17.6%,

respectively, at 98.8% RD. Zhang *et al*. [2017] developed Cu/CNT-G composites, which are synthesized through chemical reduction process and consolidated through SPS. The yield strength of Cu/CNT-G at 0.35 and 1.15 vol.% is observed to be 246.9 and 347.2 MPa, respectively.

Ullbrand *et al*. [2010] studied the influence of SPS and hot pressing in order to prepare the composites, where the carbon nanofibres (CNF) are coated with chromium for improving the adhesion bonding between the copper and CNF, and it is synthesized through electroless copper deposition technique. In addition, chromium coated over CNT prior to the deposition process improved the Cu-CNF interfaces. It is reported that the relative density of the sample obtained from hot pressing process and SPS is noted to be about 95-100% and 82-97%, respectively. It is reported that the thermal conductivity and coefficient of thermal expansion of composites made from SPS are observed to be 194 W/mK and 9.9 $\times 10^{-6}$ K^{-1}, respectively, which are found to be very significant in comparison to that of the sample prepared from the hot pressing process and their corresponding values are reported to be 104.5 W/mK and 10.1×10^{-6} K^{-1}. Nie *et al*. [2012] fabricated the Cu/CNT composite powder, where tungsten (W) is used to coat the surface of CNT to obtain a uniform dispersion and better enhancement of thermal conductivity, and then the composite powder is consolidated by SPS. It is observed that the W-CNT content less than 5 vol.% showed better dispersion in the composites and the clusters are formed with increased concentration of reinforcement. The maximum thermal conductivity of 2.5 vol.% of W-coated CNT and uncoated CNT composites is observed to be 348.5 W/mK at 99.5% RD and 329.5 W/mK at 99% RD, respectively. Raza and Khalid [2014] prepared the Cu/diamond composites at an optimized pressure of 525 MPa. The maximum density of Cu and Cu/diamond composites is obtained at the sintering condition of 925 °C- 2.5 hr and 900 °C- 2 hr, respectively. The thermal conductivity of Cu/D composites at 5 vol.% is observed to be 284 W/mK. Gao *et al*. [2016] studied the thermal conductivity of Cu/G composites, and it is reported to be 396 W/mK at 0.3wt.% G concentration. Ayyappadas *et al*. [2017] investigated the Cu/G composites prepared through mechanical mixing and consolidated through conventional and microwave sintering techniques. The electrical conductivity of Cu is observed to be 92% IACS at 89% RD and 89% IACS at 86% RD for microwave and conventional sintered samples, respectively. Zhang *et al*. [2017] reported that the electrical conductivity of Cu/CNT-G composites is observed to be 54.5 and 49.8 MS/m for 0.35 and 1.15 vol.%, respectively. It

is found that the electrical conductivity of Cu/CNT-G composites is found to be superior in comparison to that individual composite of same content.

From the above detailed analysis, it is noted that "molecular level mixing technique" is observed to produce superior characteristics of Cu/CNT composites, where the homogenous dispersion of CNT in the copper matrix is ensured. In addition, the composite is found to have the chemically stable structure and good interfacial bonding between the CNT and matrix. After comprehensive studies on the Cu/CNT composites from the published literature, the following technical gaps are noticed.

2.6 Technical Gap

- An optimum concentration of reinforcement to obtain significant improvement in both thermal and mechanical properties of the Cu/CNT composites is yet to be reported.
- Influence of the different sizes of CNT and its concentration on the properties of composites is not explored.
- Sintering and other processing parameters are required to be optimized in order to have increased relative density and other properties.
- Mechanism for the enhancement of mechanical and thermal properties of composites is not clearly understood.
- The alignment of CNT in the matrix required for studying the directional properties of the composites is to be reported.
- The effect of chemical treatment on CNT and its influence on the thermal properties of the composites are yet to be explored in detail.
- The structural damages on CNT during physical mixing and their impact on the characteristics of composites are yet to be reported in detail.
- The presence of strain and lattice defects on the CNT during synthesis of composites are to be studied in detail.
- The non-straightness effect of CNT on the thermal properties is yet to be reported in detail.
- The contact interface between the CNT and Cu is to be studied in order to understand its contribution on the thermal properties of composites.
- Cu/CNT composites are not found to be explored in different industrial applications.

2.7 Objectives of the present work

The main objective of the present work is to develop Cu/CNT composite materials and characterize them in order to explore the same for potential industrial applications in general and steel industries in particular. As the properties of the composites are found to be influenced by different variables and processing parameters, the following sub-objectives are to be carried out in order to fulfil the major objectives of the proposed study.

- To synthesize the Cu/CNT composite powder using molecular level mixing technique.
- To study the influence of processing conditions and operating parameters of compaction technique namely uniaxial compaction and cold isostatic pressing in order to improve the characteristics of the Cu/CNT composites.
- To understand the significant influence of different sintering techniques namely conventional and microwave sintering in order to improve the desired properties of the composites.
- To study the influence of size and concentration of CNT on the electrical and thermal conductivity and hardness of Cu/CNT composites.

CHAPTER 3

MATERIALS AND METHODS

3.1 Introduction

This chapter is focused on the selection of raw materials, functionalization of CNT, synthesis technique to prepare Cu/CNT composite powder and studies on the sintering kinetics of Cu and its composites. A series of studies are conducted with appropriate techniques on the test samples to study their characteristics.

3.2 Materials

Different raw materials namely Copper (II) acetate monohydrate ($Cu(COOCH_3)_2 \cdot H_2O$) with ≥ 99% purity, ethyl alcohol (C_2H_5OH) absolute 200 Proof and multi walled carbon nanotubes (CNT), which are used to synthesize copper and Cu/CNT composite powder, are procured from Sigma Aldrich, TEDIA and M/s Shenzhen Nanotech Port Co., Ltd., China, respectively. The specifications of as-received CNT are as follows: length 5–15 μm, purity 97% and ash content < 3%. The CNT having three different diameters, 10-20 nm, 20-40 nm and 40-60 nm, are used.

3.3 Functionalization and purification of CNT

To establish chemically active sites on the side walls of CNT and increase its purity level, the raw CNT is refluxed in a chemical mixture, as suggested by Esumi *et al*. [1996], where Nitric acid and Sulphuric acid are taken in the ratio of 1:3 by volume and refluxed at 140 °C for 30 min. It is then followed by multiple rinsing of CNT with distilled water using a centrifuge, where the CNT and water is separated based on their density difference due to centripetal force using REMI R-24 until the pH value of supernatant is reached about 7 and then the wet CNT is dried in a hot air oven at 100 °C for 24 hr. The process flow followed for the chemical treatment of CNT is shown in **Figure 3.1a**. The functional groups attached on the side walls of CNT are confirmed with the help of Fourier transform infrared spectroscopy (FTIR) technique. The scheme of chemical functionalization of CNT is given in **Figure 3.1b**.

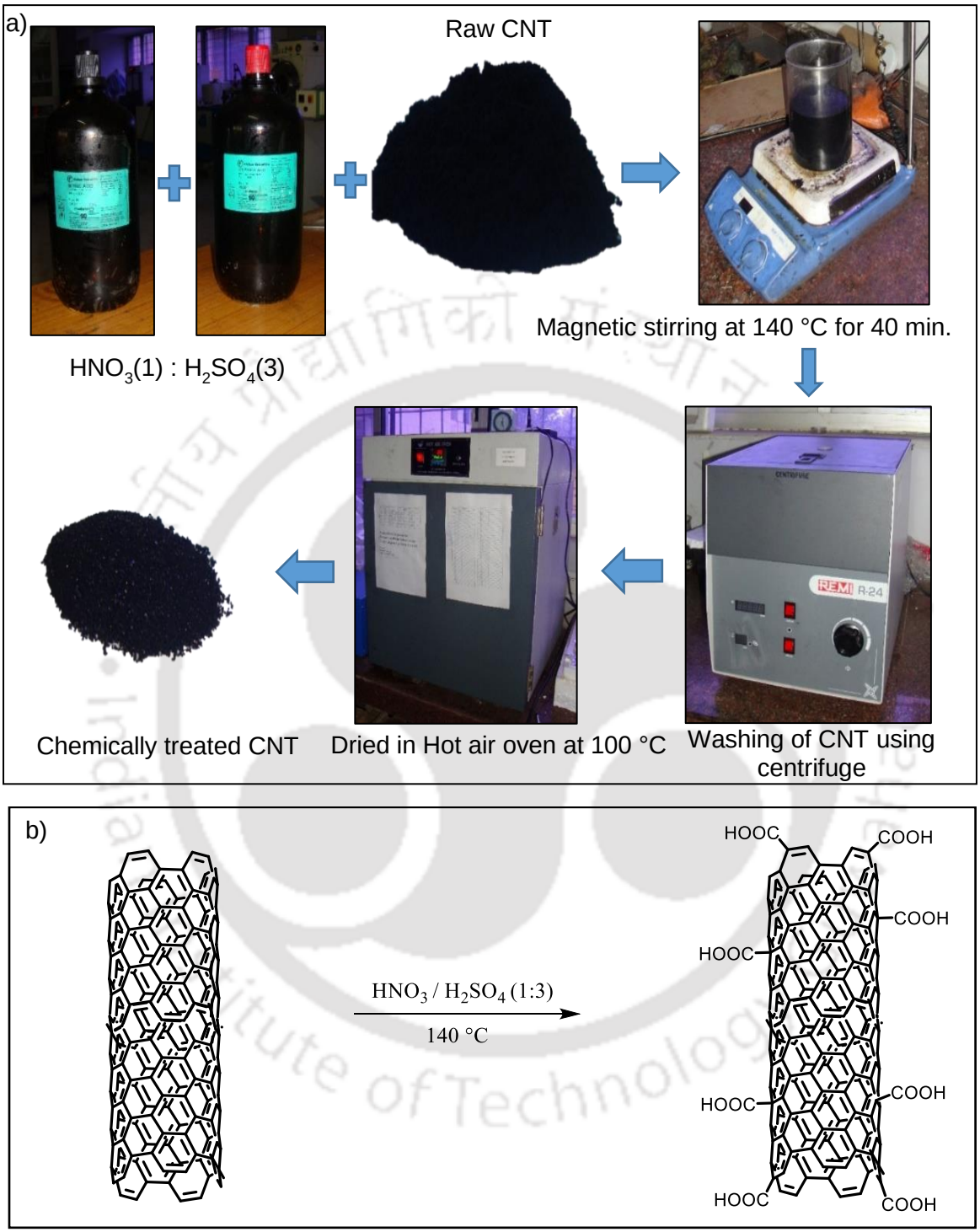

Figure 3.1 a) Schematic layout of chemical treatment of CNT, b) Scheme of chemical treatment of CNT

3.4 Preparation of Cu/CNT composites powder

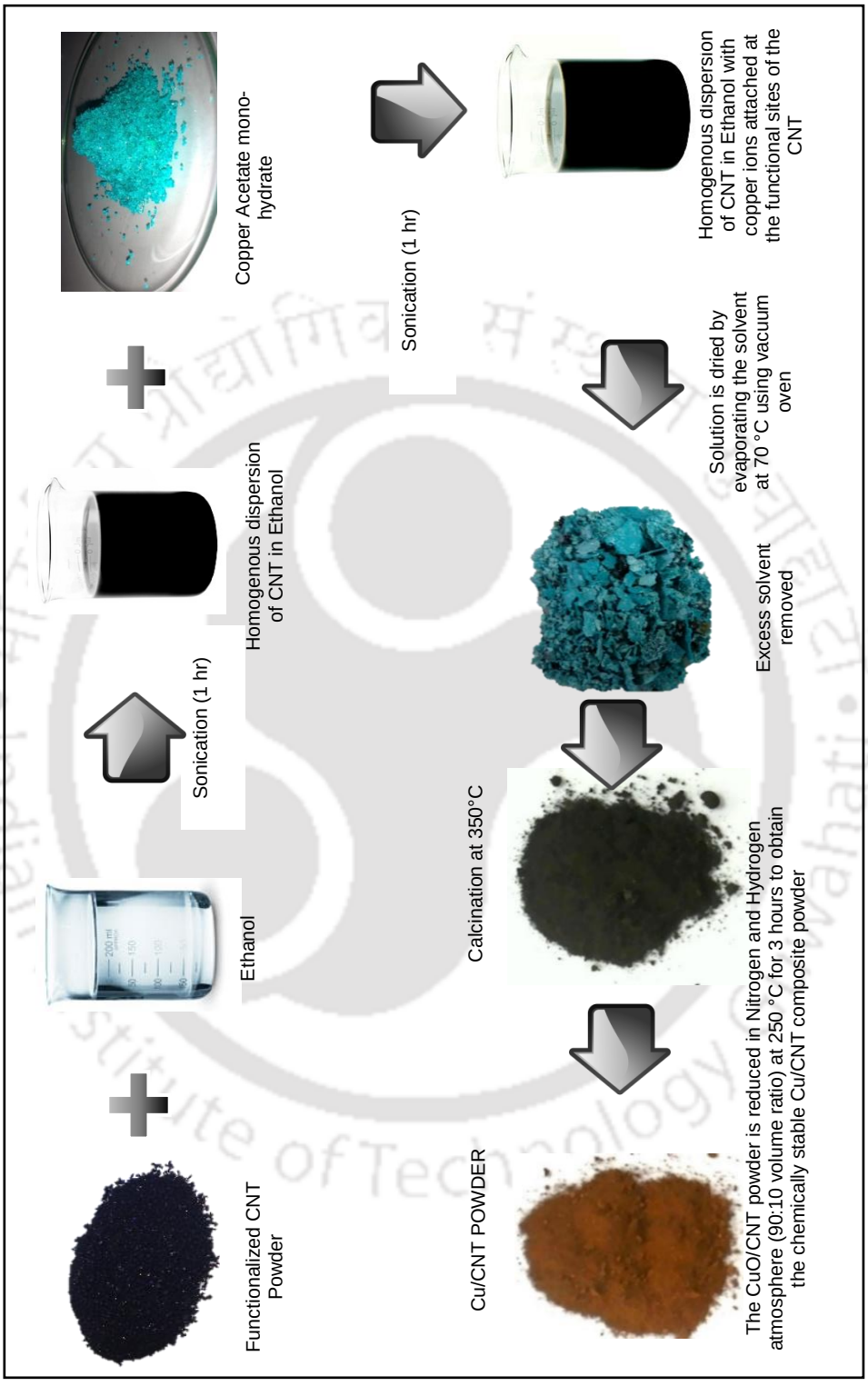

Figure 3.2 Pictorial view of different stages involved in synthesizing Cu/CNT composite powder by molecular level mixing technique

3.4.1 Synthesis procedure for copper and composite powder by molecular level mixing technique

Molecular level mixing technique is used to synthesize Cu/CNT composite powder due to its inherent advantages, which are listed in **Table 1.1**. The composite powder is synthesized by a two-step process, where the functionalized CNT is added into ethanol and sonicated in an ultrasonic bath (Ultra Met 2002 Ultrasonic Cleaner, BUEHLER) for 1 hr followed by the addition of Copper (II) acetate monohydrate to the CNT dispersed solution and further sonicated for 1 hr. The ethanol solution having Cu ions, ligands and CNT is heated in a vacuum oven at 70 °C to remove the residual ethanol. The obtained powder is calcinated at 350 °C for 3 hr to eliminate acetate, traces of ethanol and hydrates. The CuO/CNT powder is then obtained, which is finally reduced at 250 °C for 3 hr under nitrogen and hydrogen reduction environment having the volumetric ratio of 90:10, where nitrogen is mixed with hydrogen to prevent the possible embrittlement of metallic tubular furnace. Thus, the Cu/CNT composite powder is obtained after cooling down the chamber to room temperature under inert/reduction environment. A pictorial representation of the above discussed synthesis processes of Cu/CNT composite powder is shown in **Figure 3.2**.

3.5 Compaction of Cu/CNT composite powder

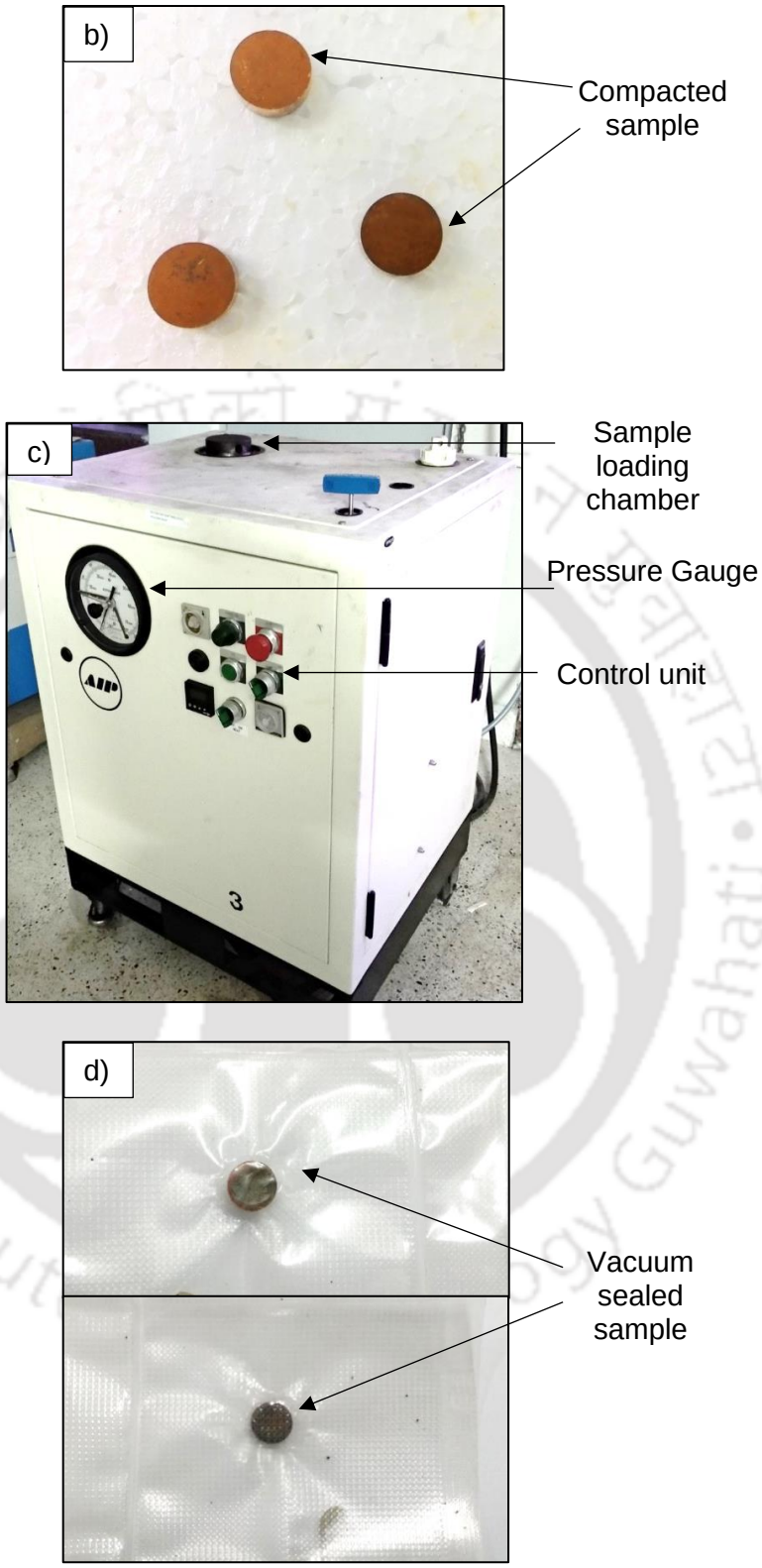

Figure 3.3 a) Universal testing machine UTE- 20, b) Uniaxially compacted samples, c) Cold Isostatic press (CIP) - AIP3-12-60C, and d) Vacuum sealed CIP compacted samples

The Cu/CNT composite powder is compacted into 8 mm diameter x 3 mm thick cylindrical pellets using an appropriate metal die set in an Universal Testing Machine (UTM) UTE-20 (FIE Ltd.), which is shown in **Figure 3.3a**. Based on the previous discussion made in **section 2.2**, an attempt is made to compact the powder sample at 800 MPa. A mixture of Zinc stearate and methanol is used as a wall lubricant as suggested by ASTM B925-08 for the smooth operation during the sample preparation process in order to get defect free green compact samples. A few samples obtained through uniaxial compaction technique are shown in **Figure 3.3b**. A Cold isostatic press (CIP), (Make; American Isostatic presses, Inc., Model: AIP3-12-60C) is used to compact the synthesized Cu/CNT composite powder and a pictorial view of the facility is shown in **Figure 3.3c**. The powder samples are compacted at 50 MPa using the UTM to get a pre-compacted sample having the desired shape and size. Further, these samples are sealed separately using a vacuum sealing unit and the sealed samples are compacted at 300 MPa under isostatic condition, which are shown in **Figure 3.3d**.

3.6 Studies on sintering kinetics of copper and composite powder

Figure 3.4 Thermomechanical Analyzer

A Thermo-Mechanical Analyser (TMA) (Model: TMA/SS6000, Hitachi High-Tech Science Corporation, Japan), which works under the principle of Linear Variable Differential Transformer (LVDT), is used to obtain the sintering parameters of the test samples proposed in the present study and the pictorial view of the facility used for the same is shown in **Figure 3.4**. A load of 100 mN is applied to ensure better contact between the sample and the probe.

A ‘R’ type (Platinum Rhodium -13% / Platinum) thermocouple is used to measure the environmental temperature of a sample with ± 0.1 °C accuracy, which is 5 mm away from the outer periphery of the sample. The sintering temperature of 900, 800, 700 and 600 ºC is selected and the sample is heated at 10 ºC/ min. till the desired sintering temperature is reached, which is maintained for 60 min. under nitrogen gas environment. The sintering kinetics of the test samples are studied in order to obtain their complete diffusion of grain boundaries.

3.7 Sintering of Cu/CNT compacted samples

The sintering of the samples is carried out in two ways: Conventional and microwave techniques. In both cases, the heating rate is maintained at 10°C/min. The pressure-less sintering is followed in a tubular furnace (Make: Thermocon, Model: Inconel type) without applying any additional load on the samples under argon gas environment. Initially, the samples are kept in an alumina boat and placed inside the furnace chamber and argon gas is used to purge the normal environment in order to avoid the oxidation of the sample during the sintering process. Once the furnace is switched on, the furnace chamber is heated up via heating coil and the heat is transferred to the samples via convection, which is maintained for 60 min. after reaching the desired working temperature. It is to be noted that the entire heating and cooling process in the furnace is done under argon gas environment in order to prevent any unwanted chemical reaction in the sample.

A 1.45 kW Industrial microwave sintering furnace (Make: Enerzi, Model: MH1514-101-V5) operating under multimode state at 2450 MHz frequency is used in the present study, where an air-cooled magnetron is used to generate the microwave. The working chamber is made of Stainless Steel-304, a reflective type, and the initial power of microwave is set at 800 W. The sample temperature is measured by an Infrared pyrometer and the temperature gradient between the environment and the sample is monitored using a ‘K’ type (Chromel/Constantan) differential thermocouple and the feedback is sent to the controller in order to reduce the same. Silicon carbide (SiC) is used as a susceptor to cover a crucible, which absorbs the radiation to heat the sample for sintering and the alumina wool is used as an insulating material over the SiC covered crucible to reduce the heat loss. All the samples are sintered at 600°C in an Argon environment for the duration of 60, 75 and 90 min. A thorough polishing is done on the sintered samples for the removal of an oxide layer, if any,

for further characterization. **Figure 3.5** shows the tubular furnace and microwave furnace, which are used to sinter the test samples.

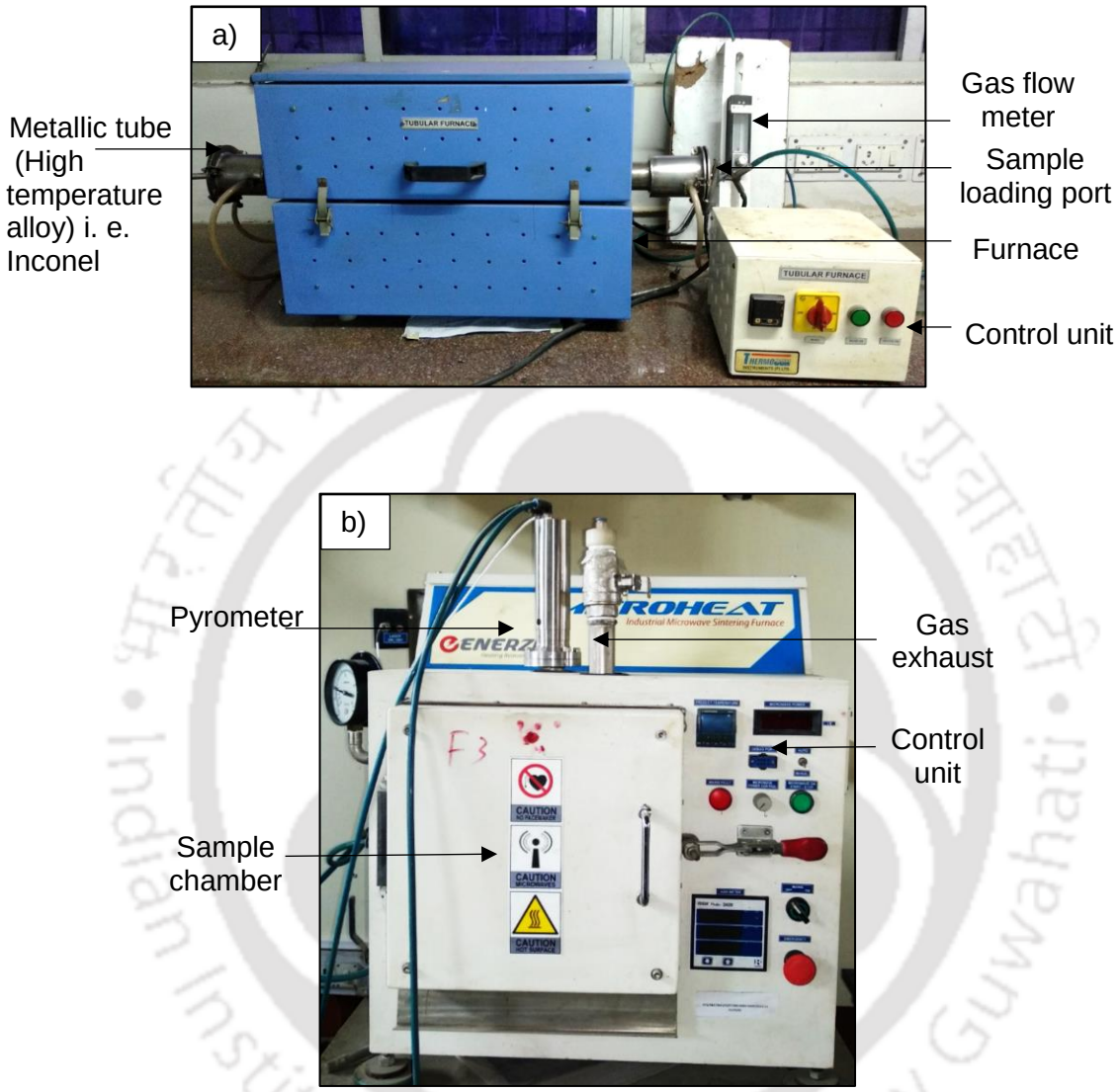

Figure 3.5 a) Conventional tubular sintering furnace and b) Microwave sintering furnace

3.8 Preparation of composite samples

The Cu/CNT composite powder having different concentration and size of CNT is synthesized using molecular level mixing technique. The concentration of CNT is varied from 0.25 to 1 wt.% with an increment of 0.25 wt.% and the CNT having diameter of 10-20 nm, 20-40 nm or 40-60 nm are used. As discussed in the previous section, different compaction and sintering techniques are used to consolidate the synthesized Cu/CNT composite powder and a detailed view of series of steps involved to prepare the composites is shown in **Figure 3.6**.

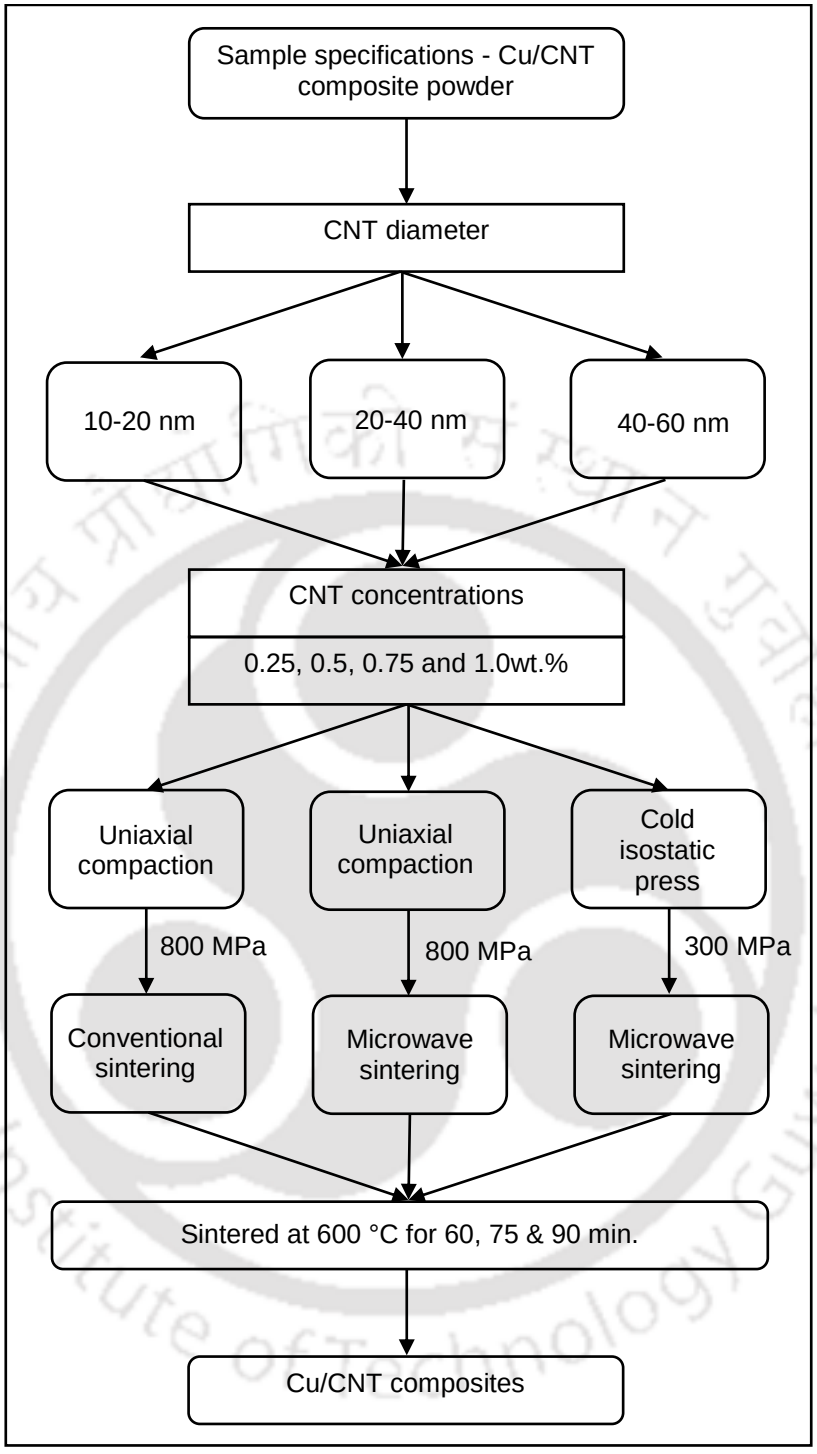

Figure 3.6 Schematic layout of preparation of Cu/CNT composites having different CNT size and its concentration through different processing techniques

3.9 Characterization of Cu/CNT composite powder and sintered sample

The synthesised powder is preserved in a desiccator before it is characterized or processed to get sintered products in order to avoid the oxidation and absorption of moisture.

3.9.1 Confirmation of chemical bonding on CNT and Cu/CNT

The effect of functionalization of CNT and the bonding between Cu and CNT are studied with the help of Fourier transform infrared spectrometer (FTIR) technique and a pictorial view of the instrument used in the present study is shown in **Figure 3.7.** An appropriate quantity of sample is mixed with potassium bromide (KBr) and it is pre-compacted at 5 MPa. An initial scan is done in order to detect the background noise without any sample. Later, the sample is kept in a transparent sample holder and it is scanned in the range of 400 - 4000 cm^{-1} wave number. The IR rays are penetrated through the KBr mixed sample and the transmitted ray gives the information about different molecular bonding based on its vibrations, rotations or stretching.

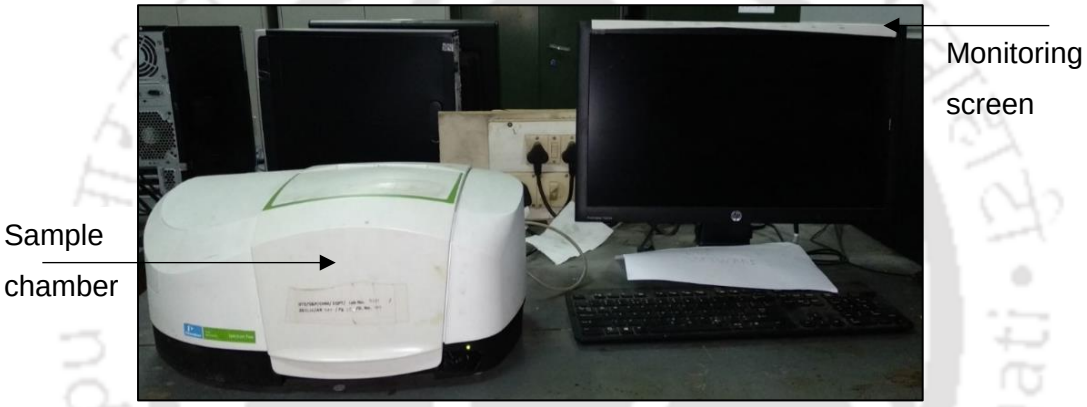

Figure 3.7 Fourier Transform Infrared Spectrometer (Make: PerkinElmer, Model: Spectrum Two)

3.9.2 Structural analysis of test samples

Crystalline structure and phases of Cu/CNT composite powder, copper and CNT are analysed through X-ray Diffractometer Make: PANalytical, Model: X'Pert powder and the photographic view of the facility is shown in **Figure 3.8**. The samples are kept in the path of X-ray beam. The generated incident X-ray beam is passed on the sample and the diffracted beams are captured by a detector. The diffraction pattern (2θ) of test samples is obtained from 20 to 95°. The scan is done under a diffracted monochromated beam Cu-Kα (1.5406 Å) radiation source, where the scanning rate and step rate are maintained at 0.03° and 0.05 s, respectively. All the analyses are carried out using high score software integrated with PANalytical system. The obtained data is noise filtered and their background details are identified for finding the full width at half maximum (FWHM). Finally, the peak corresponding to a plane is identified. Later, the peaks are compared with JCPDS (Joint

Committee on Powder Diffraction Standards) data to validate the results obtained from the present study. The strain developed during the synthesis process of Cu and Cu/CNT composite powder is calculated using the following relation:

$$\text{Strain } (\varepsilon) = \frac{\beta}{\tan\theta} \quad \text{... (3.1)}$$

Figure 3.8 X-ray Diffractometer (Make: PANalytical, Model: X'Pert powder)

3.9.3 Thermal stability analysis of test samples

Thermal characteristics of Cu/CNT composite powder, copper and CNT are studied using Thermogravimetric Analyzer (TGA), Make: Perkin Elmer Model: STA-8000, where the heating rate is maintained at 10 °C/min. for all the samples, and the facility used in the present study is shown in **Figure 3.9**. It measures the amount of weight loss or gain of a sample against the temperature or time under Argon atmosphere. Initially, the weight of the samples is measured and kept inside the furnace chamber. Then the Argon gas is passed under 1 bar at a flow rate of 20 ml/min. Once the system is stabilized, the weight of the sample is monitored and recorded. The samples are kept upto 800 °C under Argon atmosphere and the thermal stability of the same is monitored based on the weight loss throughout the process.

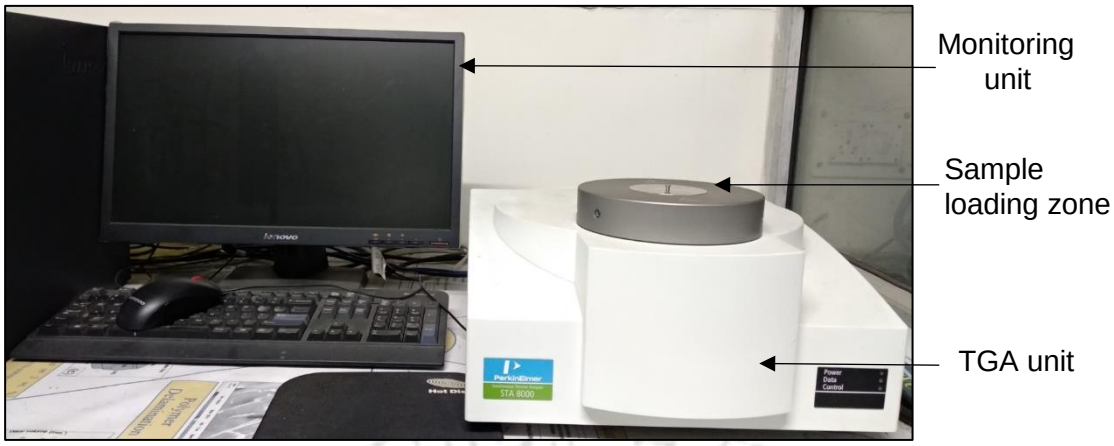

Figure 3.9 Thermogravimetric analyser (Make: PerkinElmer, Model: STA 8000)

3.9.4 Studies on the morphology of copper and Cu/CNT composite powder

Figure 3.10 Field Emission Scanning Electron Microscope (Make: Zeiss, Model: Sigma)

The morphology of Cu/CNT composite powder and copper and the dispersion of CNT in Cu are obtained by Field Emission Scanning Electron Microscope (FESEM) (Make: Zeiss, Model: Sigma). A pictorial view of the facility used in the present study is shown in **Figure 3.10.**

The morphology of CNT and the defects present in the CNT such as non-straightness, bundles, knots and kinks in the composite powder are studied using a 200 kV Transmission Electron microscopy (TEM) (Make: JEOL, Model: JEM 2100), where the electron beam penetrates through the specimen and the facility used in the present study is shown in **Figure 3.11**.

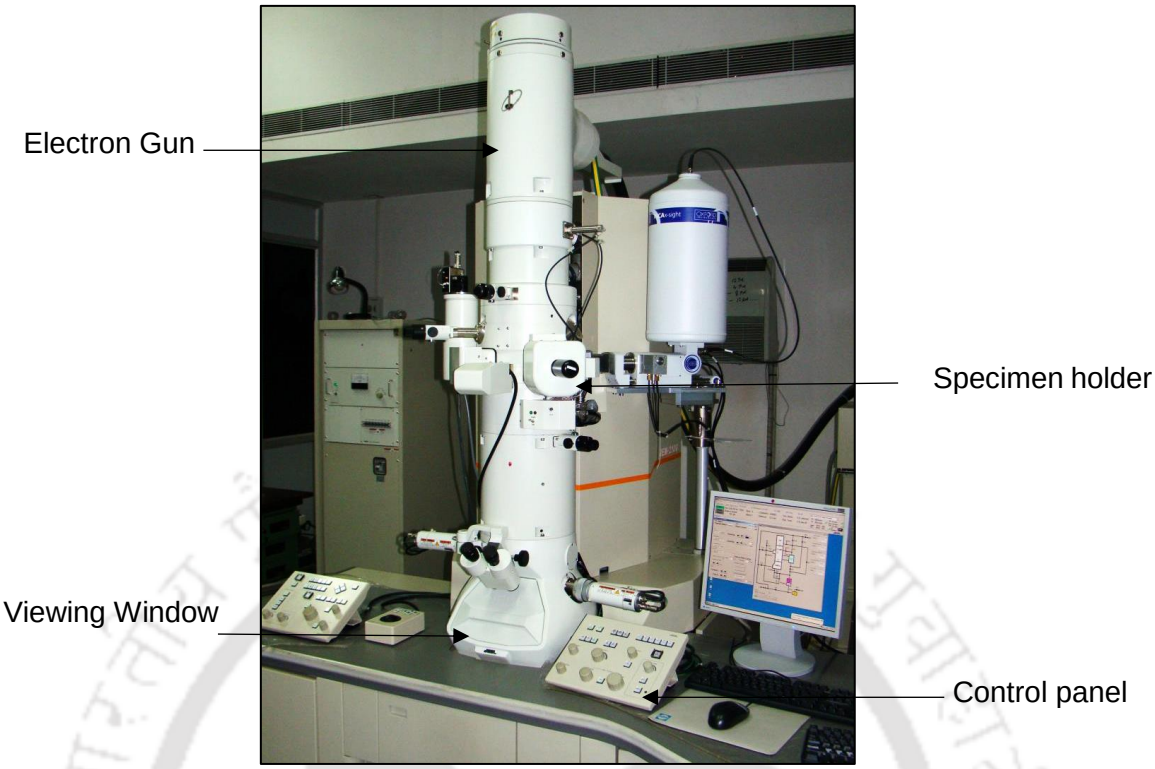

Figure 3.11 Transmission electron microscope (Make: JEOL, Model: JEM 2100)

3.9.5 Setup for density measurement of sintered samples

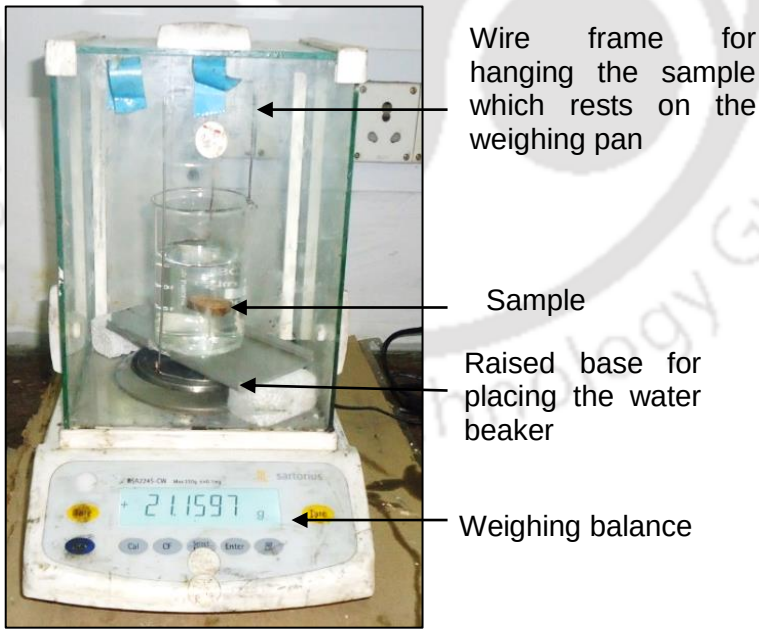

Figure 3.12 In-house setup for density measurement of sintered samples as per ASTM B962-13

Initially, the weight of samples is measured under atmospheric condition using a weighing balance. Then, the samples are immersed in oil and kept in a vacuum oven at < 7 kPa for 30 min. Then, the excess oil over the samples is wiped gently with a lint free material. It is ensured that the sample is not in contact with any oil absorbing material such as paper, cloth etc., Again, the weight of the oil impregnated samples is measured under atmospheric condition and the results are noted. A setup developed to measure the density of a sample as per ASTM B962-13 is shown in **Figure 3.12**, where weight of the sample is measured under its floating condition. Based on the Archimedes' principle, the density of Cu/CNT composites is calculated and the equation used for the same as per ASTM B962-13 is given in **Eqn**.**3.2**. The theoretical density of Cu/CNT composites is calculated using a rule of mixtures and is given in **Eqn. 3.3**. The relative density (RD) of Cu/CNT composites is calculated as per the **Eqn**. **3.4**.

$$\text{Sintered density } \rho_s = \frac{A\,\rho_w}{b-f} \quad \text{... (3.2)}$$

$$\text{Rule of mixtures } \frac{1}{\rho} = \frac{W_f}{\rho_f} + \frac{W_m}{\rho_m} \quad \text{... (3.3)}$$

$$\text{Relative density} = \frac{Sintered\ Density}{Theoretical\ density} \quad \text{... (3.4)}$$

3.9.6 Sample preparation for microscopic studies

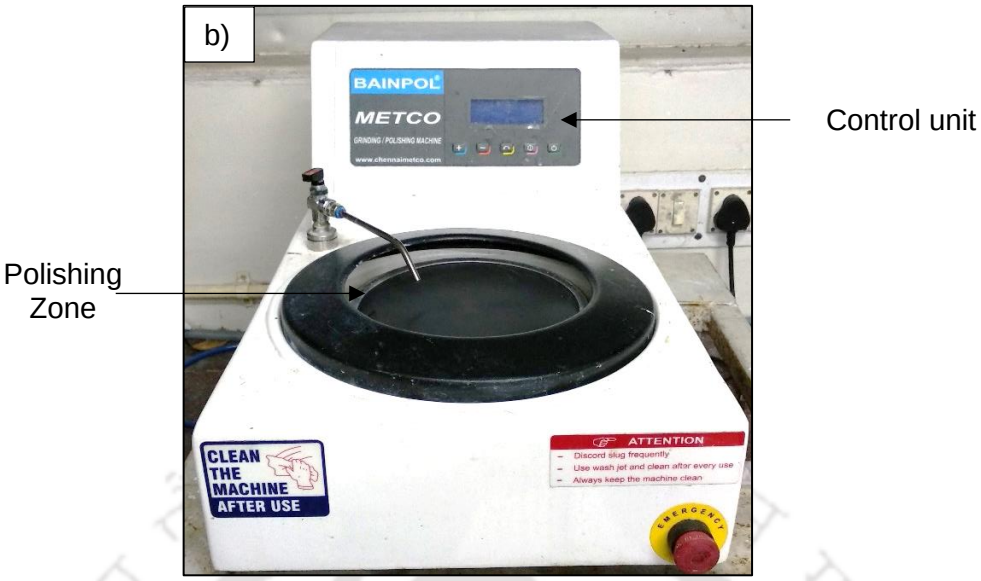

Figure 3.13 a) Pneumatic sample mounting unit and b) Polishing machine

In order to study the microstructure of the samples, the sintered products are mounted using a sample mounting press. The samples are then manually polished using 800, 1000, 1200, 1500 and 2000 grid emery sheets. Then, the lapping process is followed, which is an abrasive finishing process in order to achieve the desired surface finish, where the diamond paste is applied over the sample and polished on the soft cloth till it reaches the required mirror surface finish. Further, these samples are etched in a mixture of $FeCl_3$ and HNO_3 solution having the volumetric ratio of 1:5 for 1 min. to obtain the contrast microstructure. **Figure 3.13** shows the sample mounting unit and polishing machine used in the present study.

3.9.7 Grain size measurement

The microstructure analysis of polished sintered samples is done using an optical microscope (Make: Carl Zeiss, Model: Axiotech 100HD- 3D). All the samples are analysed with the help of AxioVision (V4.9.1.0) software in order to study the presence of voids and grain size. Initially, the sample is kept under the optical microscope, and the images are captured by image acquisition module. Subsequently, these images are processed by eliminating the unrecognized area during the image capture and highlighted with suitable spectrum of light correction. Finally, a line intercept method is used to calculate the average grain size of the samples using image analysis and interpretation module. A pictorial view of the optical microscope used in the present study is shown in F**igure 3.14**.

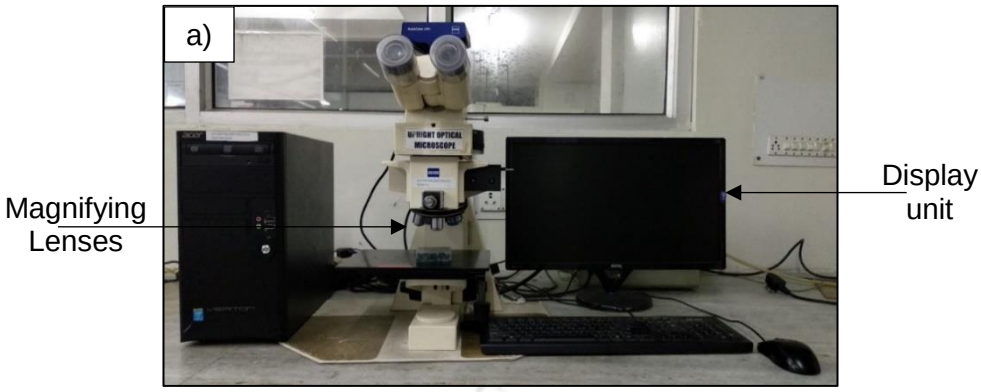

Figure 3.14 Optical microscope

3.9.8 Hardness studies on the test samples

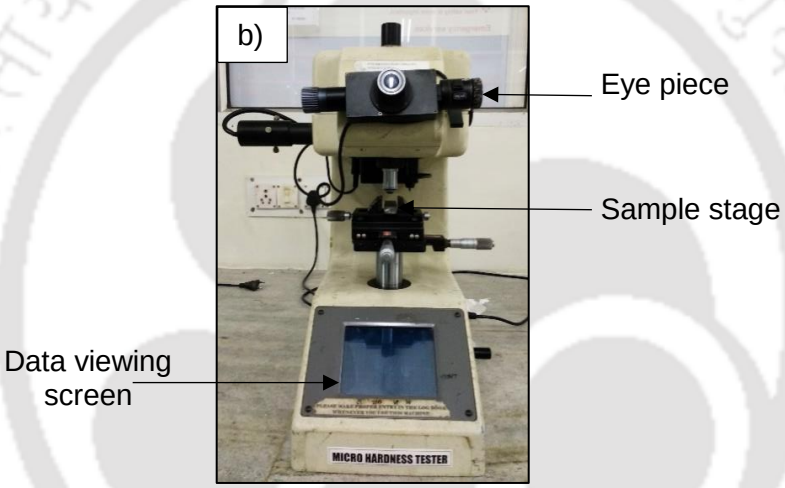

Figure 3.15 Microhardness tester

After obtaining the microstructure, the hardness of composite samples is studied with an applied force of 500 gf as per ASTM E384-16 using a microhardness tester (Make: Buehler, Model: 1600–6306). A diamond pyramid of square base having 136° ± 0.5 between opposite faces is used as an indentor. The diagonal of the indentation is noted through an eye piece and the mean value is calculated. Each sample has undergone 10 indentations in order to have the reproducibility of the results. The Vickers hardness is calculated using the **Eqn. 3.5**. The hardness of the sample is used to study the influence of concentration of CNT, size of CNT, sintering duration and sintering temperature of the composites. A pictorial view of microhardness tester is shown in **Figure 3.15.**

$$\mathrm{HV}=\frac{2F\ Sin\frac{136^{\circ}}{2}}{d^2}\ \text{i. e. HV}=1.854\frac{F}{d^2} \qquad \ldots (3.5)$$

3.9.9 Electrical and thermal conductivity studies on the test sample

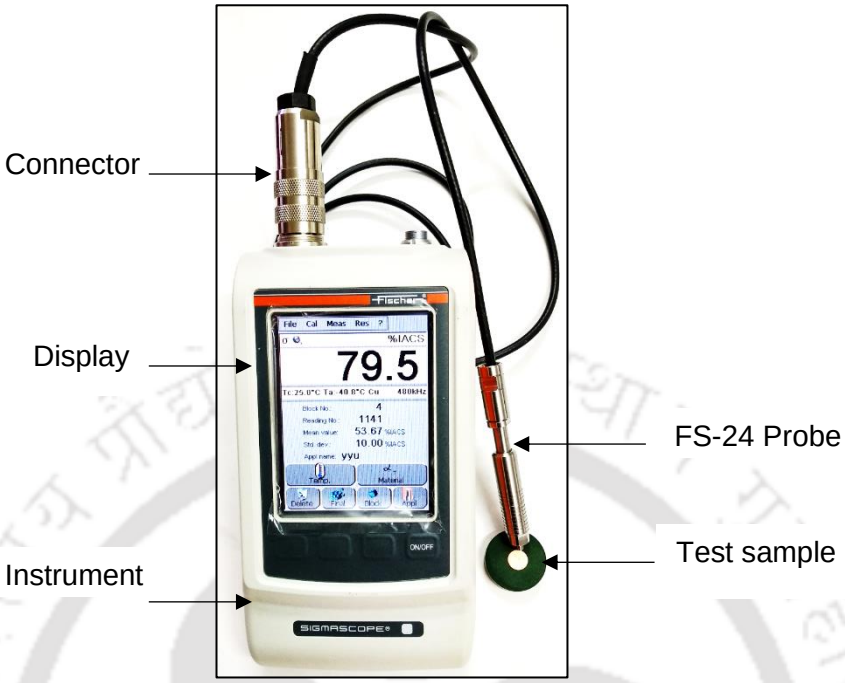

Figure 3.16 Electrical conductivity instrument - Sigmascope SMP350

An Eddy current instrument (Make: Sigmascope SMP 350, Helmut Fischer GmbH, Germany) having FS-24 probe type, shown in **Figure 3.16**, is used to study the electrical conductivity of composites in order to understand the influence of sintering duration, CNT diameter and its concentration. Since the free electron is the main source of electrical and thermal conductivity of the metallic materials, Wiedemann–Franz law, Kittel and McEuen, [2005] is used to calculate the thermal conductivity of the composites from the results of electrical conductivity (σ) data using an **Eqn. 3.6,** Kumar *et al*. [1993].

$$k = LT\sigma \quad \text{... (3.6)}$$

In each case, the results are obtained from 3 different samples synthesized after the same processing conditions in order to confirm the repeatability of the said results and the average of experimental results is reported.

CHAPTER 4

RESULTS AND DISCUSSION

4.1 Introduction

This chapter discusses thoroughly on the results of Cu/CNT composites and copper samples obtained from the present study in a systematic way. The discussion is started with characterization of Cu and composite powder and it is followed by studies on sintering behaviour of them. The results of relative density, microstructure, hardness, electrical conductivity and thermal conductivity of the composites obtained through different processing techniques are reported and discussed in detail. In addition, these results are systematically compared in order to derive the best combination of processing variables to get desired results for the proposed applications.

4.2 Characterization of Cu and Cu/CNT composite powder

4.2.1 Confirmation of chemical bonding

Figure 4.1a shows the transmittance spectra of CNT before and after its functionalization process along with CuO- 1wt.% CNT and Cu- 1wt.% CNT powder. It is observed that the transmittance spectra of as-received raw CNT showed no major peaks and the peaks noted at 1745 and 3430 cm^{-1} in the chemically treated CNT represent the C=O stretch and O-H stretch, respectively, corresponding to the peaks of acidic groups like carbonyl, phenol, and lactol. The peak observed at 1625 cm^{-1} attributes to C=C bond in CNT. The CuO/CNT sample showed the characteristic peak at 535 cm^{-1} corresponding to Cu-O stretch, as reported by Korzhavyi *et al*. [2012], along with other peaks of functionalized CNT. The appearance of Cu peak at lower wavenumber could be due to the high frequency of vibration, which is inversely proportional to mass of vibrating molecule as described by Hooke's law, Burke [1997]. During the reduction process, the CuO/CNT is reduced to Cu/CNT, where the significant peak intensity corresponding to CuO is observed to be submerged and broadened and thus the Cu/CNT composite powder is confirmed to have the chemical bonding between the matrix and reinforcement. A schematic representation of Cu ion attached over the chemically treated CNT is shown in **Figure 4.1b.**

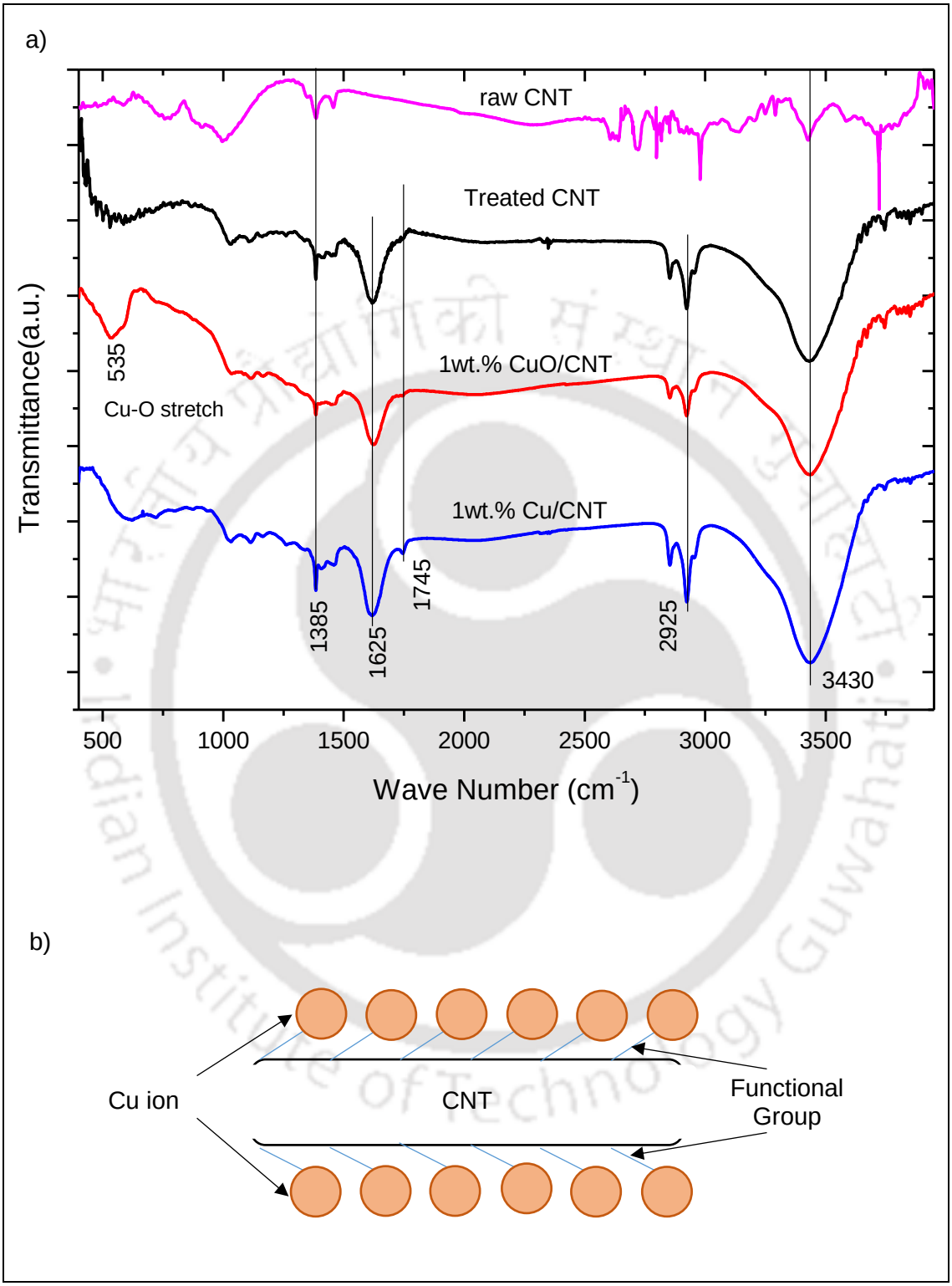

Figure 4.1 a) FTIR transmittance spectra of CNT before and after the functionalization process, CuO- 1wt.% CNT powder and Cu- 1wt.% CNT powder and b) Schematic diagram of Cu ion attachment over the CNT functional groups attached over it

4.2.2 Structural characterisation of Cu/CNT composite powder

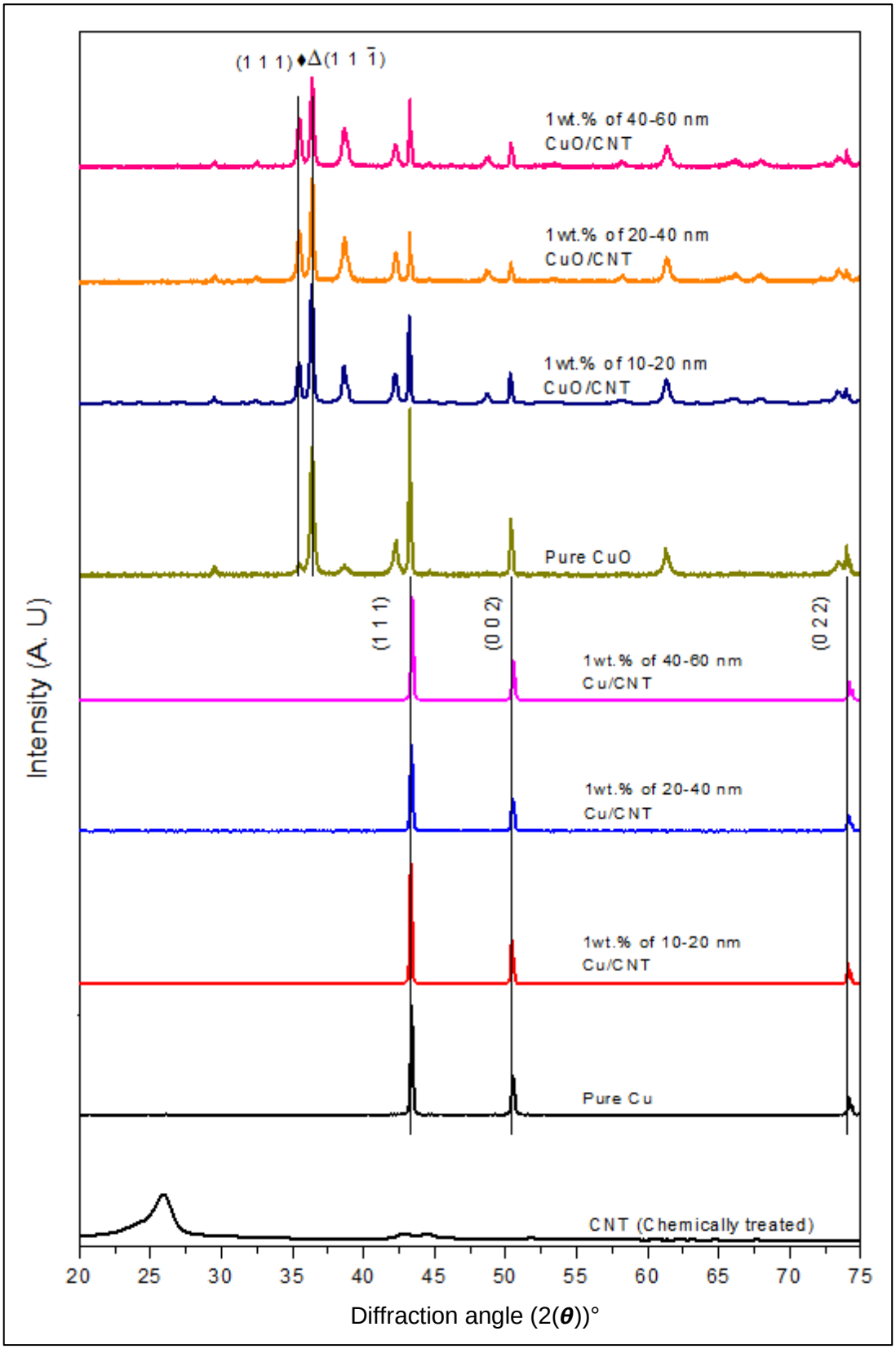

Figure 4.2 XRD pattern of CNT, CuO, Cu, CuO/CNT, and Cu/CNT composites having 10–20 nm, 20–40 nm and 40–60 nm diameter CNT at 1 wt.%

The X-ray diffractograms of CuO- 1wt.% CNT powder obtained from all types of CNT are shown in **Figure 4.2**. The peaks observed for CuO/CNT at (111) and $(11\bar{1})$ crystallographic plane correspond to tenorite phase (CuO) and cuprite phase (Cu_2O), respectively, and these patterns are in consistent with their corresponding JCPDS PDF 5-0661 and JCPDS PDF 5-0667 data. The same peaks are also noticed in copper powder synthesised through MLM technique without adding any CNT. The XRD patterns of unreinforced Cu and Cu/CNT composite powder having 1wt.% of 10-20 nm, 20-40 nm and 40-60 nm diameter CNT are also shown in **Figure 4.2**. It is observed that the XRD patterns obtained for both unreinforced Cu and Cu/CNT composite powder are found to be very similar irrespective of CNT diameter at 1wt.% of its concentration. The peaks identified at (111), (002), and (022) crystallographic planes are confirmed to follow JCPDS PDF 85-1326 and FCC structure. The major peak corresponding to CNT as per JCPDS PDF 26-1076 is also not observed at 26° in all composite powder and thus, it could be inferred that a thorough encapsulation on CNT is done by copper and there are no prominent structural changes in the Cu/CNT composite powder due to the incorporation of CNT.

4.2.2.1 Strain on the Cu and Cu/CNT composite powder due to synthesis process

Figure 4.3 shows the XRD pattern of copper and Cu- 1wt.% CNT composite powder having all types of CNT diameter at (111) plane. It is observed that the presence of strain in the composite powder is noted to be 2.17×10^{-3}, 2.16×10^{-3} and 3.24×10^{-3} for 10-20 nm, 20-40 nm and 40-60 nm diameter CNT reinforced Cu/CNT composite powder, respectively, whereas it is noticed to be 1.98×10^{-3} for pure Cu. In case of 40-60 nm diameter CNT composites, the presence of lattice strain in the composites is found to be about 1.5 times more in comparison to that of 10-20 nm and 20-40 nm diameter CNT composites. In addition, the Cu/CNT composite powder peak is observed to be similar to that of pure copper.

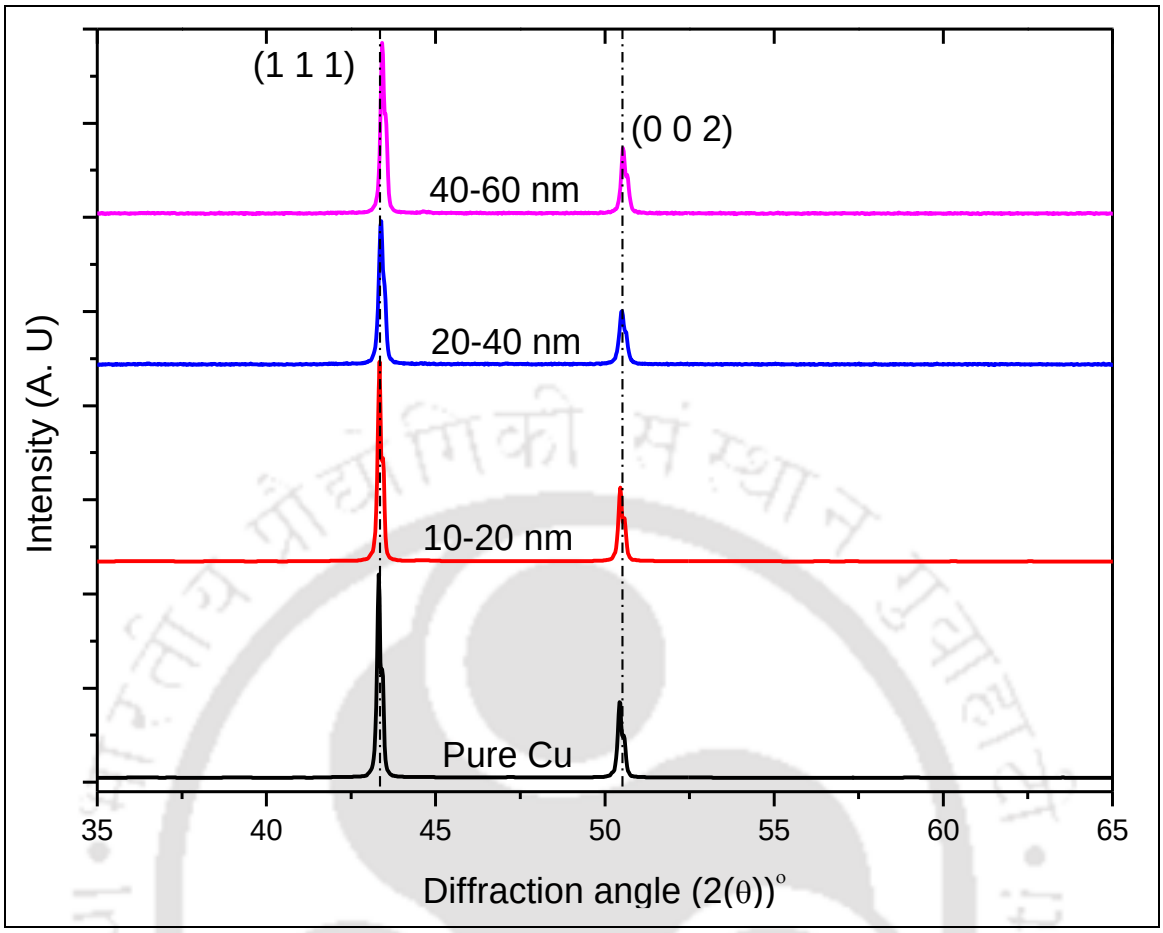

Figure 4.3 XRD pattern of Cu and Cu- 1wt.% CNT composite powder having 10–20 nm, 20–40 nm and 40–60 nm diameter CNT in the focussed region

4.2.3 Morphology of Cu and Cu/CNT composite powder

Figure 4.4 shows the FESEM images of synthesized pure copper and Cu- 1wt.% CNT composite powder having different CNT diameter in order to study the distribution pattern of CNT in the matrix, and entanglement and defects of CNT. **Figures 4.4a-b** show the morphology of copper particles obtained immediately after the reduction process, where the copper particles are observed to be glued together due to their low temperature solid-state sintering behaviour. It is noted from Guiderdoni *et al*. [2011] that the solid-state sintering of copper is observed at ~ 230°C and the same is also observed in our present study.

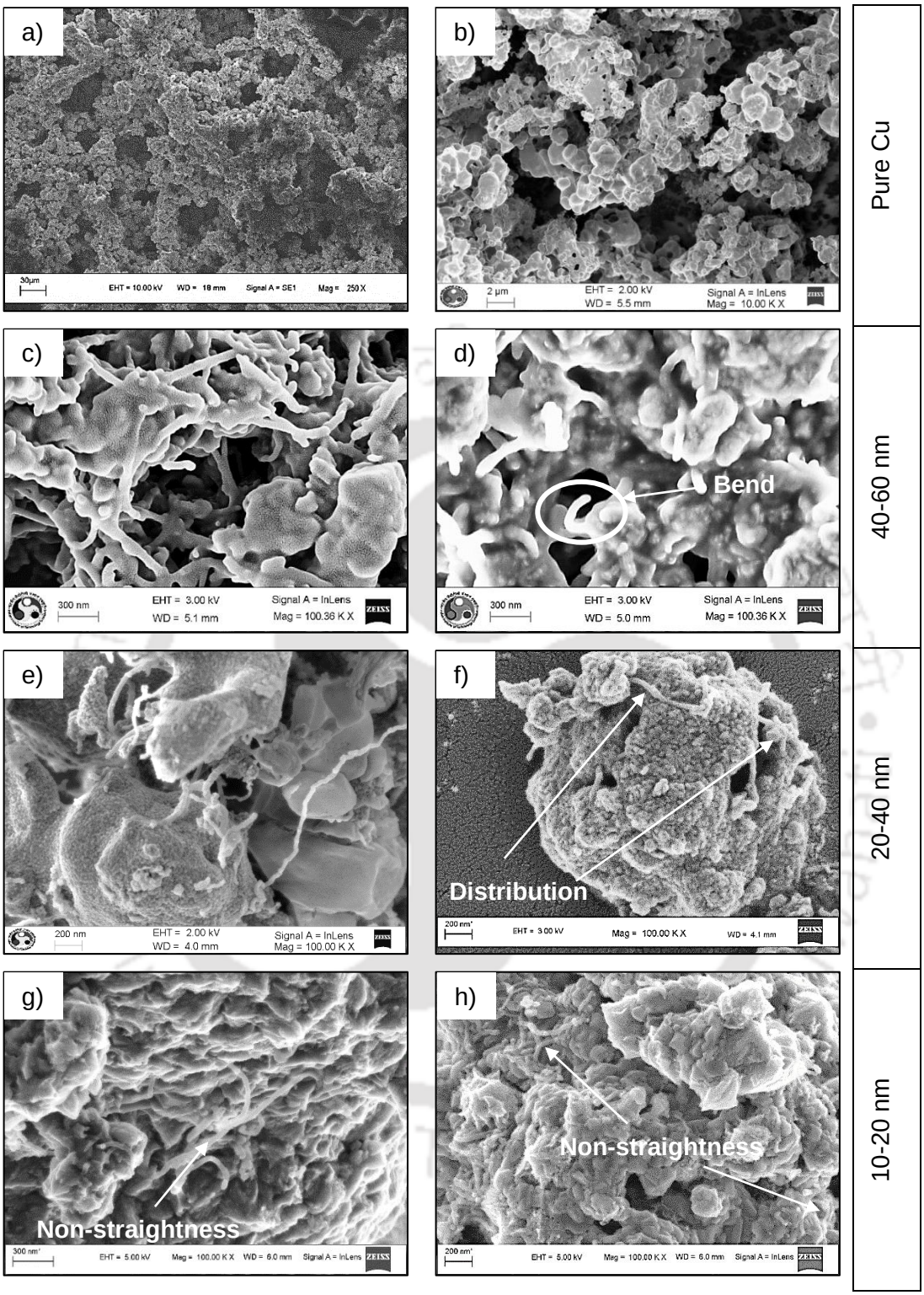

Figure 4.4 Morphology of Cu and Cu- 1 wt.% CNT composite powder a-b) Synthesized Cu powder, c-d) 40–60 nm CNT in Cu matrix, e-f) 20–40 nm CNT in Cu matrix, and g-h) 10–20 nm CNT in Cu matrix

Figures 4.4c - d, **4.4e - f** and **4.4g - h** show the microstructure of Cu- 1wt.% CNT composite powder having 40-60 nm (*l/d* = 200), 20-40 nm (*l/d* = 333) and 10-20 nm (*l/d* =

666) diameter CNT, respectively, where the non-straightness effect of CNT is observed to be increased with its aspect ratio (*l/d*). It is also observed that the CNT is distributed homogeneously and it is embedded with copper with the help of different chemical groups generated over it during the chemical treatment, which is expected to increase the rigidity of final composites. Though different kinds of defects are observed in CNT in the composite powder irrespective of its diameter, aspect ratio, chemical treatment and processing technique followed to prepare the composite powder, only bending defects are noticed significantly throughout the composite powder. As there is chemical bonding between the matrix and reinforcement, which is confirmed through FTIR studies, it is expected to improve the load bearing characteristics of the composites. It is also noted from **Figure 4.4g - h** that the 10-20 nm CNT composite powder has significant level of entanglement in comparison to that of 20-40 nm and 40-60 nm diameter CNT composite powder.

4.2.4 Studies on different defects of CNT in the composite powder

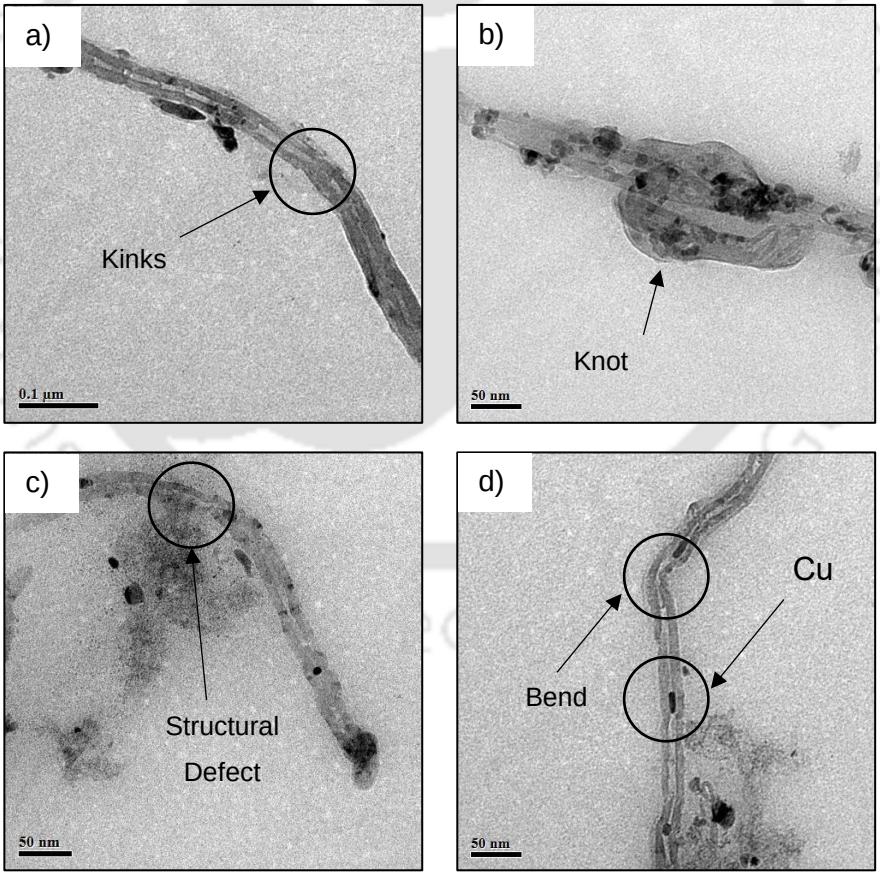

Figure 4.5 Different types of defects observed in 1wt.% 10–20 nm CNT- Cu composite powder

Figures 4.5a-d show the TEM images of different types of defects noted from 1wt.% 10-20 nm CNT- Cu composite powder, where bending of the tubes, defects/damages on the outer and inner wall of CNT, kinks, knots, and entanglement of CNT are observed. In addition, filling of copper ions inside the CNT is also noticed. Chu *et al*. [2010a] reported that the above noticed defects are expected to increase the chemical affinity towards the matrix leading to enhance the bonding strength between the matrix and reinforcement. In addition, these defects may restrict the filling pattern of composite powder in the cavity during the compaction process leading to decrease the relative density of sintered composites. These defects may also act as barriers for electron and phonon conduction leading to reduce their corresponding electrical and thermal conductivity of the composites.

4.2.5 Thermal stability of Cu and Cu/CNT composite powder

Figure 4.6 shows the thermal stability of commercially available spheroidal copper powder (Sigma-Aldrich, 10 micron), synthesized Cu powder and Cu- 1wt.% CNT composite powder, which are studied to understand their individual oxidation behaviour up to 800 °C. It is observed that the thermal stability of commercially available and synthesized copper powder is observed to follow the same trend upto 800 °C. A gradual increase in weight gain of pure Cu is noticed from 250 °C onwards irrespective of source of pure copper powder. The oxidation behaviour of Cu and Cu/CNT is observed to be saturated at 725 °C and 550 °C, respectively. The oxidation process of Cu/CNT composite powder is found to be saturated about 175 °C lower than that of respective temperature of pure copper. Due to the presence of chemical bonding between CNT and copper and the copper coating over the CNT, the oxidation process of Cu/CNT composite powder is limited to 550 °C and its thermal stability is retained from 550 °C onwards. However, the rate of oxidation of Cu/CNT composite powder is observed to be about 45 % higher that of than the synthesized copper powder, though both are observed to be saturated after attaining about 25% of weight gain. It is inferred that the oxidation temperature of composite powder is reduced to the range of 550 to 250 °C in comparison to the range of 725 to 250 °C in case of pure copper powder. Thus, the product developed using composite powder might be having less oxidation products in comparison to that of pure copper sample.

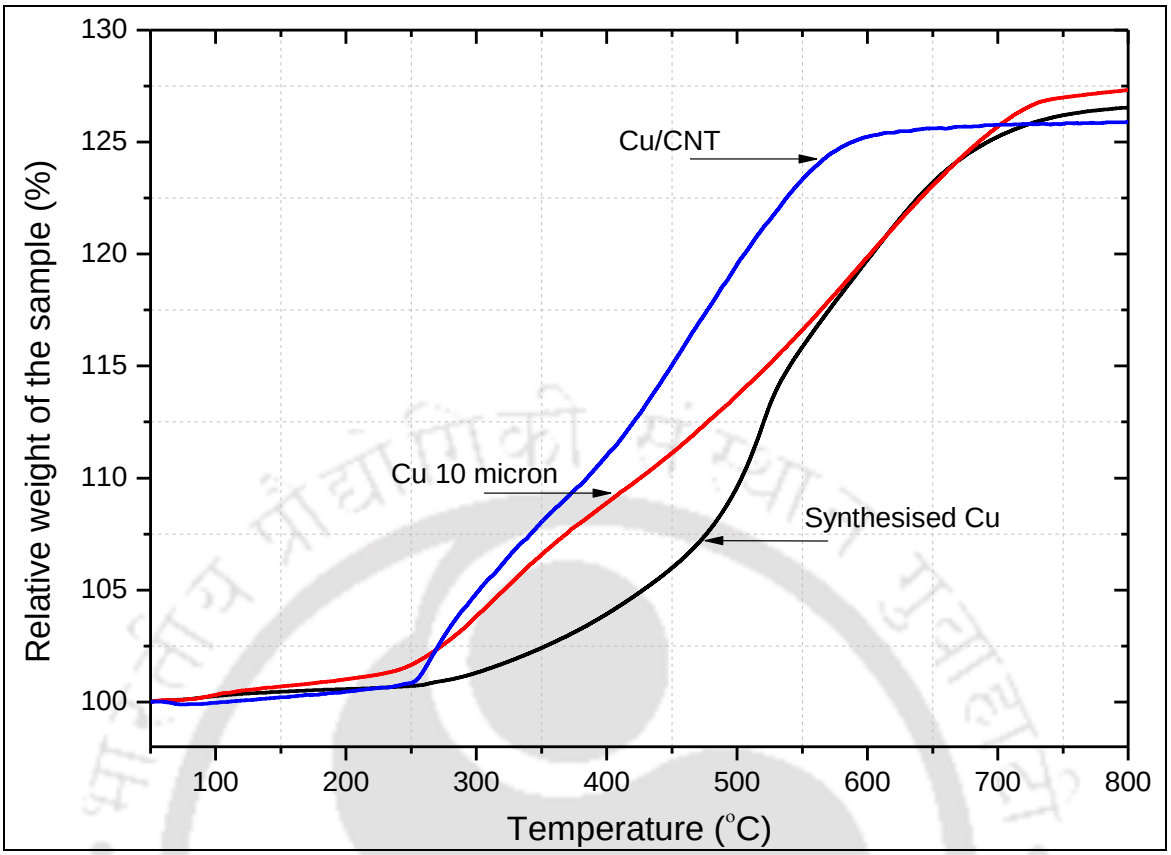

Figure 4.6 Thermal stability analysis of synthesized Cu, commercially available copper, Cu- 1wt.% CNT composite powder under Argon environment

4.3 Selection of sintering temperature of Cu and Cu/CNT composites

In order to sinter the compacted samples, it is required to finalize the sintering parameters of Cu and Cu/CNT composite test materials using TMA. It is mainly focused on finding suitable temperature and holding time in order to have the complete diffusion of grain boundaries. Based on the suitable processing parameters obtained from TMA, all the samples are sintered at the obtained sintering temperature and time, and this section discusses about the sintering kinetics of copper and its composites having different types of CNT and its concentration.

4.3.1 Sintering behaviour of copper

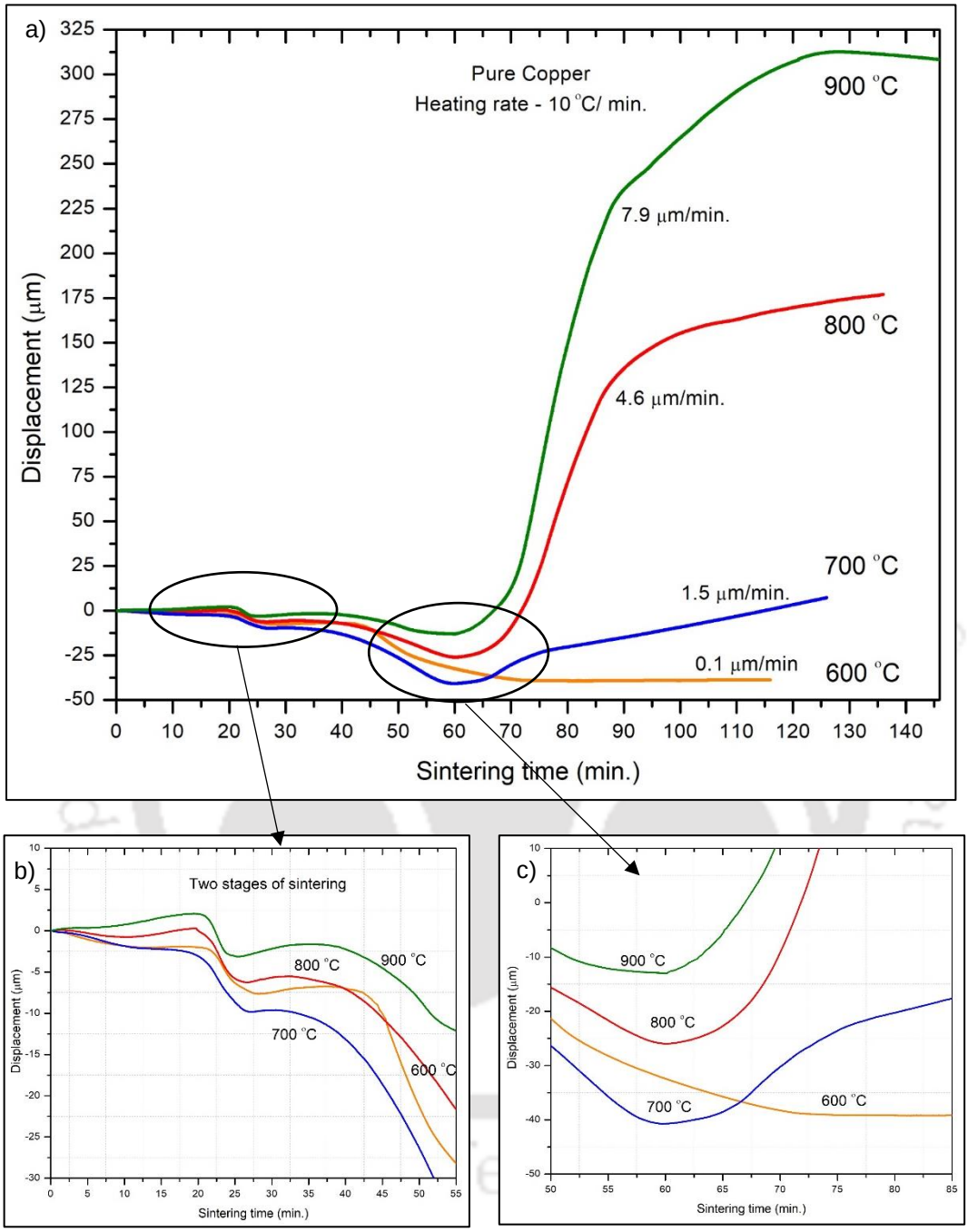

Figure 4.7 Influence of sintering temperature on copper a) overall sintering behaviour of copper against sintering time, b) two-stage sintering behaviour of copper, and c) transition region of diffusion-expansion zone of copper

Figure 4.7a shows the sintering behaviour of copper sample against sintering duration at different temperature. The sample is heated till the desired temperature at the heating rate of 10 ºC/min. and then it is maintained for 60 min., where a two-stage diffusion

process is observed for the copper sample irrespective of sintering temperature and it is clearly shown in **Figure 4.7b**. It is noted from **Figure 4.7c** that the diffusion of the sample is observed to be completed around 60 min. in case of 700, 800 and 900 ºC and 81 min. in case of 600 ºC sintering temperature. At any sintering temperature, the diffusion process of a test sample is continued till 650 ± 10 ºC and 61 ± 1 min. and then the sample is started to expand irrespective of sintering temperature except at 600 ºC sintered sample, where the diffusion process is observed to be continued till 81 min. It is noted that the thermal energy supplied till 600 ºC is sufficient enough to complete the diffusion process of the sample and it is expanded during its isothermal condition. It is noted that there is also no significant physical changes i.e. diffusion and expansion of grain boundaries during rest of the period of isothermal condition in case of 600 ºC sintered sample. The rate of expansion is observed to be the least at 600 ºC in comparison to that of rest of the sintering temperature considered in the present study. At 900 and 800 ºC, the pattern of sintering of pure copper during diffusion and expansion is observed to be very similar, where the rate of grain growth is found to be dominated after complete diffusion of the sample. It is also expected to have an irregular grain growth, which might be helpful to reduce the number and size of voids by filling the same during the growth of grains and it is also confirmed from the microstructural studies.

It is noted from **Figure 4.7b** that the first stage of sintering process is started at 210 ºC and completed at around 310 ºC. Then, the second stage of sintering is continued from 440 ºC onwards, where the final stage of complete diffusion of grain boundaries is progressed further. It is observed from **Figure 4.7c** that the rate of diffusion is noted to be 0.80, 0.92, 1.11 and 1.22 µm/min., at 600, 700, 800 and 900 ºC, respectively, and it is increased with sintering temperature. In addition, the time taken to have a complete diffusion of grain boundaries is observed to be not significantly varied in the temperature range of 700-900 ºC in comparison to that of 600 ºC sintering**.** It is clearly noted that the increase of sintering temperature from 600 to 900 ºC reduced the total diffusion time and it is observed to significantly influence the rate of diffusion and the rate of expansion, which is clearly depicted from **Figure 4.7**. In addition, it is expected to have the maximum and minimum size of grains, respectively, at 900 and 600 ºC sintering temperature, which are also confirmed through their microstructural analysis.

The diffusion process of copper is observed to follow two stages: 1) shrinkage occurs during the neck formation between two particles at the initial stage of sintering to the

maximum strain of 3%, Kang [2005]; 2) the grain boundary diffusion takes place at the intermediate stage, where the maximum shrinkage occurs. In addition to the above and the interaction between the particles, the voids present in the samples are being detached and isolated against each other. Thus, the shape of voids becomes irregular during the course of sintering due to grain growth. The size of grains is also found to be increased with temperature, where the driving force generated by sintering process during the grain boundary diffusion and pressure generated within the entrapped voids present along the grain boundaries become equal. It led to limit further shrinkage/densification process. Thus, the void isolation occurs during the sintering process of the sample; 3) During the second stage of sintering, the number of isolated voids is expected to be significantly reduced leading to increase the relative density of the samples. Among the above discussed 2 stages of diffusion process during the sintering, the removal of isolated voids or bringing the same from interior to surface level is one of the major challenging processes and the same might have assisted the grain growth upto some extent during the excessive sintering process leading to reduce the hardness of the sample. These above discussed phenomena on the sintering duration are well supported by Kang [2005].

4.3.2 Sintering behaviour of Cu/CNT composites

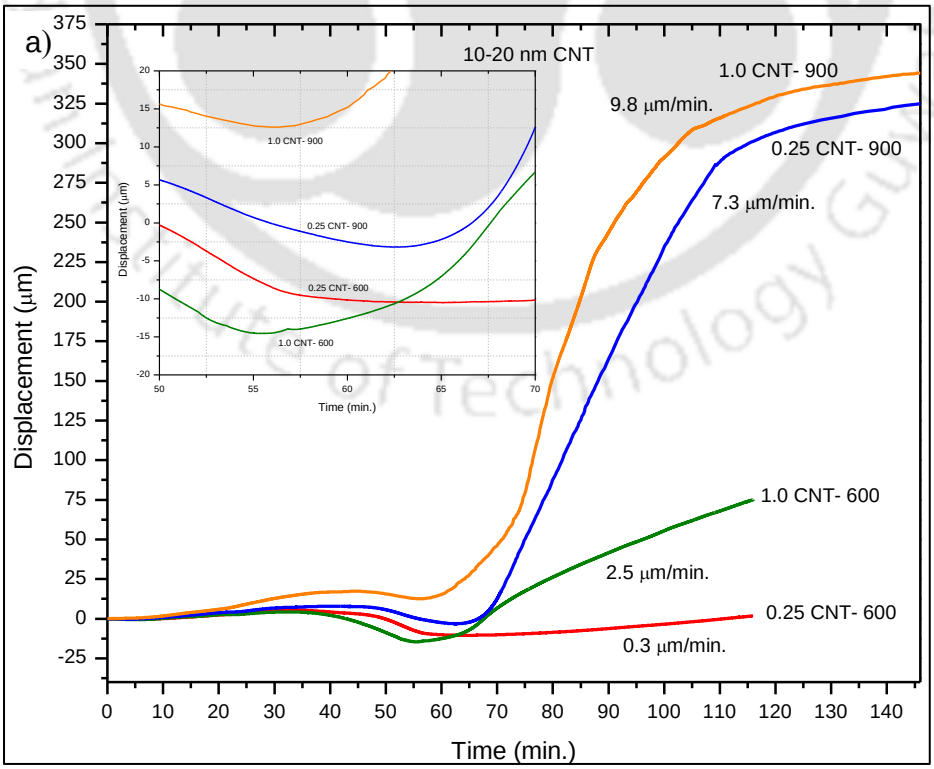

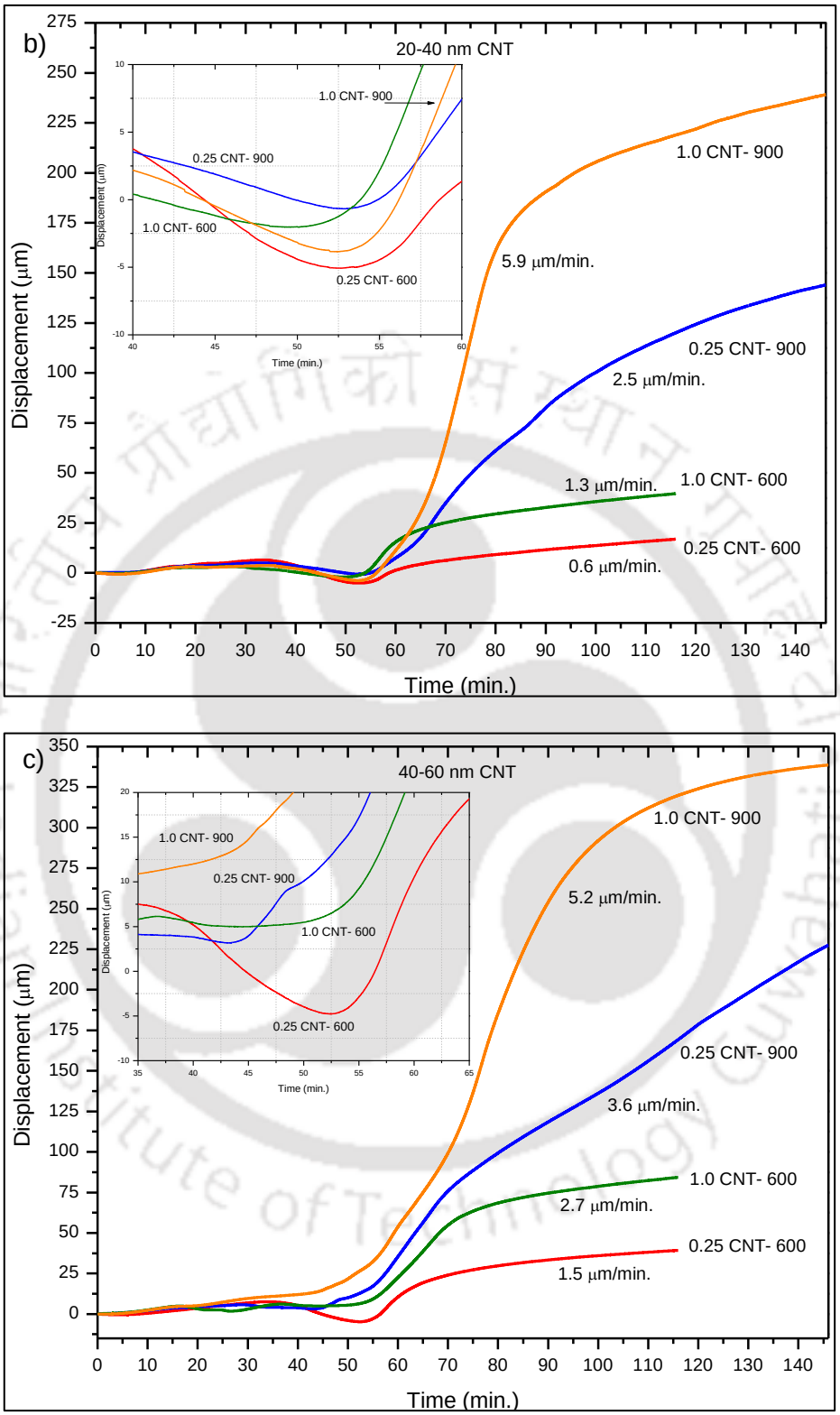

Figure 4.8 Sintering behaviour of Cu/CNT composites at 900 ºC and 600 ºC held for 60 min., a) 0.25 and 1.0wt.% of 10-20 nm , b) 0.25 and 1.0wt.% of 20-40 nm, and c) 0.25 and 1.0wt.% of 40-60 nm

Figures 4.8a, 4.8b and 4.8c show the sintering behaviour of 0.25 and 1wt.% CNT reinforced copper composites having 10-20 nm, 20-40 nm and 40-60 nm diameter CNT, respectively, where the composites are sintered at 600 and 900 ºC for 60 min. It is observed from **Figure 4.8a** that the diffusion process of 0.25wt.% CNT composites is completed at 65 min. and then the expansion is followed at a very slow rate of 0.3µm/min. at 600 ºC. In case of 1wt.% composites, the time required to have the complete diffusion is reduced to 56 min., which is followed by the expansion at 2.5 µm/min. At 600 ºC, the required diffusion time of 0.25 and 1wt.% CNT composites is reduced by 20 and 31%, respectively, in comparison to that of pure copper. In addition, the diffusion time required for 1wt.% composites at 600 ºC is reduced by 13% in comparison to that of 0.25wt.% composite sample. The rate of expansion of diffused grain at 0.25wt.% CNT composites is not found to be significant at 600 ºC in comparison to that of 900 ºC sintering temperature. The diffusion of sample at 0.25wt.% composites at 900 ºC is observed to be completed at 63 min. followed by drastic increase of rate of expansion of the sample. When the CNT concentration is increased from 0.25 to 1wt.% in the composites, the diffusion process at 900 ºC is completed at 57 min. and the expansion of composite is noted to be 9.8 µm/min. and their corresponding reduction of diffusion time and increase of expansion rate are reported to be 9 and 30% in comparison to that of 0.25wt.% composites. It is inferred that the addition of CNT increased the available surface area for the heat transfer in the Cu/CNT composite powder leading to reduce the sintering time irrespective of sintering temperature.

It is observed from **Figure 4.8b** that the diffusion of composite samples having 20-40 nm diameter CNT is completed at 53 ± 1 min. irrespective of CNT concentration and sintering temperature, which is observed to be reduced by 34 and 13% at 600 and 900 ºC, respectively, compared to that of pure copper. Once diffusion is completed, the sample sintered at 600 ºC is expanded at the rate of 0.6 and 1.3 µm/min. at 0.25 and 1.0wt.% CNT reinforced composites, respectively, and the corresponding values are increased to 2.5 and 5.9 µm/min. at 900 ºC sintering. The expansion of test samples is observed to be linearly increased after completing their diffusion process at 600 ºC sintering irrespective of CNT concentration. In addition, the rate of expansion of 20-40 nm diameter CNT based composites is observed to be decreased in comparison to that of 10-20 nm diameter CNT based composites corresponding to their respective concentration at 900 ºC. When the diameter of CNT is increased in the composites, it is observed to significantly influence the

rate of diffusion, rate of expansion and sintering duration at any desired sintering temperature.

It is observed from **Figure 4.8c** that the composite samples having 0.25 and 1wt.% of 40-60 nm diameter CNT completed their diffusion at 52 and 43 min. at 600 ºC, respectively. The rate of expansion of 1wt.% CNT composites is observed to be 1.8 times more in comparison to that of 0.25wt.% CNT composites at 600 ºC. In addition, the rate of expansion of 0.25wt.% composites is observed to be 1.5 and 3.6 µm/min., respectively, at 600 and 900 ºC. At 900 ºC, the time required to complete the diffusion of 0.25wt.% CNT composite is decreased by about 28% in comparison to that of copper. The rate of expansion is observed to be increased with sintering temperature and CNT concentration, where the maximum value is observed at 1wt.% of CNT composites and 900 ºC sintering irrespective of CNT diameter and the same is observed to be decreased with sintering temperature, and CNT concentration and increased with CNT diameter. These might be due to the presence of effective chemical bonding between Cu and CNT, which is assisted by the functional groups attached on the CNT. It is inferred that the presence of CNT and large amount of heat accelerated the diffusion process at higher sintering temperature and it reduced the expansion rate in comparison to that of pure copper. Unlike pure copper sample, the first-stage sintering is not observed at 250 ºC irrespective of CNT diameter and its concentration.

It is noted that only a single stage sintering process is observed in the composites irrespective of CNT diameter and its concentration. It could be due to the large surface area of CNT, which has controlled the rate of heat transfer, initial surface level diffusion process and the rate of diffusion. As the 40-60 nm diameter CNT has approximately 11 and 4 times more surface area, respectively, compared to that of 10-20 nm and 20-40 nm diameter CNT, it helped to reduce the corresponding time taken to have the complete diffusion at 900 ºC by 18.2 and 31.2% at 0.25wt.% and 14.4 and 21% at 1wt.% CNT. The sintering time required for 40-60 nm diameter CNT composites at 600 ºC is reduced by 2.4 and 19.8% at 0.25wt.% and 11.9 and 19.2% at 1wt.%, respectively, in comparison to that of 20-40 nm and 10-20 nm diameter CNT composites. The rate of expansion is increased with CNT diameter at 0.25wt.% and 600 ºC. Though the sintering behaviour of the composites is observed to be influenced by the sintering temperature, increase in surface area of CNT led to significantly reduce the sintering time required to have complete diffusion.

4.3.3 Analysis of diffusion time requirement of Cu/CNT composites

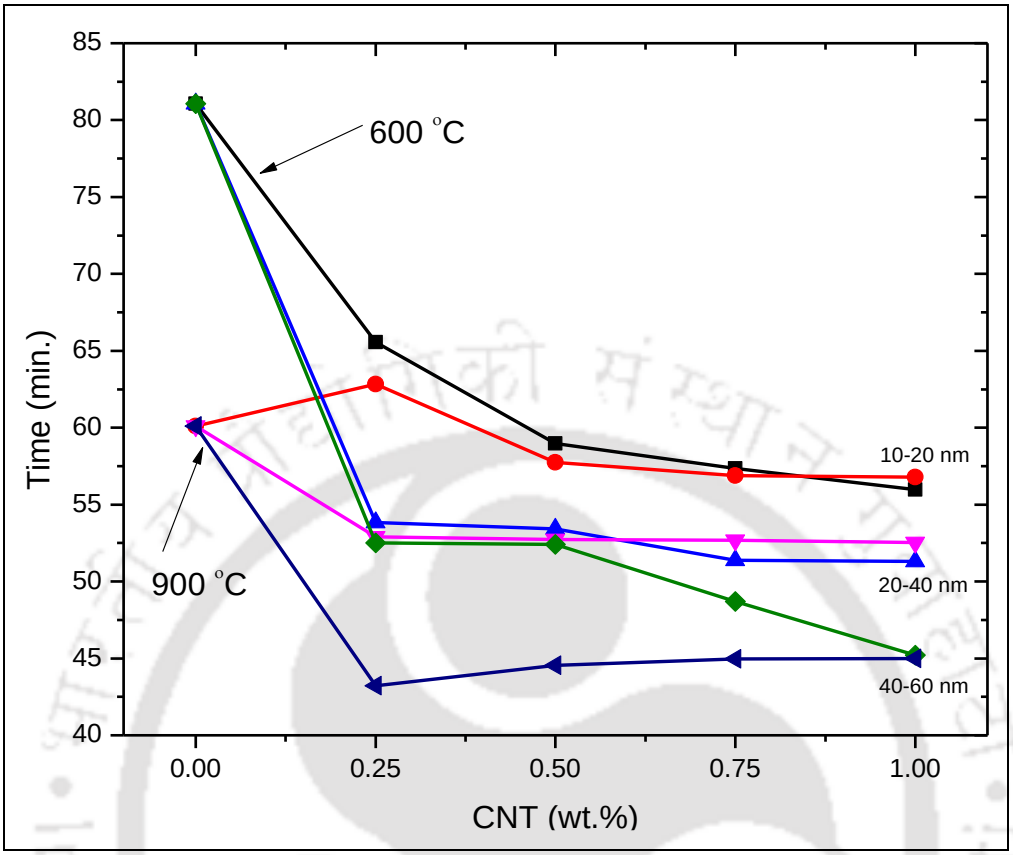

Figure 4.9 Diffusion time requirement of copper based composites against CNT diameter, its concentration and sintering temperature

Figure 4.9 shows the diffusion time requirement of test samples having different diameter of CNT against its concentration at 600 and 900 ºC. In case of pure copper, the rate of diffusion of grain boundaries is observed to be considerably influenced by the temperature, where the sample sintered at 600 ºC consumed about 81 min. in order to have a complete diffusion of grain boundaries, and it is reduced to 61 min. at 900 ºC corresponding to 26% reduction of diffusion time. In case of 20-40 nm and 10-20 nm diameter CNT based composites, the diffusion time is observed to be varied within ±1.5 min. corresponding to 5% deviation irrespective of sintering temperature and its concentration. In 40-60 nm diameter CNT composites, the maximum diffusion time is found to be reduced by 35 and 46% for 0.25 and 1.0wt.%, respectively, at 600 °C in comparison to that of pure copper. It is also noted that the diffusion time of 40-60 nm diameter CNT composites at 900 ºC is reduced by 8% till 0.75wt.% CNT composites and it is converged at 1wt.% CNT concentration in comparison to a sample sintered at 600 ºC. It is noticed that the diffusion time required for the composites having 20-40 nm diameter CNT at 600 ºC is reduced by

35% irrespective of CNT concentration in comparison to that of copper, whereas the 10-20 nm diameter CNT composites showed a significant reduction of diffusion time varying from 19 to 31% with an increase of CNT concentration. The composites sintered at 900 ºC showed about 5, 12 and 26% of reduction of diffusion time, respectively, for 10-20 nm, 20-40 nm and 40-60 nm diameter CNT composites irrespective of CNT concentration in comparison to that of pure copper. In general, it is observed that the addition of CNT irrespective of its diameter is found to have significant influence on reducing the diffusion time of composites in comparison to that of pure copper. Though the CNT diameter is found to have a great influence on the diffusion time of composites, its concentration is not found to have much impact on the same.

Based on the study, it is found that the Cu and Cu/CNT can be sintered at 600 °C for 60 min. However, sintering studies on the composites are also extended to 75 and 90 min. in order to study the influence of sintering duration on material behaviour.

4.3.4 Sintering mechanism of test samples

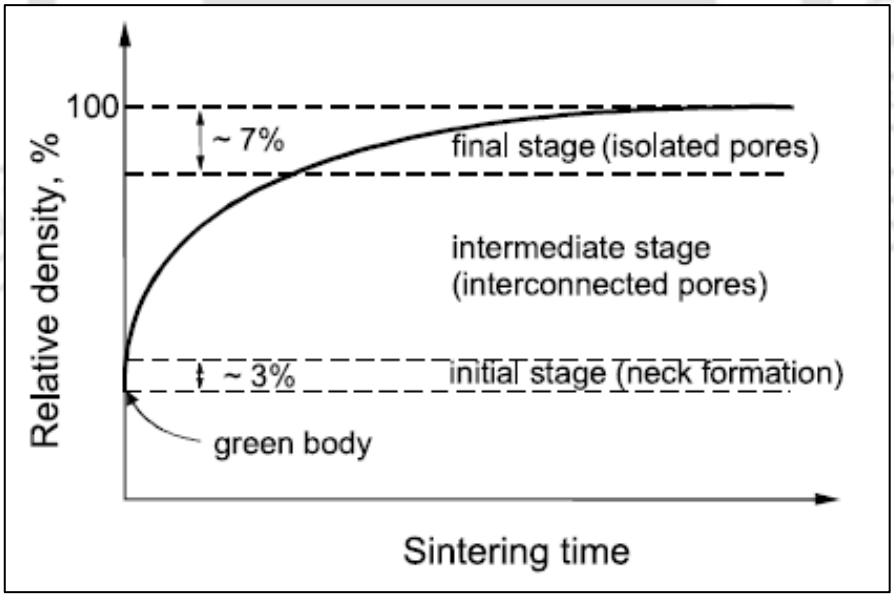

Figure 4.10 Different stages of densification of test samples against sintering duration, Kang [2005]

A schematic representation of different densification stages of a compressed sample during the sintering process against sintering duration is shown in **Figure 4.10**, Kang, [2005], and it is reported that the initial stage of sintering is limited to 3% enhancement of RD, where the neck formation is expected to occur between the grains. At an intermediate stage, the maximum diffusion of grain boundaries is found to occur and the RD is increased

up to 93% and it is followed by final stage of sintering, where the isolated pores are noticed apart from increasing the RD in order to obtain the maximum possible RD of the sample. It is assumed that (i) the particles are uniform in size; (ii) the pores are evenly distributed and thus, the densification and shrinkage of the compacted samples are observed to occur uniformly throughout the sample.

In Cu/CNT composites, it is noted that the dimensional change of the composites at the neck formation zone is observed to be in the range of 1.9 to 10.7 μm for all types of CNT concentration and its size. Thus, the change in density of any sample is expected to be insignificant for the composites. At an intermediate stage, the diffusion of grain boundaries of composites are observed to be similar in comparison to that of pure copper. However, the closure of interconnected and isolated pores are expected to delay the grain boundary diffusion due to the restriction created by CNT and the entrapped pores present within grain boundaries, which might increase the sintering time in order to achieve the maximum possible density of the composites. In the present study, densification of composites is found to be saturated after 60 min. of sintering beyond which expansion of grain is noticed.

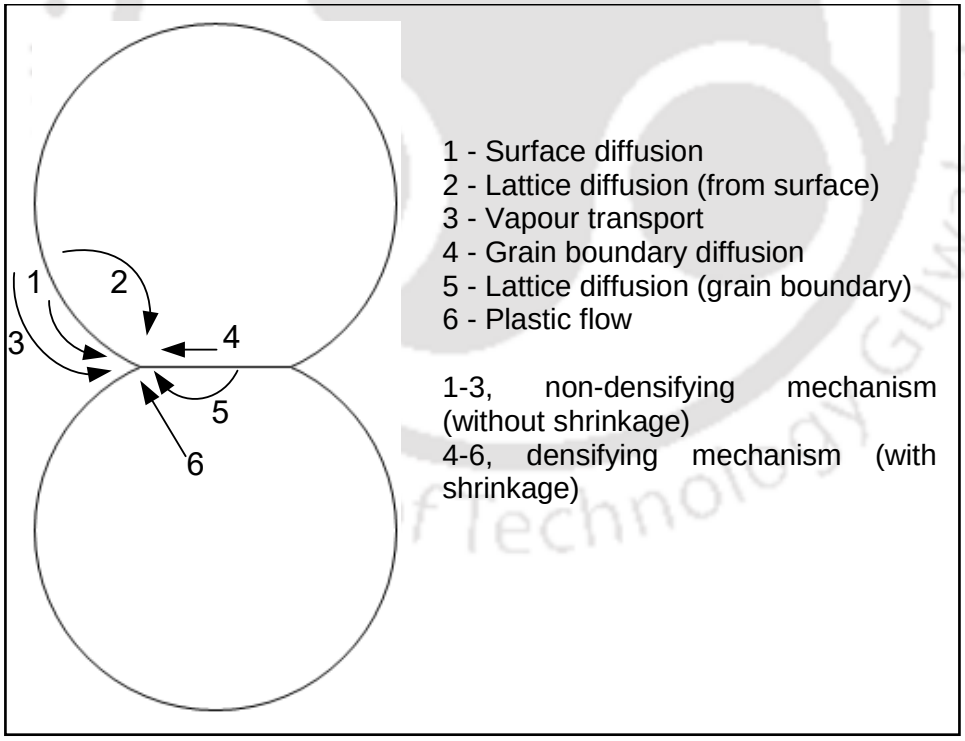

Figure 4.11 A schematic representation of a two-particle model, Zak Fang [2010]

Figure 4.11 shows the sintering mechanism of a two-particle model and the path of suggested mechanism. It is reported that the sintering of grains is found to follow different

mechanisms namely, surface diffusion, lattice diffusion from surface, vapour transport, grain boundary diffusion, lattice diffusion from grain boundary and plastic flow, where the former 3 mechanisms contributed to non-densification process without any shrinkage, whereas the later 3 mechanisms led to densification process with shrinkage of grains. It is noted that the non-densification mechanism assisted to have neck formation leading to have neck growth and coarsening of particles without any shrinkage effect. The later is found to reduce the available driving energy and increase the distance between the grain boundaries during the diffusion process and thus, it led to have reduced densification during the sintering process. In case of densifying mechanism, the plastic flow around the neck region caused the growth of neck leading to have significant shrinkage, which contributed to have maximum densification of sintered products. It is also noted that the grain boundary diffusion is the important mechanism in the metallic materials, where the plastic flow during the sintering is expected to occur at an initial stage of sintering and the densification noticed during this stage is expected to be within 3%, as reported by Kang [2005]. Due to the presence of grain boundaries in a polycrystalline phase, the driving energy is expected to be decreased due to the reduction of free surface area and its contribution to grain growth led to reduce the progress of densification. In addition, the size of void and its shape are changed due to the grain boundary diffusion, and these effects decreased the densification process during the sintering process.

In the present study, the copper sample is observed to have the maximum strain of 1% during the initial stage of sintering process irrespective of sintering temperature. The enhanced densification of copper sample at 600 °C is due to the fact that the energy supplied during the sintering process at 10 °C/min. till 600 °C is noted to be sufficient enough to have complete grain boundary diffusion without immediate grain growth and thus, it is found to reduce the number of voids present in the sintered sample. However, the effect generated over the sample during the compaction process is expected to limit the maximum achievable density. When the sintering temperature is increased to 700 °C and above, the excess heat supplied beyond the sintering process assists to have non-uniform grain boundary diffusion and possible expansion of them. In addition, the continuous supply of heat over the sample beyond the desired requirements of sintering helped to form irregular grains and these boundaries led to generate more number of voids leading to decrease the relative density of the sample.

It is also noted that the size of grain is found to be in different ranges under the experimental conditions and these grains are expected to rearrange themselves during the compaction process leading to have randomly distributed and different sizes of voids in the compacted samples. It is also noticed that the rearrangement of copper grains and their attraction among them led to solid state sintering even at low temperature. During the sintering process, diffusion among grain boundaries is occurred and it is expected to reduce the size and number of voids in comparison to that of green compacts. Due to irregular grain size and its rearrangement among themselves happening during the compaction process, the region between grain boundary to neck is noted to be non-uniform, where more flow of material is expected to reduce the radius of curvature during the sintering process. By doing the parametric studies along with processing variables, the number and sizes of voids could be reduced. In some cases, a non-uniform dense sample is obtained due to the presence of irregular voids leading to have reduced RD. As the distribution of different size of grains is expected to play an important role in the sintering process to get the desired RD and other characteristics, different processing techniques and variables are followed in the present study.

4.4 Relative density of Cu/CNT composites obtained through different processing techniques

In order to study the quality of sintered products of pure copper and Cu/CNT composites, the relative density of test samples is calculated using their actual and theoretical density, where the experimental values are obtained as per Archimedes' principle and the theoretical density is calculated using the rule of mixtures. This section discusses about the relative density of Cu/CNT composites obtained from the different processing techniques in order to study the influence of CNT size and its concentration, compaction technique, and sintering techniques on the same.

4.4.1 Relative density of Cu/CNT composites processed through uniaxial compaction and conventional sintering

4.4.1.1 Relative density of Cu/CNT composites against CNT type

The following section discusses about the RD of Cu and Cu/CNT composites obtained at different sintering duration against different CNT diameter.

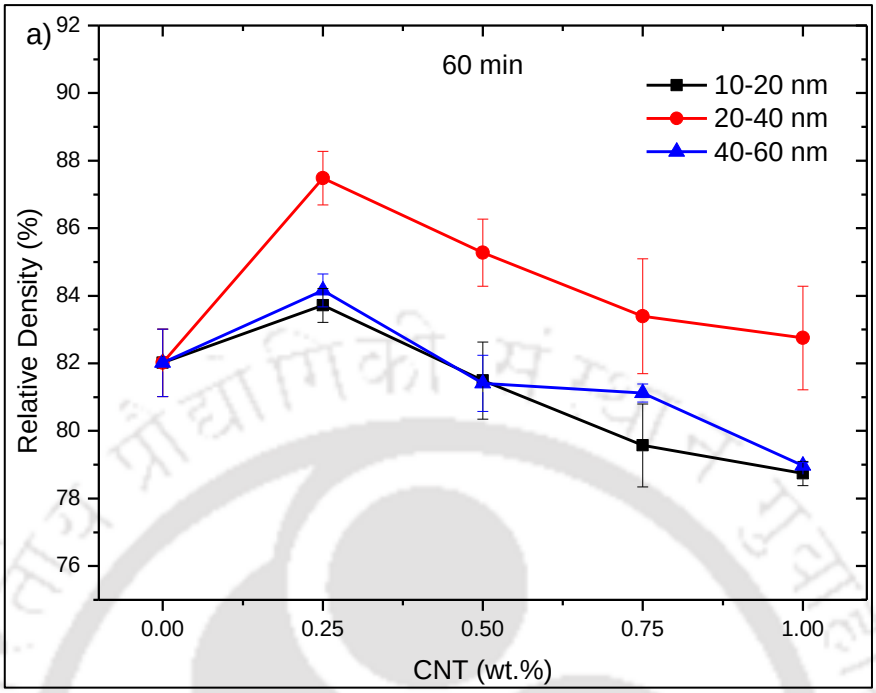

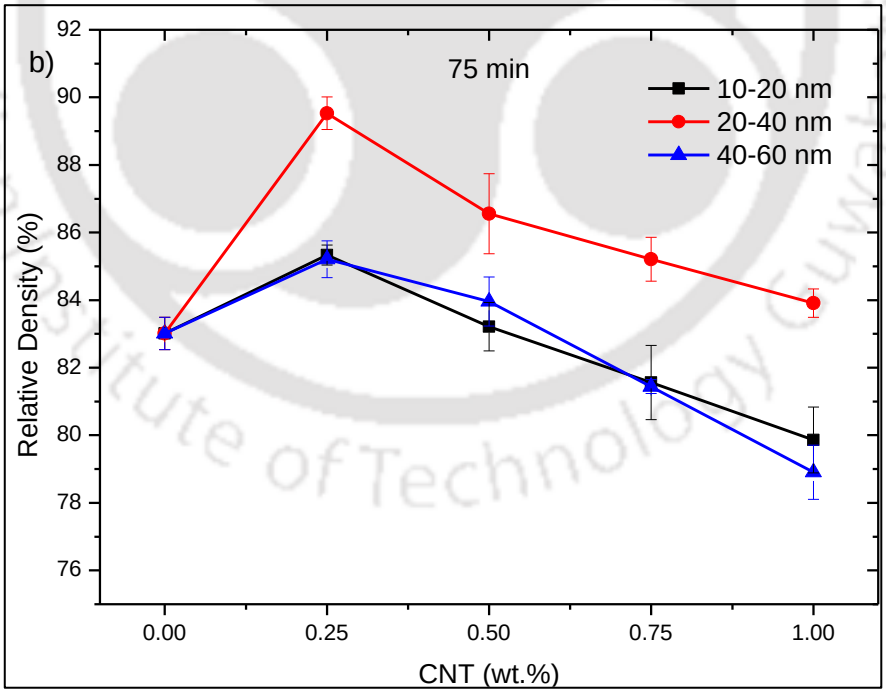

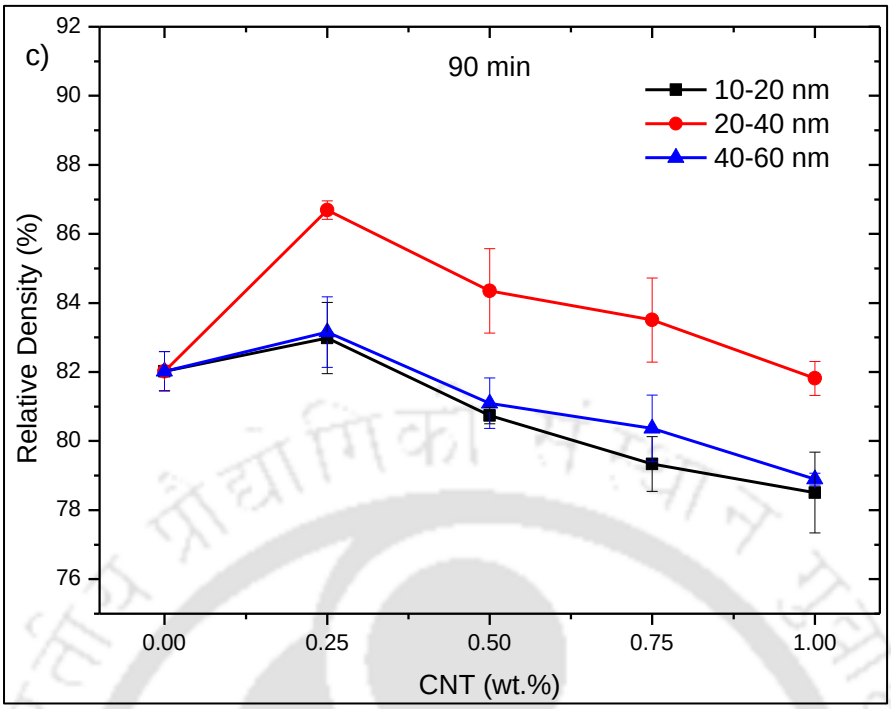

Figure 4.12 Relative density of UA-CS processed Cu/CNT composites having 10-20 nm, 20-40 nm and 40-60 nm diameter CNT sintered at 600 ℃ for a) 60 min., b) 75 min. and c) 90 min.

Figures 4.12a, b and c show the relative density (RD) of Cu/CNT composites having 40-60 nm, 20-40 nm and 10-20 nm diameter CNT, which are sintered at 600 ºC for 60, 75 and 90 min., resepctively. It is noted from **Figure 4.12a** that the maximum RD is observed to be 82% and 87.5% for pure copper and its composite having 0.25wt.% of 20-40 nm diameter CNT, respectively at 60 min. of sintering. It is also noted that the RD of 20-40 nm CNT reinforced composites showed significant enhancement in comparison to that of 10-20 nm and 40-60 nm diameter CNT reinforced composites. Irrespective of diameter of CNT, the composites having 0.25wt.% CNT showed the highest RD and then it is started to decrease with an increase of CNT concentration. Beyond 0.25wt.% CNT concentration, the RD of 10-20 nm and 40-60 nm CNT reinforced composites is observed to be lower than that of pure copper. From 0.5wt.% onwards, the RD of 20-40 nm CNT composites is not significantly varied and the results are found to be within the limit of experimental deviation. The lowest RD is observed to be 78.7% at 1wt.% of 10-20 nm CNT composites. Except 20-40 nm diameter CNT reinforced composites, the RD of rest of the composites is not affected by different sizes of CNT and its concentration.

It is observed from **Figure 4.12b** that the maximum and minimum RD of 75 min. sintered composites is observed to be 89.5% at 0.25wt.% of 20-40 nm diameter CNT and 79% at 1.0 wt.% of 40-60 nm diameter CNT composites, respectively. It is also noted that the RD of 20-40 nm diameter CNT composites showed significant improvement in comparison to that of 60 min. of sintering time. The results observed in case of 10-20 nm and 40-60 nm CNT reinforced composites are found to be within the limit of experimental deviation. It is inferred that the desired characteristics of the composites are expected to be the highest at 0.25wt.% CNT due to its improved RD irrespective of CNT diameter. It is observed from **Figure 4.12c** that the RD of composites is observed to be 82.9, 86.7 and 83.2% for 10-20 nm, 20-40 nm and 40-60 nm reinforced composites, respectively at 0.25wt.% for 90 min. of sintering time and the RD of pure copper is noted to be 82%. The RD of composites is observed to be decreased beyond 0.25wt.% of CNT irrespective of its diameter. It is also observed that the RD of 20-40 nm diameter CNT composites sintered at 90 min. is found to be the lowest in comparison to that of 60 and 75 min. sintered sample irrespective of CNT concentration. It is inferred that the CNT diameter considered in the present study is not found to dominate the RD of composites except for 20-40 nm diameter CNT.

4.4.1.2 Relative density of Cu/CNT composites against sintering duration

The following section discusses about the RD of Cu and Cu/CNT composites having different diameter of CNT and its concentration obtained against different sintering duration.

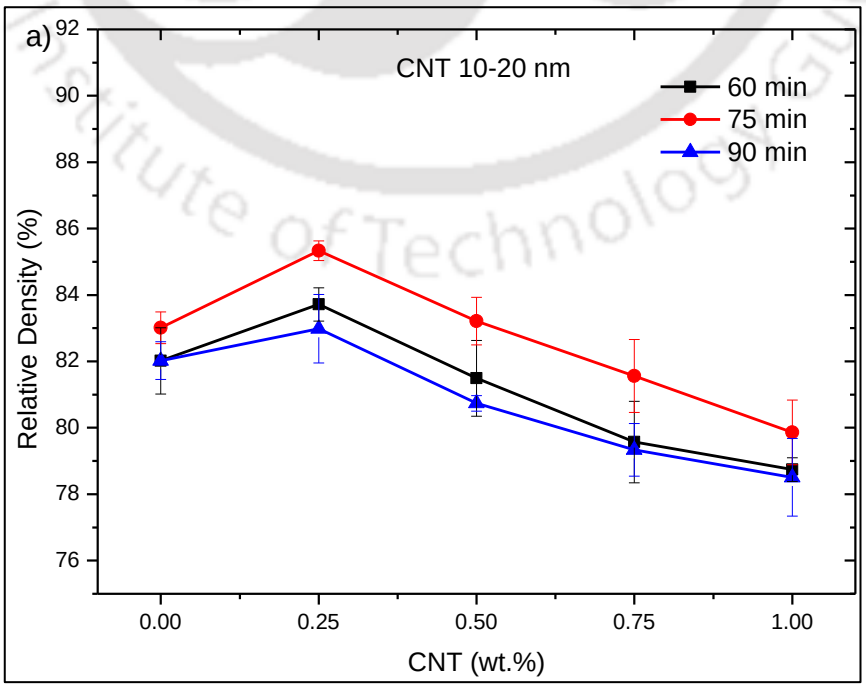

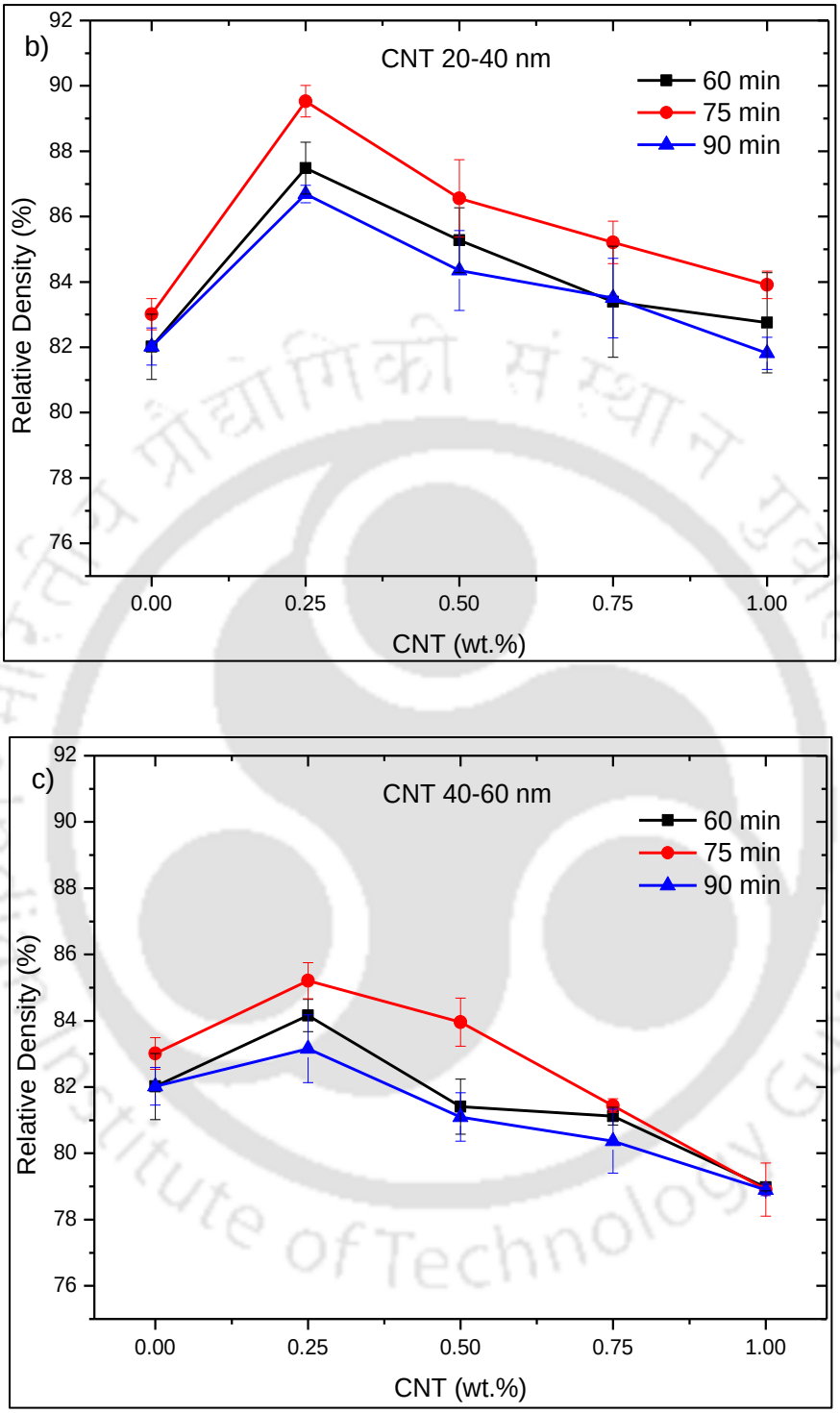

Figure 4.13 Relative density of UA-CS processed Cu/CNT composites having a) 10-20 nm, b) 20-40 nm, and c) 40-60 nm diameter CNT reinforcement against different sintering time

Figure 4.13 shows the influence of sintering time on the RD of copper and CNT composites having all types of CNT and its concentration. It is observed from **Figure 4.13a**

that the composites having 0.25wt.% of 10-20 nm diameter CNT showed the maximum RD of 85.3% at 75 min. of sintering. It is also observed that the sample sintered at 90 min. showed the lowest RD in comparison to that of 60 min. sintered sample. In general, the RD of composites is observed to have the reduced RD in comparison to that of pure copper except for 0.25wt.% content irrespective of sintering time. It is also observed that the RD of composites having 0.75 and 1wt.% is found to be within its experimental deviation at 60 and 90 min. of sintering time. It is observed from **Figure 4.13b** that the 0.25wt.% of 20-40 nm diameter CNT reinforced composites showed the maximum RD at 75 min. of sintering time. It is also observed that the RD of 75 min. sintered composites is found to have a similar trend in comparison to that of 90 min. of sintering time and it is found to be decreased after 75 min. of sintering time. It is also observed that the RD of composites is noted to be improved upto 0.75wt.% in comparison to that of pure copper irrespective of sintering time. At 90 min. of sintering time, the RD of composites at 1wt.% CNT is found to be within the limit of experimental deviation as that of pure copper. It is noticed that the 20-40 nm CNT size showed better relative density in comparison to that of 10-20 nm CNT size at 75 min. of sintering time. It is depicted from **Figure 4.13c** that the maximum RD is observed to be 85% at 0.25wt.% of 40-60 nm CNT composites after 75 min. of sintering time. Beyond 0.75wt.% content, the RD of composites is observed to be converged irrespective of sintering duration. It is also observed that the RD of composites showed a similar trend irrespective of CNT concentration at 75 and 90 min. of sintering time. In addition, the RD of 40-60 nm and 10-20 nm diameter CNT composites showed a similar trend at 75 min. of sintering time, where the lowest RD of the composites is observed to be 79% at 1wt.% CNT concentration for 40-60 nm diameter CNT in comparison to that of 10-20 nm and 20-40 nm diameter CNT composites at the same CNT concentration. It is inferred that the sintering time is not significantly influenced the relative density of the composites having 40-60 nm CNT size.

The reasoning for the above discussed observation on the RD of copper and Cu/CNT composites processed through UA-CS technique is discussed below: the heat generated during the uniaxial compaction process due to the presence of friction among the particles caused by their rearrangement is expected to induce cohesion among the powder surfaces leading to have surface diffusion, Kang [2005]. During the uniaxial compaction (UA), the compaction pressure is limited within the impacting zone or threshold level and not able to transfer the pressure through entire thickness of the sample along the longitudinal axis leading to have reduced RD. In addition, the conventional sintering process is carried at

normal atmospheric pressure (pressure-less) under protective environment, which might not have assisted to remove the entrapped air generated during the compaction process leading to retain different sizes of voids. These are observed and reported from microstructural studies, and it caused to decrease the RD of the sample. In case of conventional sintering process, the heat is generated by heating coils and transmitted to the samples via radiation, conduction and convection, where the heat transfer phenomenon from surface to core is expected to be strongly influenced by the quality of the samples or defects present in the sample and it will be reflected in the final sintered products, Yadoji *et al*. [2003]. During the sintering, the movement of grains is very much limited, and they are not allowed to rearrange among themselves. Under such condition, the sintering process might not have complete diffusion and produced voids in the sample and thus, it reduced the RD of the sample.

The lowest RD obtained for 40-60 nm diameter CNT composites irrespective of sintering duration in comparison to other types of CNT composites might be due to the fact that the presence of copper inside the CNT and coating over the CNT through its functionalized sites significantly restricted the grain growth of copper during the sintering process in order to fill the voids. The copper ions attached to the functional groups of CNT and considerable filling within the tubular structure of CNT are expected to restrict the flowability of composite powder and its rearrangement during the uniaxial compaction. The dominance of above factors is high at larger diameter of CNT and its concentration due to significant increase of its surface area and volume. Moreover, the CNT is expected to absorb maximum part of compaction pressure due to its high Young's modulus, which reduced the intensity of compaction process. It led to least proportion of force being used to compact the powder causing the increased number of voids and their sizes. Thus, the composites are expected to have a large number of different sizes of voids at higher concentration of CNT and its diameter leading to reduce the RD of composites, which is also confirmed through their microstructural studies. The dominance of above discussed effects is increased from 0.5wt.% CNT onwards and reached their maximum at 1wt.% CNT irrespective of its diameter leading to decrease the RD of composites. The improved RD of composites is observed at 0.25 wt.% CNT along with dense microstructure due to the presence of lower concentration of CNT.

In case of 20-40 nm and 10-20 nm diameter CNT composites, the quantity of Cu filled and coated over the CNT is expected to be about 60 and 30 %, respectively, in comparison to that of 40-60 nm diameter CNT composites and thus it provides good

flexibility and rearrangement of the composite powder during its compaction leading to increase the RD of composites at 0.25wt.% CNT after the sintering process. Though the flexibility of 10-20 nm diameter CNT composites is not restricted by the presence of copper during the compaction process, the existence of non-straightness and randomness of CNT due to its high aspect ratio, 666 in this case, and reduced diameter of CNT could have formed more number of kinks and bends, Chu *et al*. [2010a]. It is also confirmed from their microstructural studies through TEM, leading to produce a significant number of voids with different sizes causing the reduction of RD of composites. The intensity of above discussed phenomena is increased significantly at a higher concentration of CNT and thus, the RD of composites is decreased with an increase of CNT concentration beyond 0.25wt.%.

Since the maximum RD of composites is achieved at 75 min. of sintering irrespective of CNT diameter, it indicated that the number of voids and their sizes formed during the compaction process within the grain boundaries are reduced due to grain growth occurred during the sintering process. Though the samples sintered at 90 min. are expected to have the highest grain growth, the internal pressure exerted by the voids against the grain growth might be higher than the pressure generated during the grain growth leading to retain the number of voids generated during the compaction process. Thus, there is less number of grain diffusion during the sintering process leading to have reduced the RD of composites. Due to increased interaction between CNT and copper at 1wt.%, the CNT is expected to restrict the movement of grain growth and thus, it led to reduce the RD of Cu/CNT composites irrespective of CNT diameter.

4.4.2 Relative density of Cu/CNT composites processed through uniaxial compaction and microwave sintering

4.4.2.1 Relative density of Cu/CNT composites against CNT type

The following section discusses about the RD of Cu and Cu/CNT composites obtained at different sintering duration against different CNT diameter.

Figure 4.14 shows the RD of Cu and Cu/CNT composites having the CNT diameter of 10-20 nm, 20-40 nm and 40-60 nm processed through uniaxial compaction and microwave sintering against CNT concentrations, where the samples are sintered at 600°C for the duration of 60, 75 and 90 min. In general, it is observed that the RD of 20-40 nm diameter CNT composites is found to be the highest as compared to that of 10-20 nm and 40-60 nm diameter CNT composites at any concentration of reinforcement and sintering

duration reported in the present study. It is also noted that the maximum RD of Cu/CNT composites is achieved at 0.25wt.% of CNT irrespective of its diameter and sintering duration and then it began to decrease against increase in the concentration of CNT.

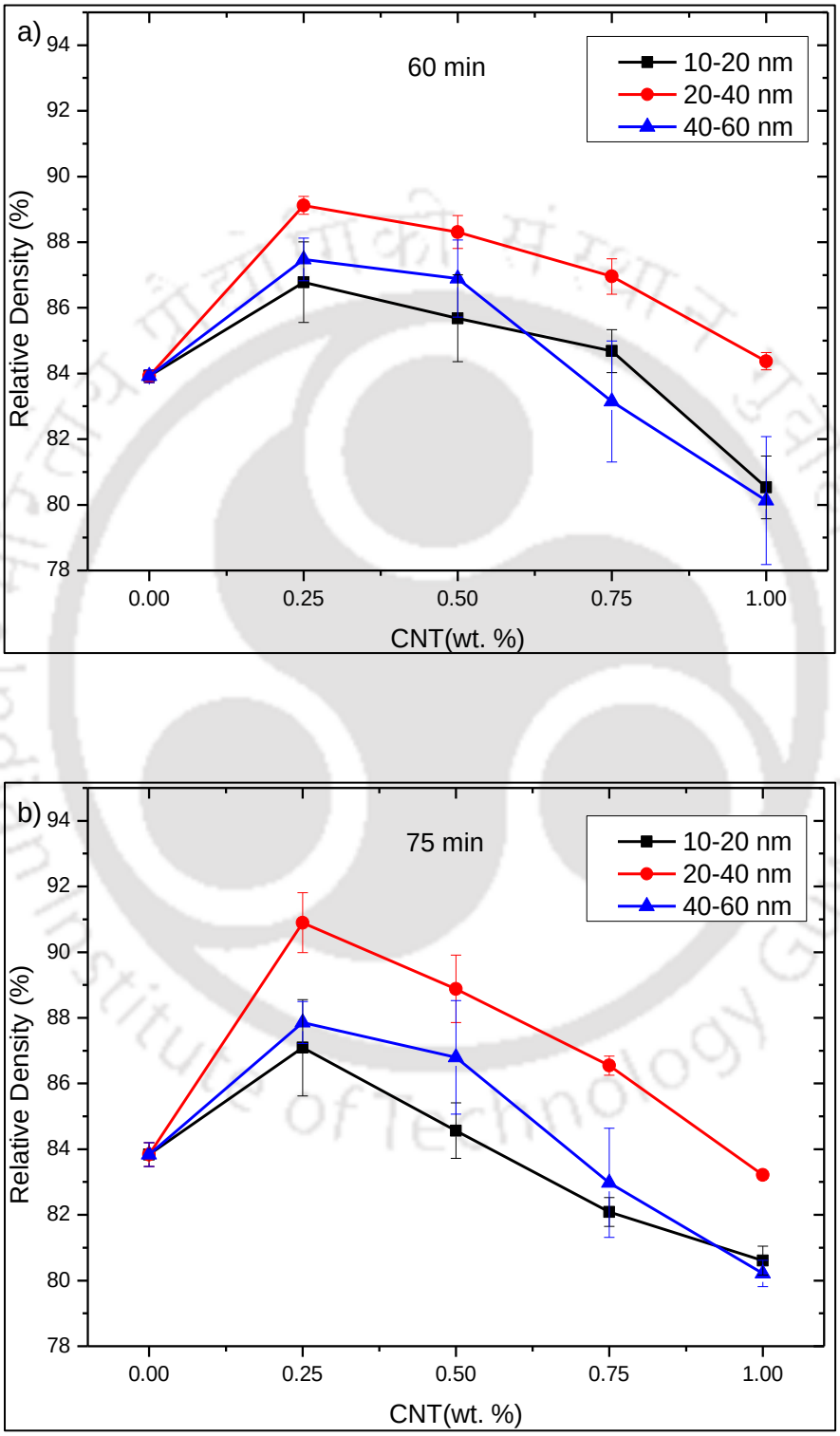

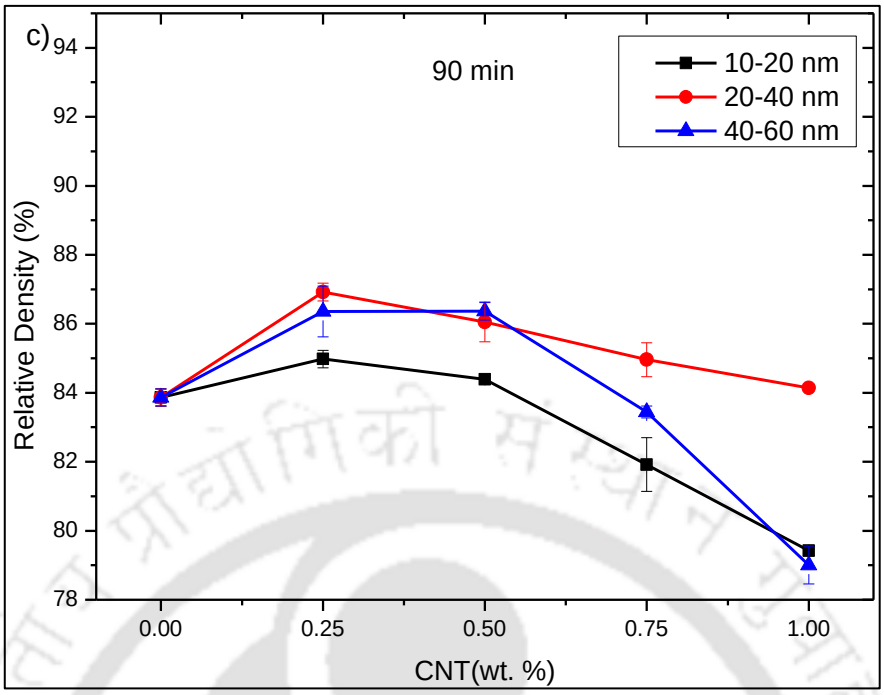

Figure 4.14 Relative density of UA-MW processed Cu/CNT composites having 10-20 nm, 20-40 nm and 40-60 nm diameter CNT sintered at 600 ℃ for a) 60 min., b) 75 min. and c) 90 min.

Figure 4.14a shows the RD of all types of composites sintered at 60 min., where the maximum RD of pure copper is observed to be about 83.9 % and it is increased to 89.1% at 0.25wt.% of 20-40 nm CNT reinforcement. The RD of copper is observed to be increased with reinforcement of CNT and the enhancement is reduced at 40-60 nm diameter CNT composites in comparison to that of 20-40 nm diameter CNT reinforced composites irrespective of reinforcement concentration. When the CNT concentration is increased beyond 0.25wt.%, the composites having 10-20 nm and 40-60 nm diameter CNT at 0.5wt.% showed approximately the same RD of composites as that of 0.25wt.% CNT and then it is reduced beyond 0.5wt.% and converged at 1wt.% CNT, where the RD is not found to be influenced against CNT size.

Figures 4.14b and **4.14c** show the RD of copper and Cu/CNT composites sintered at 600°C for 75 min. and 90 min., respectively. It is observed from **Figure 4.14b** that the maximum RD of composites is observed to be 90.9% for 20-40 nm diameter CNT at 0.25 wt.% after 75 min. of sintering. It is also observed that the 10-20 nm and 40-60 nm diameter CNT reinforced composites showed the reduced RD in comparison to that of pure copper beyond 0.75wt.% CNT and converged, where significant influence of CNT diameter is not

observed. It is observed from **Figure 4.14c** that the maximum RD of 86.9% is observed for 0.25 wt.% of 20-40 nm diameter CNT composites at 90 min. of sintering. In all cases, the RD of composites obtained after 90 min. of sintering is the lowest in comparison to that of the samples sintered at 60 and 75 min. The RD of 0.25 and 0.5wt.% of 10-20 nm and 40-60 nm diameter CNT reinforced composites is observed to be approximately 2-3% higher than that of pure copper and it is reduced and converged beyond 0.5wt.% CNT. However, the 20-40 nm diameter CNT composites retained their improvement of RD in comparison to that of pure copper till 1wt.% irrespective of sintering duration used in the present study.

4.4.2.2 Relative density of Cu/CNT composites against sintering duration

The following section discusses about the RD of Cu and Cu/CNT composites having different diameter of CNT and its concentration obtained against different sintering duration.

An influence of sintering time and concentration of CNT on RD of copper is shown in **Figures 4.15a-c** for the different diameter of CNT. In general, it is observed that the maximum RD is obtained at Cu- 0.25wt.% CNT composites irrespective of sintering time and diameter of CNT. The RD of composites is observed to be decreased with an increase of CNT concentration beyond 0.25wt.%. In case of 1wt.% of any CNT diameter, the RD of composites is found to have no influence on sintering time. The RD of composites obtained at 90 min. of sintering is observed to be the lowest in comparison to that of rest of the samples. In addition, there is no significant influence of the RD of copper against different sintering duration. It is observed from **Figure 4.15a** that the maximum RD of 87.1% is obtained at 0.25wt.% of 10-20 nm diameter CNT reinforced copper after 75 min. of sintering. It is also observed that the RD of composites is increased with sintering time up to 75 min. irrespective of CNT diameter and then it is decreased, and the lowest RD of 79.4% is observed at 1.0wt.% CNT and 90 min. of sintering. The average enhancement of RD of composites at 0.25wt.% CNT and 75 min. of sintering is observed to be in the range of 3% in comparison to that of copper. Moreover, there is no significant influence of 60 and 90 min. of sintering on RD of composites beyond 0.25wt.% CNT reinforcement, where the RD of composites is observed to be converged and it is lower than that of pure copper at 0.75 and 1wt.% of CNT.

Figure 4.15b shows the RD of 20-40 nm diameter CNT composites against different sintering duration, and the maximum RD of 90.9% is observed at 0.25wt.% CNT and 75 min. of sintering, where the influence of different sintering time is well distinguished unlike

10-20 nm and 40-60 nm diameter CNT composites. Beyond 0.25wt.% CNT, the RD of composites is observed to converge irrespective of sintering duration.

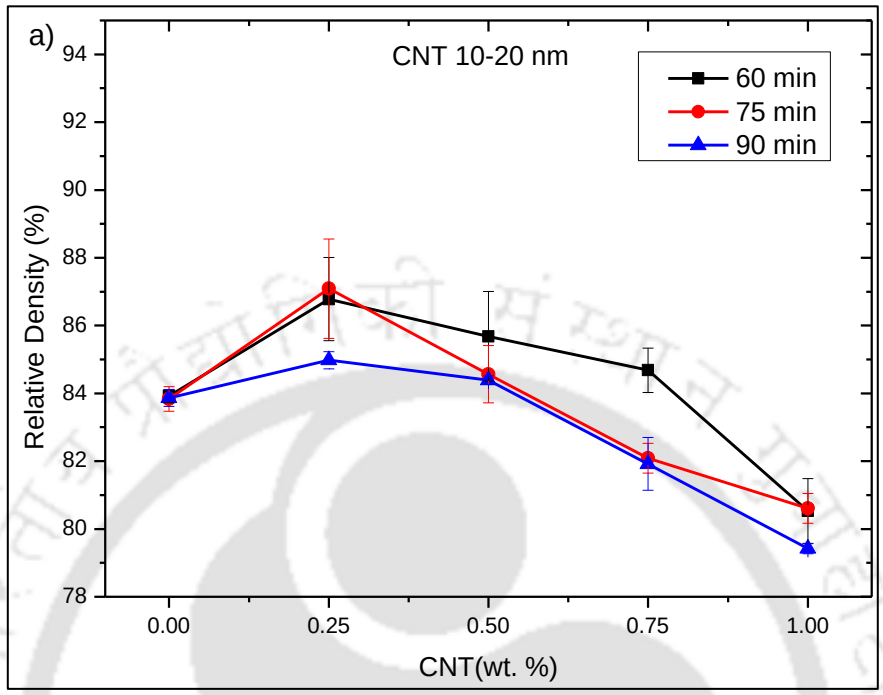

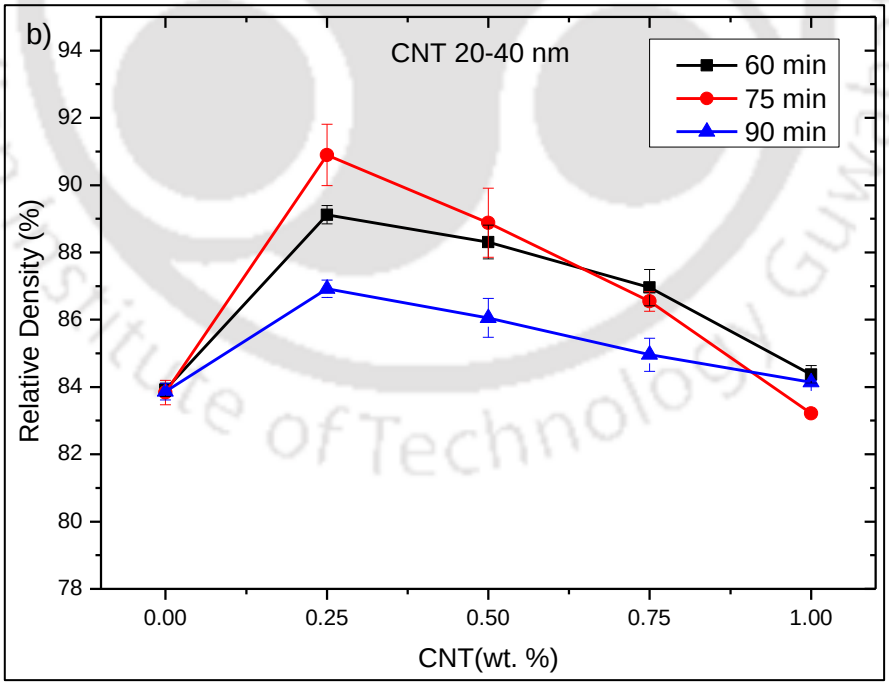

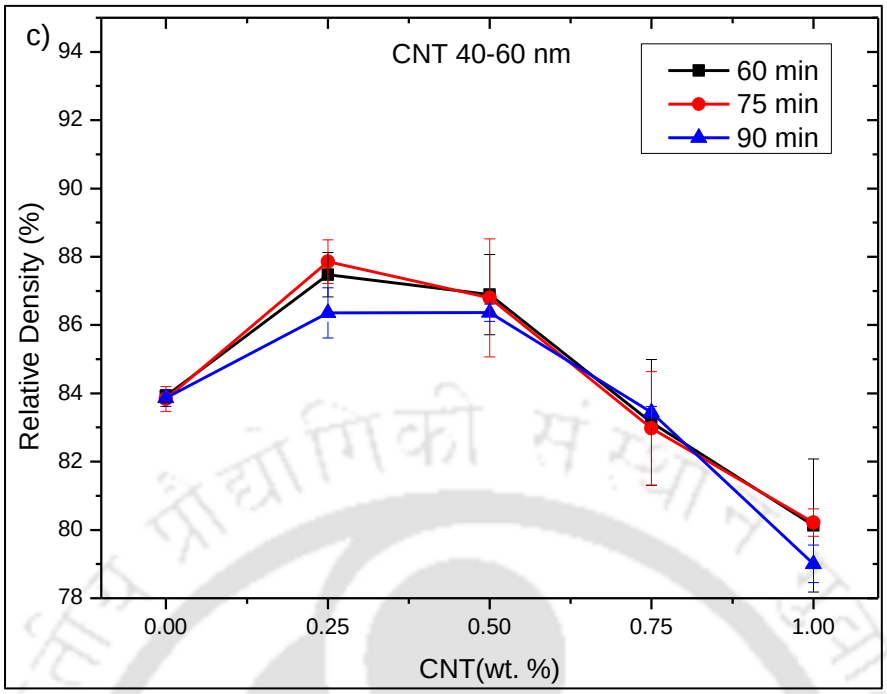

Figure 4.15 Relative density of UA-MW processed Cu/CNT composites having a) 10-20 nm, b) 20-40 nm, and c) 40-60 nm diameter CNT reinforcement against different sintering time

It is observed from **Figure 4.15c** that the RD of 40-60 nm diameter CNT reinforced composites is not found to be influenced by the sintering duration and CNT concentration except at 0.25wt.% CNT. It is also observed that the RD of composites is reduced beyond 0.5wt.% CNT in comparison to that of copper. It is noted that the RD of 1wt.% of 40-60 nm diameter Cu/CNT composites is observed to be 79% at 90 min. of sintering and it is the lowest RD in comparison to that of 20-40 nm and 10-20 nm diameter CNT composites irrespective of sintering duration and CNT concentration.

Apart from the previous discussion made on RD of UA-CS processed Cu and Cu/CNT composites, the effect of microwave sintering is found to be very much significant in comparison to that of conventionally sintered samples. The microwave energy is absorbed by the samples due to its penetration across the same leading to have volumetric heating, where the presence of varying heat from core to surface is eliminated by using a susceptor and insulation around the sample, as supported by Rajkumar and Aravindan [2009] and thus, the RD of UA-MW processed composites is observed to be improved in comparison to that of UA-CS processed composites irrespective of CNT size and its concentration.

4.4.3 Relative density of Cu/CNT composites processed through cold isostatic pressing and microwave sintering

4.4.3.1 Relative density of Cu/CNT composites against CNT type

The following section discusses about the RD of Cu and Cu/CNT composites obtained at different sintering duration against different CNT diameter.

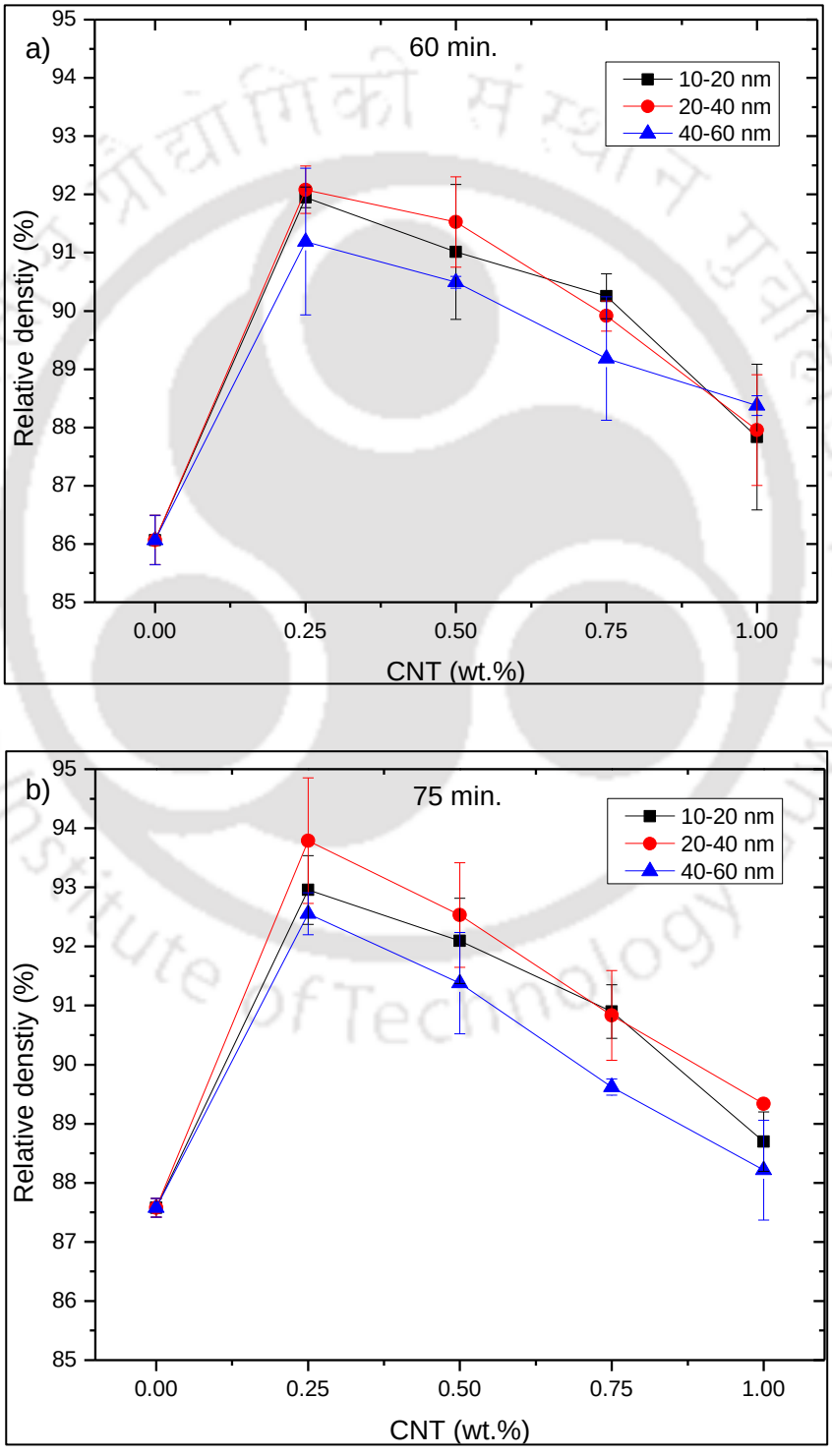

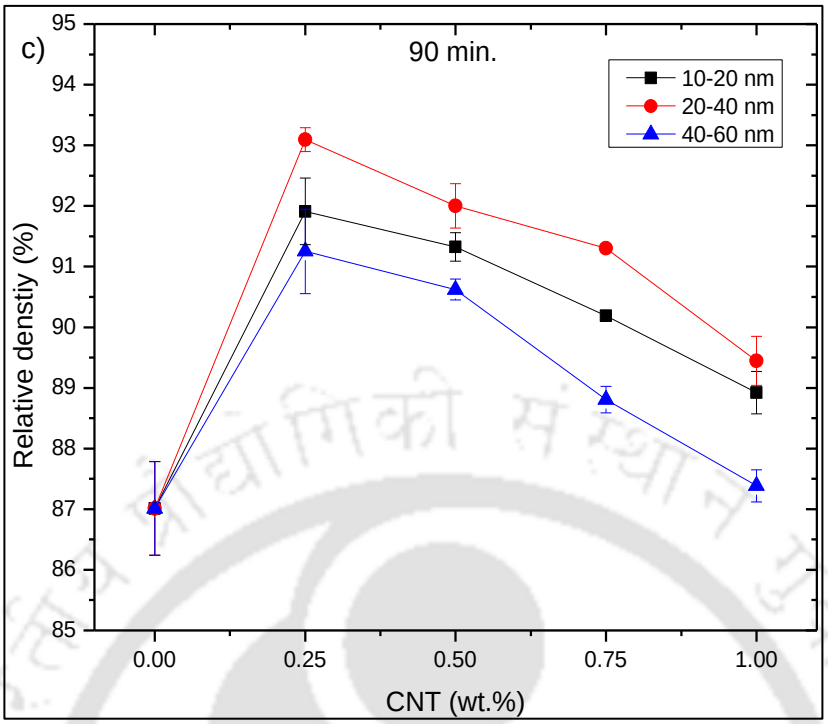

Figure 4.16 Relative density of CIP-MW processed Cu/CNT composites having 10–20 nm, 20–40 nm and 40–60 nm diameter CNT sintered at 600 °C for a) 60 min, b) 75 min. and c) 90 min.

Figure 4.16 shows the relative density (RD) of CIP compacted-microwave sintered Cu and Cu/CNT composites having the CNT diameter of 10-20 nm, 20-40 nm and 40-60 nm against their concentrations and sintered at 600°C for the duration of 60, 75 and 90 min. It is noted that the maximum RD of Cu-CNT composites is obtained at 0.25wt.% of CNT irrespective of its diameter and sintering duration and then it began to decrease against increase of CNT concentration. **Figure 4.16a** shows the RD of all types of composites sintered at 60 min., where the maximum RD of pure copper is observed to be about 86.1% and it is increased to 92.1% at 0.25wt.% of 20-40 nm CNT reinforcement. Beyond 0.25wt.%, the RD of composites is observed to be decreased irrespective of CNT size and it is further reduced at 40-60 nm diameter CNT reinforcement in comparison to that of 20-40 nm diameter CNT reinforced composites irrespective of reinforcement concentration. It is also observed that the RD of the composites is decreased with an increase of CNT concentration and converged at 1wt.% CNT irrespective of its diameter. The 10-20 nm CNT reinforced composites showed a similar kind of enhancement in comparison to that of 20-40 nm CNT composites.

Figures 4.16b and **4.16c** show the RD of copper and Cu/CNT composites obtained through CIP and sintered at 600°C for 75 min. and 90 min. sintering duration, respectively. It is observed from **Figure 4.16b** that the maximum RD of 92.9, 93.8 and 92.5% is obtained, respectively, for 10-20 nm, 20-40 nm and 40-60 nm diameter CNT for Cu- 0.25 wt.% CNT composites at 75 min. of sintering. It is also observed that the 20-40 nm and 40-60 nm diameter CNT reinforced composites showed a similar type of decreasing trend beyond 0.25wt.%. The RD of composites is observed to be improved in comparison to that of pure copper irrespective of CNT diameter, where a gradual improvement of RD of the composites is noted irrespective of CNT diameter and its concentration in comparison to that of 60 min. sintered sample. It is observed from **Figure 4.16c** that the maximum RD of 20-40 nm CNT composites having 0.25wt.% is observed to be 93.1% at 90 min. of sintering. It is noted that the RD of 40-60 nm diameter CNT composites is observed to be the lowest in comparison to that of 10-20 nm and 20-40 nm diameter CNT reinforced composites. In addition, the 20-40 nm CNT diameter reinforced composites are observed to have the maximum RD in comparison to that of 10-20 nm and 40-60 nm diameter CNT reinforced composites. It is inferred that the size of CNT and its concentration are observed to be significant to obtain the highest RD of composites, which are obtained through CIP followed microwave sintering technique.

4.4.3.2 Relative density of Cu/CNT composites against sintering duration

The following section discusses about the RD of Cu and Cu/CNT composites having different diameter of CNT and its concentration obtained against different sintering duration.

Figure 4.17a-c shows the RD of Cu and its composites against sintering time on different diameter of CNT and its concentration, where the results are obtained through CIP followed by microwave sintering. In case of 1wt.% of any CNT diameter, the RD of composites is found to have no significant influence against sintering time. The RD of composites obtained at 60 min. of sintering is observed to be the lowest irrespective of CNT size and its concentration. It is observed from **Figure 4.17a** that the maximum RD of 10-20 nm diameter CNT reinforced composites is observed to be 92.9% at 0.25wt.% and 75 min. of sintering time. It is also observed that the trend noticed on the RD of the composites is found to be very similar for 60 and 75 min. sintering time and the RD of the composites at 1wt.% CNT concentration is observed to be converged and the results are found to be within the experimental deviation irrespective of sintering time. The samples sintered at 60 and 90

min. are not found to show any significant difference in improving the RD of the composites irrespective of CNT concentration.

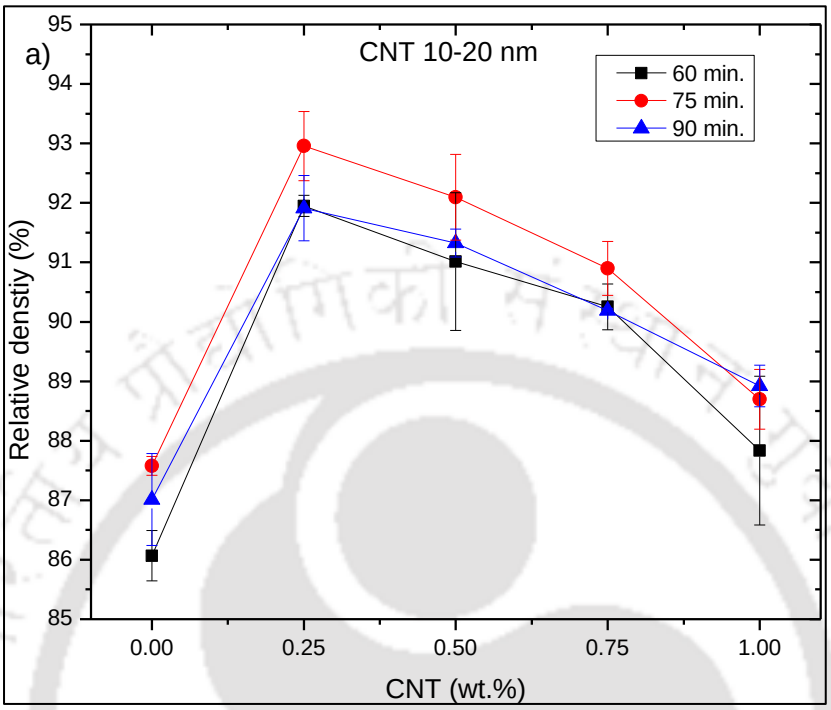

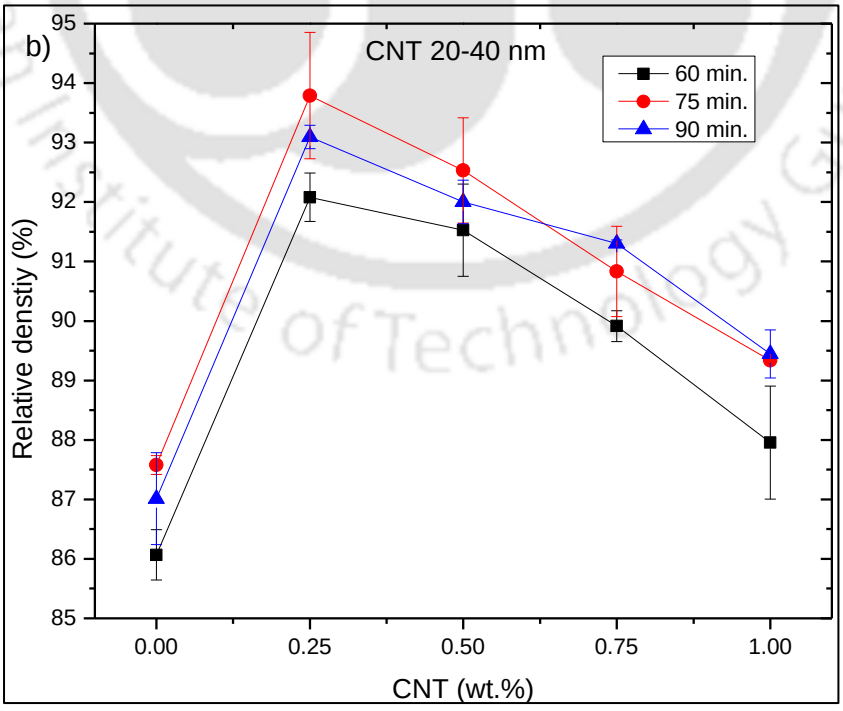

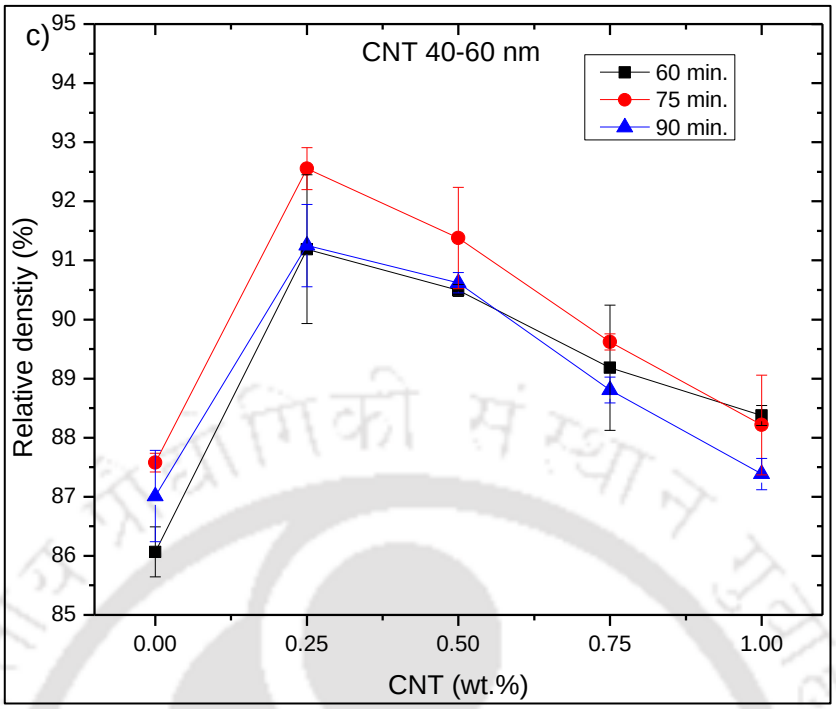

Figure 4.17 Relative density of CIP-MW processed Cu/CNT composites having a) 10-20 nm, b) 20-40 nm, and c) 40-60 nm diameter CNT reinforcement against different sintering time

Figure 4.17b shows the RD of 20-40 nm diameter CNT composites, and the maximum RD of 93.9% is observed at 0.25wt.%, where significant influence of sintering time is noticed. Similar to 10-20 nm CNT reinforced composites, the sample sintered at 60 min. of sintering time is found to have the lowest value of RD for the composites irrespective of CNT concentration. It is observed from **Figure 4.17c** that the RD of 40-60 nm diameter CNT is not found to have any significant difference between 60 and 90 min. sintering and the maximum RD is noted to be 92.5% at 0.25wt.% for 75 min. sintering time. It is also observed that the RD of 1wt.% CNT composites converged at 60 and 75 min. of sintering time and the 40-60 nm CNT diameter composites showed the lowest RD at 90 min. of sintering time.

In summary, the RD of CIP-MW processed composites is found to have a significant influence on the size of CNT and it is observed to be improved irrespective of CNT diameter and its concentration in comparison to that of pure copper and rest of the processed techniques. It is also noted that the compaction technique played an important role in order to improve the RD of the composites irrespective of CNT type and its concentration. The RD of CIP-MW processed composite sample is noted to be highly improved in comparison

to that of pure copper and other samples processed through other techniques. The RD of 20-40 nm diameter CNT composites is observed to be the highest and have much significant influence in all kind of processing techniques.

4.5 Comparison of Uniaxial and CIP compaction process

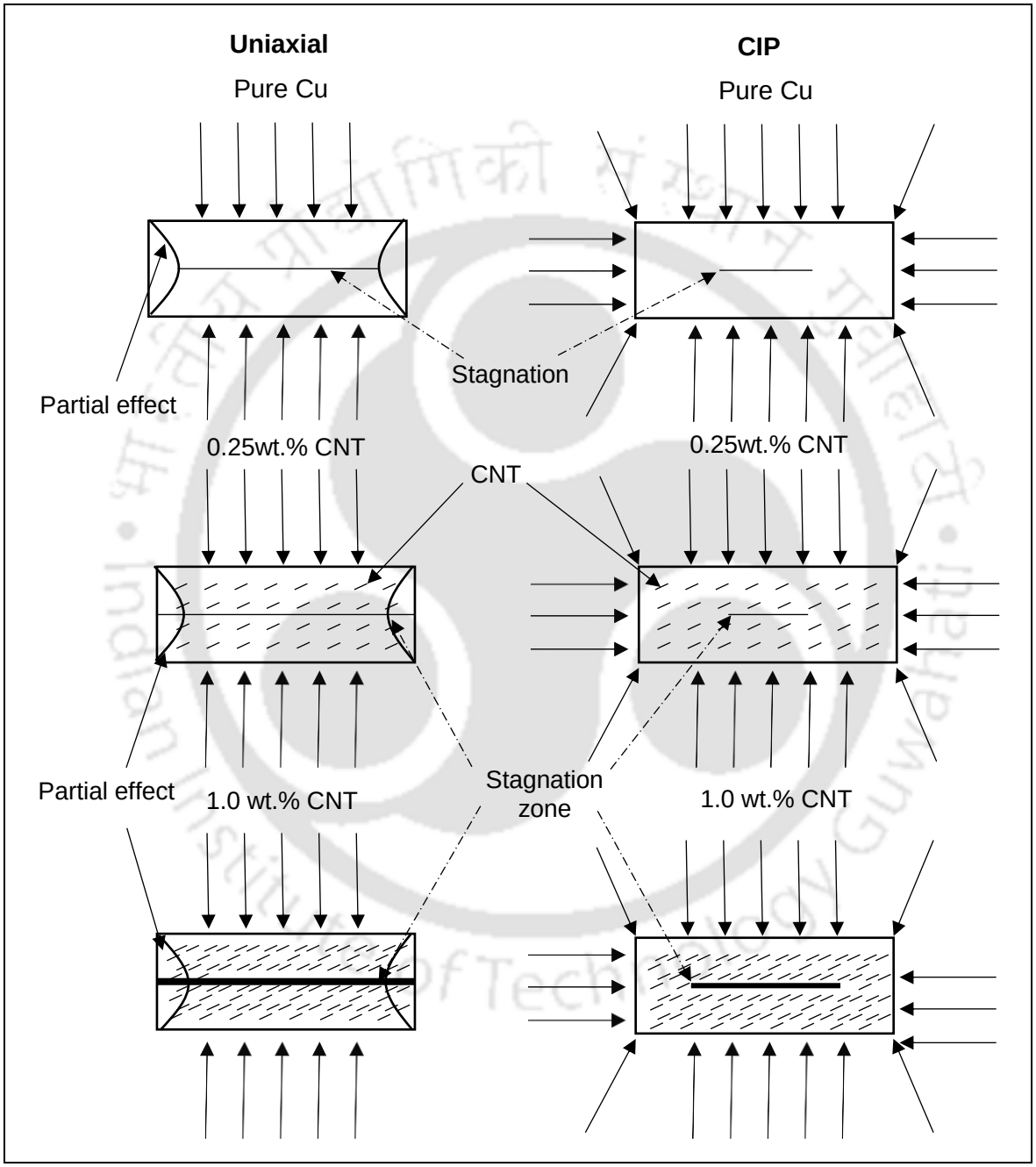

Figure 4.18 Schematic representation of CIP and UA compaction of copper and Cu/CNT composite powder

Figure 4.18 shows the schematic representation of CIP and UA compaction process of copper and Cu/CNT composite powder at 0.25 and 1wt.% of CNT. In case of CIP

compacted pure copper sample, the applied pressure is evenly distributed throughout the sample. However, the same is not observed in case of uniaxial compaction, where a strong presence of stagnation zone is believed to be present. The generation of stagnant zone is expected to be present irrespective of compaction technique. However, its volume is limited by the CIP process in comparison to that of uniaxial compaction process. In the stagnation zone, only a part of compaction pressure is transferred to the sample during the uniaxial compaction process, whereas the intensity of stagnant zone is very much limited and it is evenly distributed in case of CIP compaction, which allows the redistribution of powder effectively during its compaction process in comparison to that of UA compaction process. In addition, the CIP technique has produced homogeneous distribution of pressure in all direction, whereas UA compacted sample is expected to provide varying pressure along the longitudinal direction due to the generation of stagnation zone along with edge effect, which is also supported by An *et al*. [2015]. The pressure generated at the entrapped void during the UA compaction is expected to be significantly high in comparison to that of CIP compaction. Thus, the RD of CIP processed samples is expected to be very high in comparison to that of UA sample, and it is also reported by Eksi *et al*. [2004]. As no external pressure is applied during the sintering process, it is expected to retain the isolated pores present in the sample irrespective of their location and the movement of voids from interior to the surface level is also not noticed, Kang [2005]. In case of CIP-MW process, the characteristics of compacted sample are expected to have maximum penetration of heat within the sample due to its low porosity and thus, the improved RD of the composites is observed in all cases of CIP-MW processed sample in comparison to that of UA-MW processed sample.

Since the CNT has inherent self-lubrication characteristics, the friction generated within the composite powder during the compaction process is expected to be reduced at 0.25wt.% CNT concentration irrespective of its size and thus, it assists to transfer the total compaction pressure on the powder sample to increase the RD of composites. The addition of CNT beyond 0.25wt.% in the composite powder decreased the effective compaction pressure applied over the sample due to its high strength, Qian *et al*. [2002], which absorbs the partial compaction force leading to generate a more number of voids in the sample, Feng *et al*. [2005]. As the penetration depth of compressive force is reduced due to increased concentration of CNT, it is expected to increase the thickness of the stagnation zone, where complete diffusion is limited during the sintering process leading to reduce the RD of

composites. As the compaction pressure used in UA technique is 2.67 times higher in comparison to that of CIP technique, the absorbed energy by CNT is expected to be much higher leading to have many kind of defects on the sample and it is expected to induce some kind of residual stresses on the sample. As there is no compaction on lateral side of the powder sample, the UA compacted samples are expected to have poor diffusion in lateral direction, as supported by An *et al*. [2015], which leads to reduce the overall RD of the composites in comparison to that of CIP sample and it is schematically shown in **Figure 4.18**. The above discussed effects are expected to be very high at higher concentration of CNT due to the presence of pressure gradient while compacting the composite powder sample irrespective of compaction technique and thus, the RD of the composites at higher concentration of CNT is observed to be reduced.

4.6 Microstructure of sintered copper and Cu/CNT composite samples

This section mainly discusses about the microstructure of copper and Cu/CNT composite samples, where the influences of grain size, size of voids, void distribution, CNT diameter and the concentration of reinforcement against different processing techniques are discussed in detail. As the composites having 0.25wt.% and 1.0wt.% CNT showed the maximum and minimum characteristics of the composites, respectively, the microstructures of the said composites obtained through different processing techniques are reported.

4.6.1 Microstructure of uniaxial compaction and conventional sintering (UA-CS) processed copper and Cu/CNT composite samples

Figures 4.19a, b and c show the microstructure of copper sintered at 600 °C for 60, 75 and 90 min., respectively, obtained through UA-CS technique. It is noted that the shape of voids is observed to be different and it has a good number of grains having the size of approximately 4.1 ± 0.1 µm irrespective of sintering duration. In order to study the effect of CNT diameter and its concentration, the composite samples having 0.25 and 1wt.% CNT concentration of 10-20 nm, 20-40 nm and 40-60 nm diameter CNT sintered at 600 °C against the sintering duration of 60, 75 and 90 min. are studied and their micrographs are shown in **Figure 4.19d - u**. It is observed from **Figure 4.19d- l** and noted from **Table 4.1** that the size of grains is observed to be in the range of 4.29 ± 0.05 µm to 4.76 ± 0.1 µm for all types of composites having 0.25wt.% CNT and the presence of a very few number of voids in the composites. It is also observed that a number of voids irrespective of CNT diameter is found to be less and the grains are closely packed. **Figures 4.19m-u** show the microstructure of

Cu- 1wt.% CNT composites, where the grain size of composites is observed to be in the range of 5.6 ± 0.12 µm to 6.35 ± 0.12 µm for all types of composites tested in the present study and they also have a significant number of voids irrespective of CNT diameter and sintering time. It is inferred that the grain size of the composites is increased with an increase of CNT diameter, its concentration and sintering time.

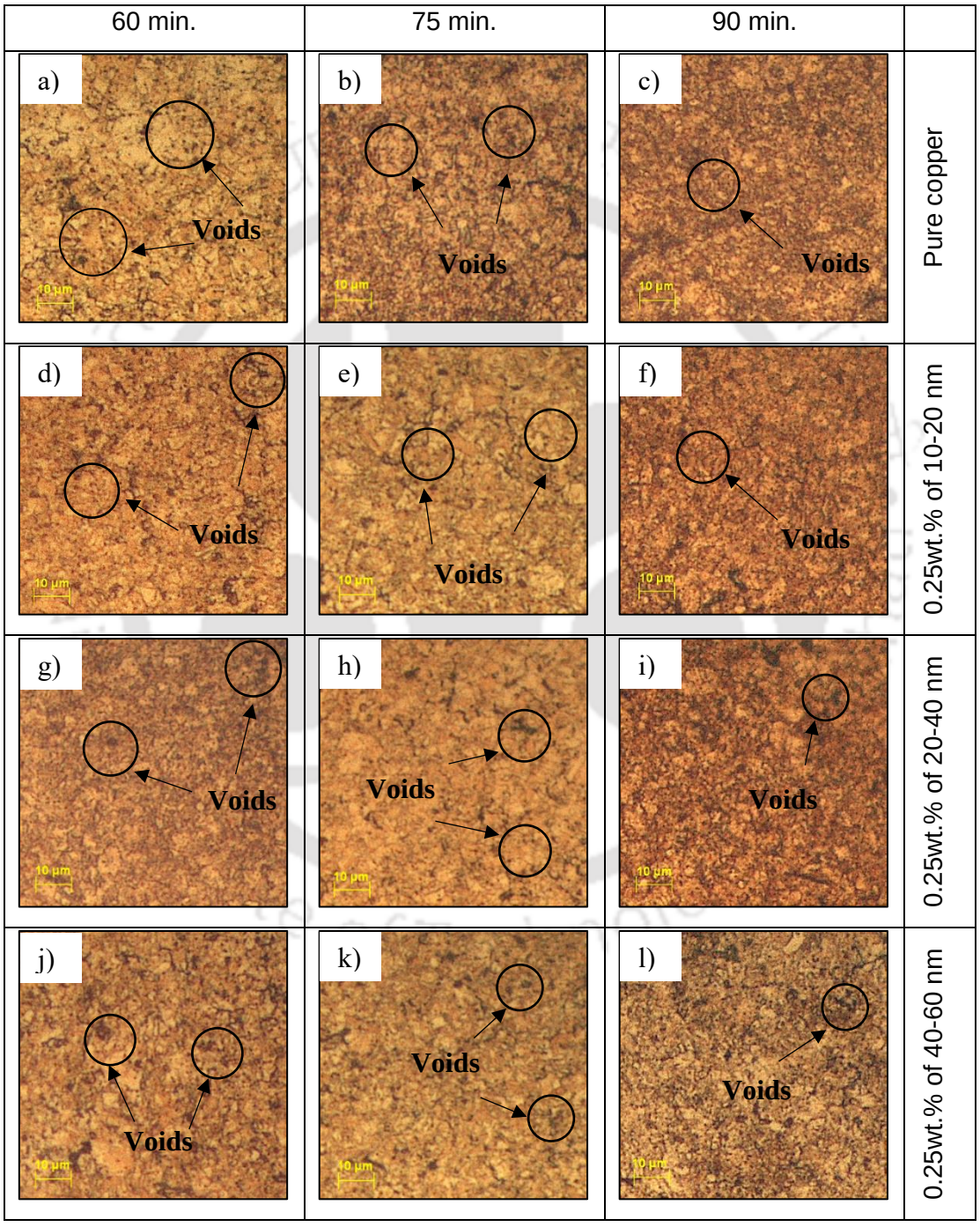

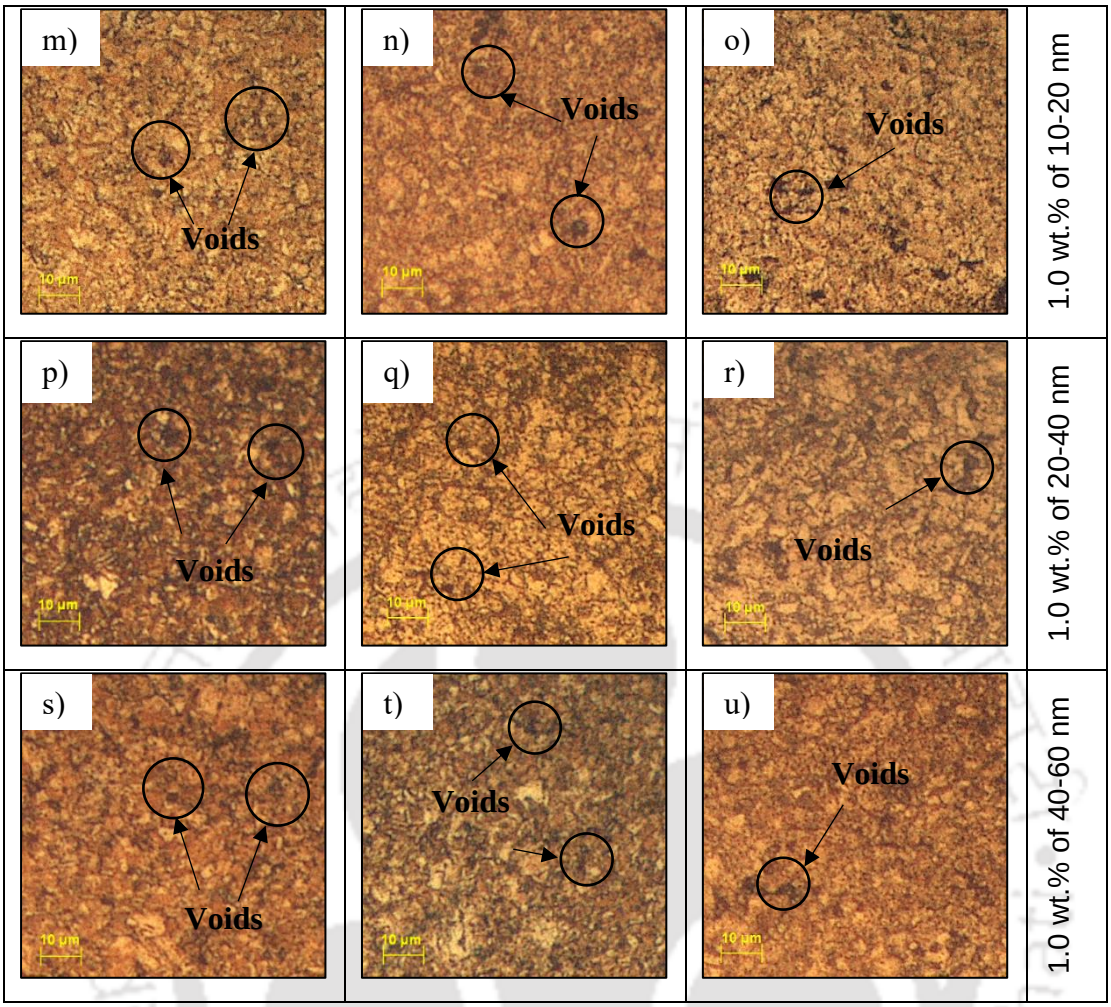

Figure 4.19 Microstructure of UA-CS processed Cu and Cu/CNT composites sintered at 600 °C for 60, 75 and 90 min. (a-c) pure copper, (d-f) 0.25wt.% of 10-20 nm CNT composites, (g-i) 0.25wt.% of 20-40 nm CNT composites, (j-l) 0.25wt.% of 40-60 nm CNT composites, (m-o) 1wt.% of 10-20 nm CNT composites, (p-r) 1.0wt.% of 20-40 nm CNT composites and (s-u) 1.0wt.% of 40-60 nm CNT composites

Table 4.1 reports the summary of above observation, where the grain size of Cu and Cu/CNT composites obtained through UA-CS processed technique is reported for all CNT diameter and their concentration against different sintering duration. It is observed that the grain size of pure copper and Cu/CNT composites is noted to be increased with sintering duration. It is noted that the average enhancement of grain size of the composites at 0.25wt.% is observed to be 5.5, 11, and 16% for 10-20 nm, 20-40 nm and 40-60 nm irrespective of sintering duration, respectively. In addition, it is noted that the grain size of the composite is increased with CNT diameter irrespective of its concentration. In case of Cu- 1wt.% CNT composites, the average enhancement of grain size is observed to be 37, 42, and 55% for 10-

20 nm, 20-40 nm and 40-60 nm diameter CNT composites in comparison to that of pure copper, respectively, irrespective of sintering duration.

Table 4.1 Average grain size of UA-CS processed Cu/CNT composites sintered at 600 °C against different sintering duration

CNT diameter	**Grain size (µm)**				
	Pure Cu	**0.25wt.%**	**0.5wt.%**	**0.75wt.%**	**1.0wt.%**
60 min.					
10-20 nm	4.02 ± 0.05	4.29 ± 0.12	4.71 ± 0.15	5.05± 0.15	5.56 ± 0.09
20-40 nm		4.47 ± 0.10	4.82 ± 0.20	5.35 ± 0.30	5.71 ± 0.30
40-60 nm		4.70 ± 0.07	5.25 ± 0.30	5.78 ± 0.12	6.25 ± 0.10
75 min.					
10-20 nm	4.12 ± 0.06	4.32 ± 0.08	4.88 ± 0.10	5.20 ± 0.20	5.59 ± 0.13
20-40 nm		4.56 ± 0.16	5.05 ± 0.09	5.36 ± 0.09	5.78 ± 0.02
40-60 nm		4.75 ± 0.07	5.20 ± 0.21	5.75 ± 0.15	6.32 ± 0.05
90 min.					
10-20 nm	4.18 ± 0.09	4.39 ± 0.10	4.99 ± 0.02	5.34 ± 0.03	5.74 ± 0.07
20-40 nm		4.65 ± 0.11	5.05 ± 0.09	5.46 ± 0.10	5.98 ± 0.10
40-60 nm		4.84 ± 0.10	5.35 ± 0.08	5.98 ± 0.07	6.49 ± 0.06

4.6.2 Microstructure of uniaxial compaction and microwave sintering (UA-MW) processed copper and Cu/CNT composite samples

Figures 4.20a-c show the microstructure of pure copper sintered in a microwave furnace, where the average grain size of 4.09 ± 0.1 µm is noticed irrespective of sintering duration. It is also noticed that the number and size of voids along the grain boundaries are observed to be increased with sintering duration. **Figures 4.20d-f** and **Table 4.2** show the microstructure of 0.25 wt.% 10-20 nm diameter CNT reinforced Cu/CNT sintered composites, where the average grain size is observed to be 4.22 ± 0.01 µm along with less number of voids irrespective of sintering duration. Similarly, **Figures 4.20g-i** and **4.20j-l** show the microstructure of Cu- 0.25wt.% CNT composites reinforced with 20-40 nm and 40-60 nm diameter CNT, respectively, sintered at 600 °C for 60, 75 and 90 min. and their corresponding average grain size is observed to be 4.41 ± 0.11 µm and 4.54 ± 0.08 µm. It is

observed from **Figure 4.20d-l** that the number of voids is significantly reduced and the grains are observed to be closely packed. Due to low concentration, a dense microstructure is noticed at 0.25wt.% CNT, which helped to improve the hardness of the composites in comparison to that of other types of composites. It is also noted that the increased grain size is expected due to strong interfacial bonding between the CNT and Cu.

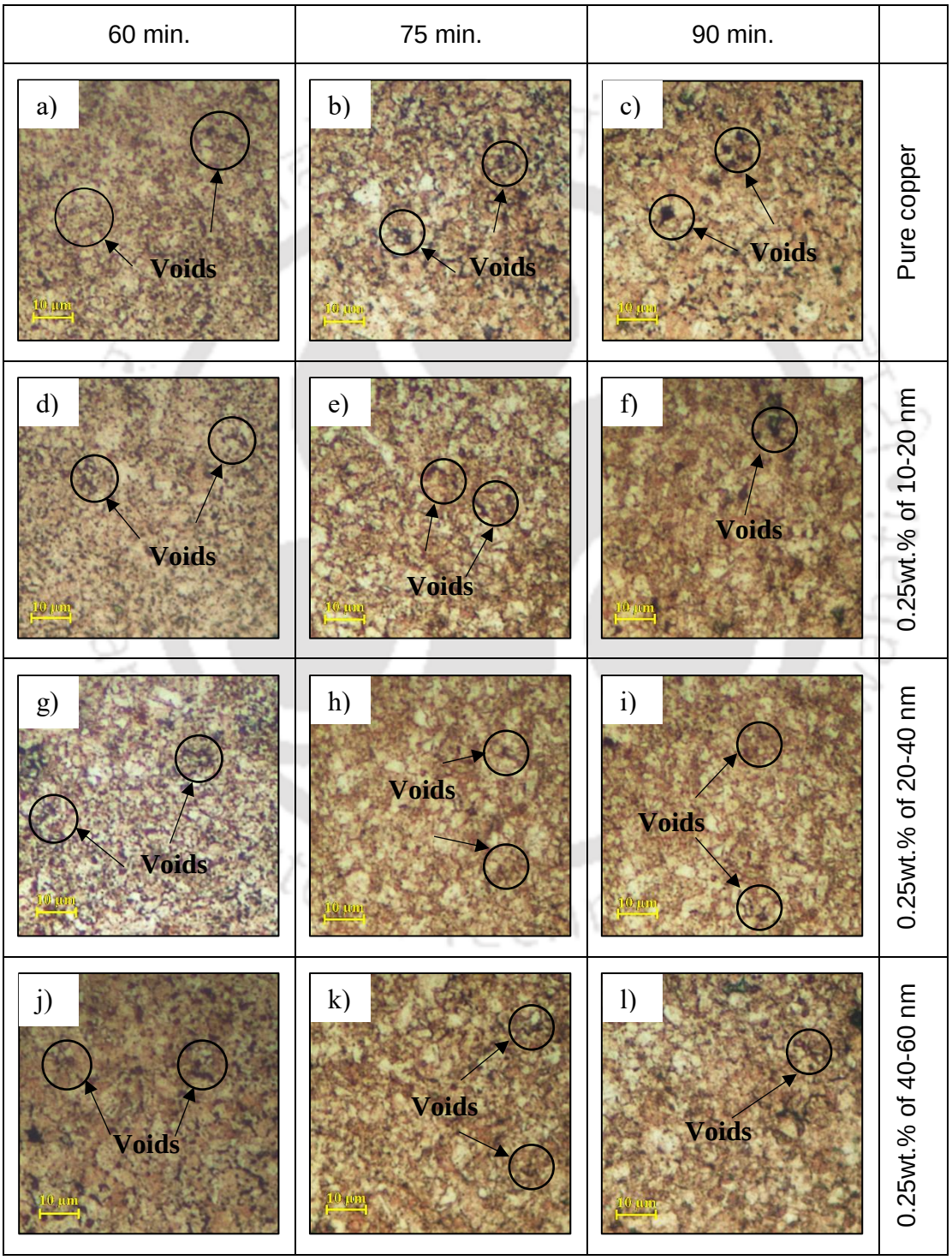

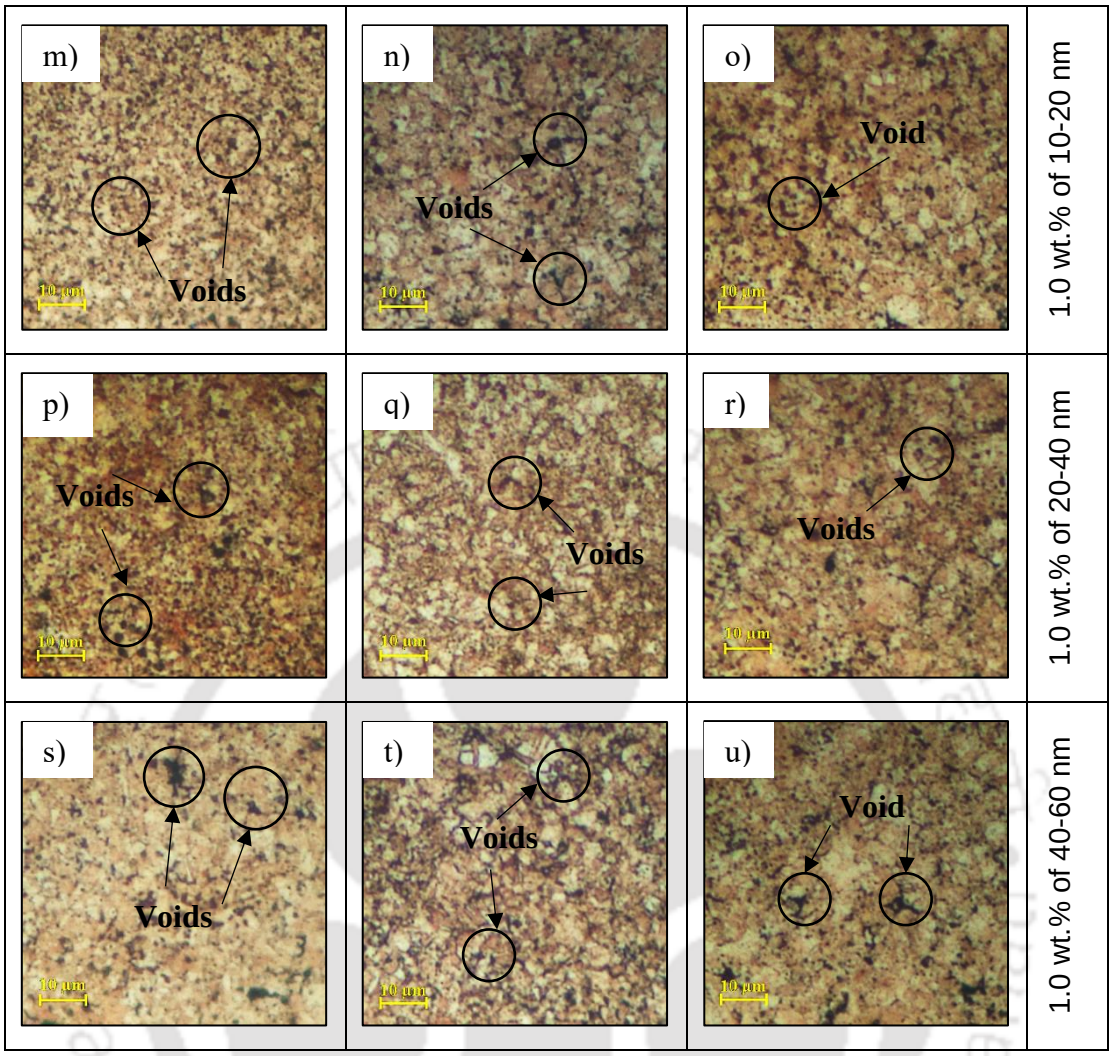

Figure 4.20 Microstructure of UA-MW processed Cu and Cu/CNT composites sintered at 600 °C for 60, 75 and 90 min. (a-c) pure copper, (d-f) 0.25wt.% of 10-20 nm CNT composites, (g-i) 0.25wt.% of 20-40 nm CNT composites, (j-l) 0.25wt.% of 40-60 nm CNT composites, (m-o) 1wt.% of 10-20 nm CNT composites, (p-r) 1.0wt.% of 20-40 nm CNT composites and (s-u) 1.0wt.% of 40-60 nm CNT composites

Figures 4.20m-o, **4.20p-r** and **4.20s-u** show the microstructure of Cu- 1wt.% CNT composites having 10-20 nm, 20-40 nm and 40-60 nm diameter CNT, respectively and their corresponding average grain size is observed to be 5.57 ± 0.07, 5.77 ± 0.11 and 6.16 ± 0.14 µm. In addition, the presence of voids at Cu- 1wt.% CNT composites is found to be significant with an increase of sintering time in comparison to that of Cu- 0.25wt.% CNT composites irrespective of CNT diameter. This can be attributed to the intensity of restriction in particle rearrangement, which is the highest at 1wt.% composites due to the enhancement of stiffness of CNT. It is noticed that all CNT composites are observed to have a large size of grains and voids, which is noted to be higher at 1wt.% in comparison to that of 0.25wt.%

Cu/CNT composites. It is also noticed that the size of grains and number of voids present in the UA-MW processed composites are found to be significantly reduced in comparison to that of UA-CS processed composites at the respective concentration. In addition, the size of voids and their concentration are increased with CNT diameter and its concentration and sintering time in case of both UA-CS and UA-MW processed samples.

Table 4.2 reports the summary of above discussion on grain size of UA-MW processed Cu and Cu/CNT composites having all CNT concentration against different sintering duration. It is observed that the maximum enhancement of grain size of Cu-0.25wt.% CNT composites is observed to be 11% for 40-60 nm diameter CNT irrespective of sintering duration. In case of 10-20 nm diameter CNT composites, the enhancement of grain size is found to be within the experimental deviation in comparison to that of pure copper for all sintering duration. It is also observed that the grain size of composites is linearly increased with an increase of CNT concentration and the average enhancement of grain size is noted to be 25, 39 and 52% for 0.5, 0.75 and 1wt.% CNT composites, respectively, in comparison to that of pure copper.

Table 4.2 Average grain size of UA-MW processed Cu/CNT composites sintered at 600 °C against different sintering duration

CNT diameter	**Grain size (µm)**				
	Pure Cu	**0.25wt.%**	**0.5wt.%**	**0.75wt.%**	**1.0wt.%**
60 min.					
10-20 nm	4.04 ± 0.10	4.15 ± 0.12	4.55 ± 0.09	4.98 ± 0.10	5.51 ± 0.09
20-40 nm		4.30 ± 0.08	4.77 ± 0.20	5.18 ± 0.21	5.65 ± 0.05
40-60 nm		4.45 ± 0.06	4.90 ± 0.15	5.45 ± 0.15	6.05 ± 0.08
75 min.					
10-20 nm	4.08 ± 0.06	4.21 ± 0.07	4.77 ± 0.10	5.10 ± 0.05	5.56 ± 0.11
20-40 nm		4.40 ± 0.13	4.89 ± 0.09	5.31 ± 0.11	5.78 ± 0.05
40-60 nm		4.55 ± 0.06	5.20 ± 0.07	5.73 ± 0.15	6.11 ± 0.07
90 min.					
10-20 nm	4.15 ± 0.09	4.30 ± 0.10	4.77 ± 0.09	5.24 ± 0.10	5.74 ± 0.07
20-40 nm		4.52 ± 0.04	4.98 ± 0.30	5.36 ± 0.05	5.98 ± 0.10
40-60 nm		4.62 ± 0.07	5.26 ± 0.07	5.89 ± 0.11	6.49 ± 0.06

4.6.3 Microstructure of cold isostatic pressing compaction and microwave sintering (CIP-MW) processed copper and Cu/CNT composite samples

60 min.	75 min.	90 min.	
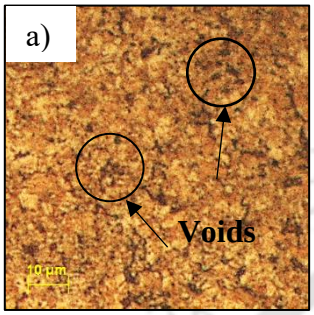	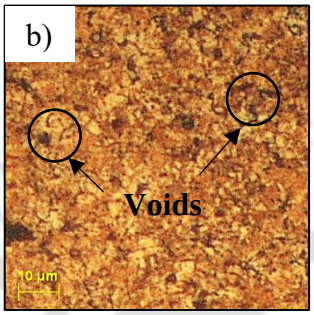	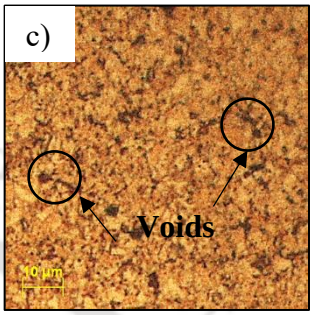	Pure copper
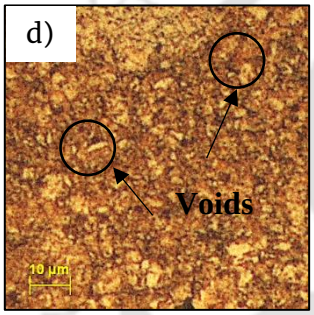	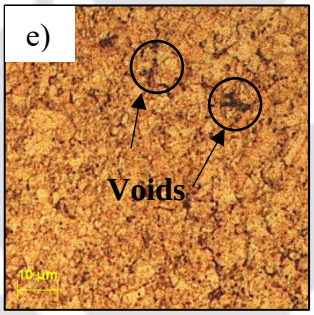	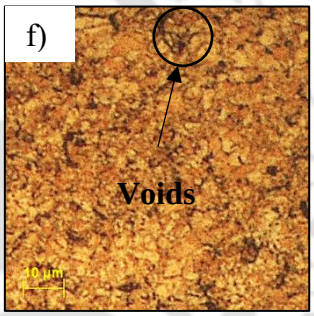	0.25wt.% of 10-20 nm
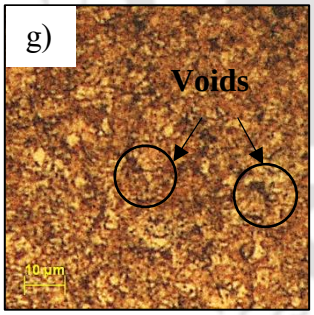	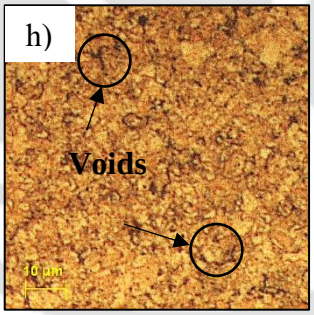	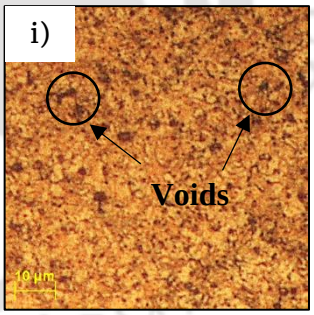	0.25wt.% of 20-40 nm
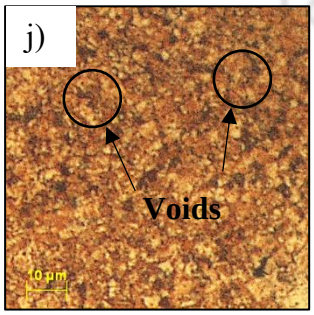	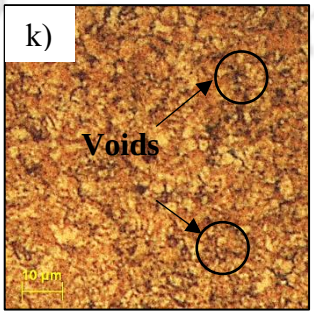	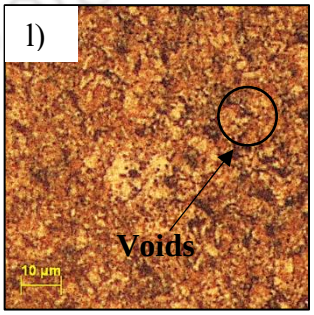	0.25wt.% of 40-60 nm

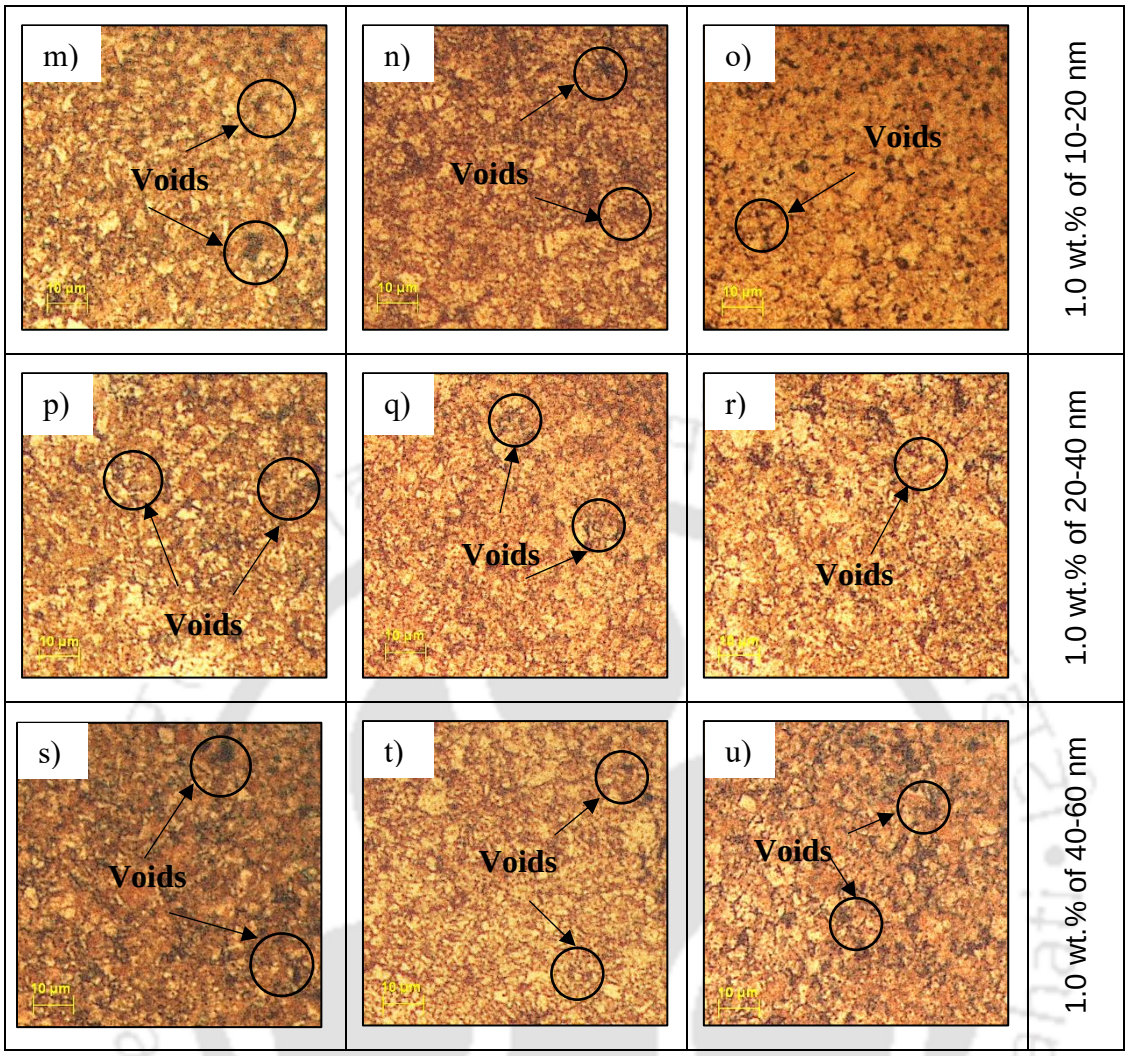

Figure 4.21 Microstructure of CIP-MW processed copper and Cu/CNT composites sintered at 600 °C for 60, 75 and 90 min. (a-c) pure copper, (d-f) 0.25wt.% of 10-20 nm CNT composites, (g-i) 0.25wt.% of 20-40 nm CNT composites, (j-l) 0.25wt.% of 40-60 nm CNT composites, (m-o) 1wt.% of 10-20 nm CNT composites, (p-r) 1.0wt.% of 20-40 nm CNT composites and (s-u) 1.0wt.% of 40-60 nm CNT composites

Figure 4.21 shows the microstructure of Cu and its composites having 0.25wt.% and 1.0wt.% CNT concentration obtained through CIP-MW technique after 60, 75 and 90 min. of sintering for all types of CNT diameter. It is observed from **Figure 4.21a-c** that the change in grain size of copper is observed to be insignificant against the sintering duration and the average size is observed to be 4.05 ± 0.05 µm. It is noted from the microstructure of copper that the grains obtained from CIP-MW technique are found to be densely packed in comparison to that of UA-CS and UA-MW processed samples. It is observed from **Figures 4.21d-l** that the number of grains is found to be more at 0.25wt.% concentration and the average grain size is found to be 4.32 ± 0.18 µm irrespective of CNT diameter, where the

maximum grain size is observed to be 4.55 ± 0.01 µm for 40-60 nm diameter CNT reinforced composites. The grains are densely packed and voids are not noticed significantly in the CIP-MW processed composites in comparison to that of UA-CS and UA-MW processed samples. At 1wt.% CNT composites, the number of voids is observed to be increased with sintering duration and the size of grains is increased from 5.52 ± 0.10 µm to 6.08 ± 0.15 µm with an increase of CNT diameter, which are observed in **Figure 4.21m-u** and reported in **Table 4.3**. In addition, the CIP-MW processed composites are found to have the least grain size and very less number of voids irrespective of CNT diameter, its concentration and sintering duration in comparison to that of UA-CS and UA-MW processed composites. It is inferred that the selection of processing technique is found to play an important role for obtaining the dense microstructure and controlled size of grains in the composites.

Table 4.3 Average grain size of CIP-MW processed Cu/CNT composites sintered at 600 °C against different sintering duration

CNT diameter	**Grain size (µm)**				
	Pure Cu	**0.25wt.%**	**0.5wt.%**	**0.75wt.%**	**1.0wt.%**
60 min.					
10-20 nm	4.01 ± 0.05	4.06 ± 0.05	4.52 ± 0.15	4.98 ± 0.10	5.45 ± 0.07
20-40 nm		4.26 ± 0.11	4.73 ± 0.06	5.12 ± 0.07	5.61 ± 0.13
40-60 nm		4.47 ± 0.09	4.92 ± 0.12	5.45 ± 0.09	5.95 ± 0.04
75 min.					
10-20 nm	4.04 ± 0.09	4.11 ± 0.05	4.64 ± 0.12	5.10 ± 0.05	5.51 ± 0.09
20-40 nm		4.33 ± 0.09	4.86 ± 0.08	5.25 ± 0.10	5.69 ± 0.03
40-60 nm		4.49 ± 0.10	5.17 ± 0.10	5.66 ± 0.11	6.05 ± 0.02
90 min.					
10-20 nm	4.11 ± 0.10	4.19 ± 0.07	4.76 ± 0.10	5.20 ± 0.07	5.60 ± 0.10
20-40 nm		4.42 ± 0.10	5.05 ± 0.20	5.42 ± 0.10	5.75 ± 0.06
40-60 nm		4.55 ± 0.08	5.24 ± 0.05	5.91 ± 0.30	6.25 ± 0.05

Table 4.3 reports the summary of above discussion on the average grain size of Cu and Cu/CNT composites processed through CIP-MW technique against different sintering duration. The average enhancement of grain size of Cu- 0.25wt.% CNT composites in comparison to that of copper is noted to be 2, 7 and 11% for 10-20 nm, 20-40 nm and 40-60 nm diameter CNT, respectively, irrespective of sintering duration. It is noted that the enhancement pattern of grain size of CIP-MW processed composites is observed to be decreased irrespective of CNT diameter in comparison to that of other processing techniques.

4.7 Hardness of Cu/CNT composites obtained through different processing techniques

The following section is dealt with the hardness of composites obtained through different processing techniques having different types of CNT and its concentration. The results obtained from the present study are discussed below in detail.

4.7.1 Hardness of uniaxial compaction and conventional sintering (UA-CS) processed Cu/CNT composite samples

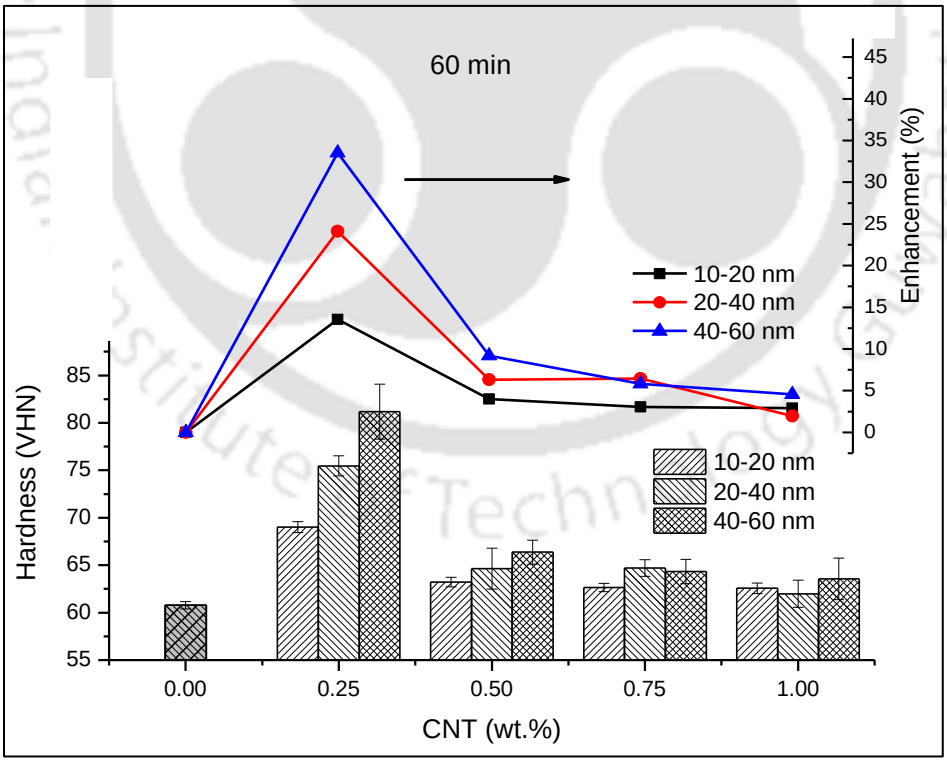

Figure 4.22 Hardness and its enhancement of UA-CS processed Cu/CNT composites having 10-20 nm, 20-40 nm and 40-60 nm size CNT sintered at 600 ℃ for 60 min.

Figure 4.22 shows the hardness and its enhancement of Cu/CNT composites having all CNT size and its concentrations sintered at 60 min. and it is noted that the hardness of pure copper is observed to be 60.8 ± 0.4 VHN at 82% RD and the maximum hardness is observed to be 69 ± 0.6 VHN at 83.7% RD, 75.4 ± 1.1 VHN at 87.5% RD and 81.2 ± 2.9 VHN at 84.2% RD for 10-20 nm, 20-40 nm and 40-60 nm diameter CNT reinforced composites, respectively, at 0.25wt.% CNT and the corresponding enhancement in comparison to that of pure copper is observed to be 14, 24 and 34%**.** It is also observed that the enhancement of hardness of the composites having the CNT concentration of 0.5 to 1wt.% irrespective of CNT diameter is found to vary within 10% in comparison to that of pure copper. Within the above specified range, the average hardness and its enhancement of said composites are observed to be 63.8 ± 0.67 VHN and 5%, respectively. The hardness of the composites is converged at 1wt.% for all type of CNT and it is found to be within the limit of experimental deviation.

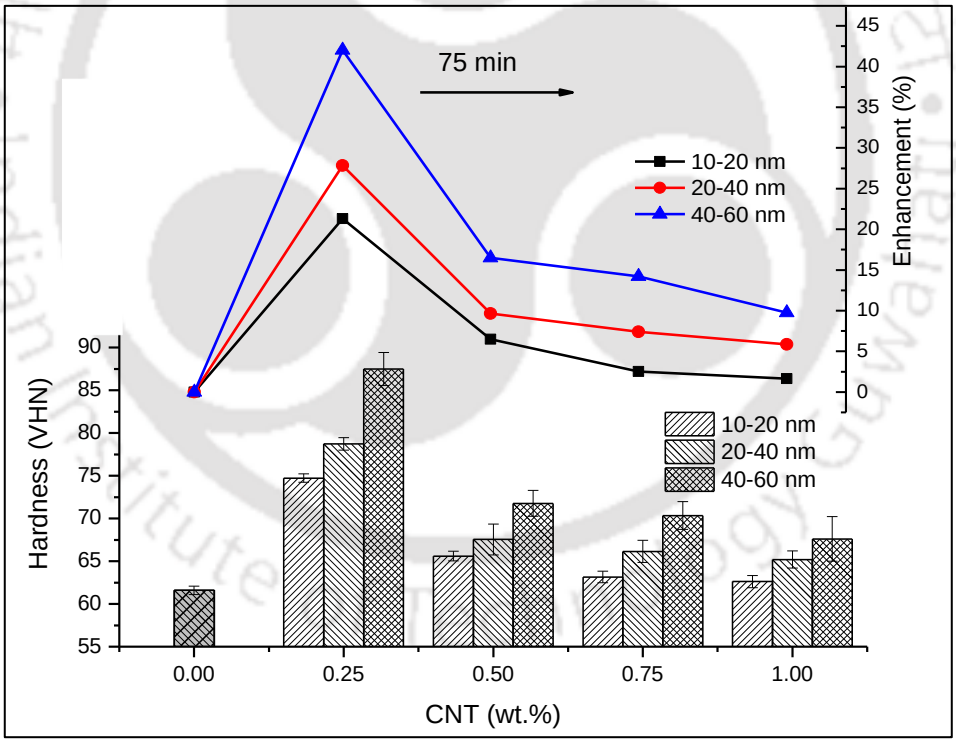

Figure 4.23 Hardness and its enhancement of UA-CS processed Cu/CNT composites having 10-20 nm, 20-40 nm and 40-60 nm size CNT sintered at 600 ℃ for 75 min.

Figures 4.23 shows the hardness of Cu/CNT composites sintered at 75 min. and its enhancement. It is noted that the maximum hardness of the composites having 10-20 nm, 20-40 nm and 40-60 nm diameter CNT is observed to be 74.7 ± 0.5 VHN at 85.3% RD, 78.7

± 0.7 VHN at 89.5% RD and 87.5 ± 1.9 VHN at 85.2% RD, respectively, at 0.25wt.% CNT. It is also observed that the hardness of 40-60 nm diameter CNT composites is found to be significant in comparison to that of 10-20 nm and 20-40 nm diameter CNT composites irrespective of CNT concentration. It is noted that the hardness of pure copper is not found to be significant with an increase of sintering time and it is observed to be 61.6 ± 0.5 VHN at 83% RD. It is observed from that the enhancement of hardness of composites having 10-20 nm, 20-40 nm and 40-60 nm diameter of CNT having 0.25wt.% CNT is noted to be 21, 28 and 42%, respectively, in comparison to that of pure copper. When the results are compared with that of 60 min. of sintering duration, the composites sintered at 75 min. are observed to show about 9% enhancement of hardness for 10-20 nm and 40-60 nm diameter CNT composites, and it is limited to 4% in case of 20-40 nm diameter CNT composites.

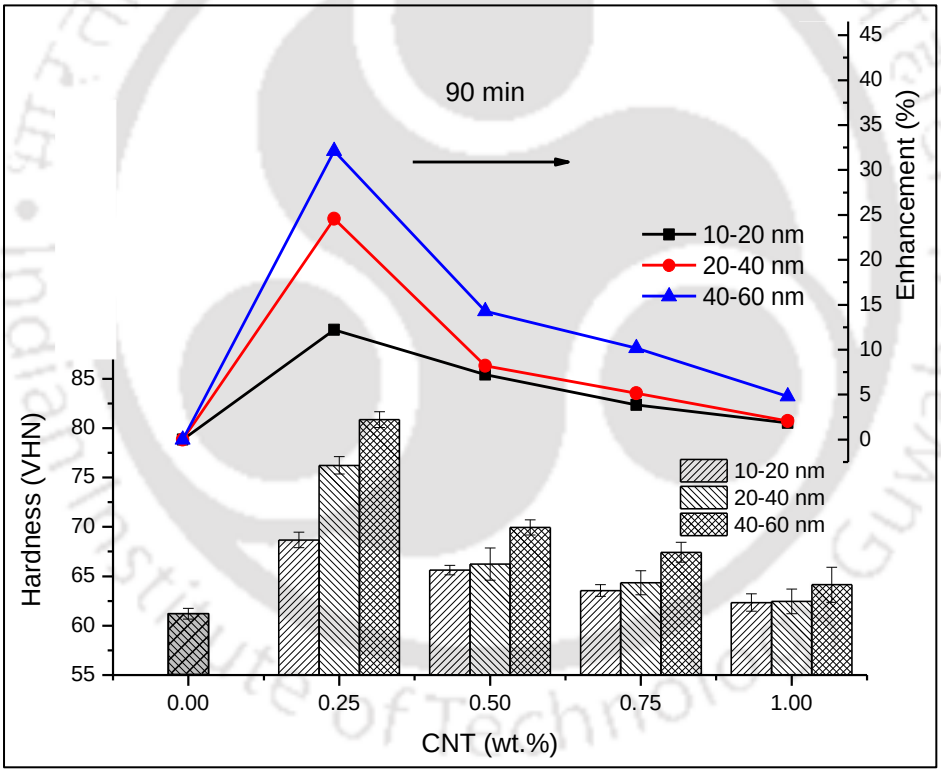

Figure 4.24 Hardness and its enhancement of UA-CS processed Cu/CNT composites having 10-20 nm, 20-40 nm and 40-60 nm size CNT sintered at 600 ℃ for 90 min.

Figures 4.24 shows the hardness and its enhancement of 90 min. sintered Cu/CNT composites. It is observed that the hardness of Cu/CNT composites having 40-60 nm diameter CNT at 0.25wt.% for 90 min. of sintering is noted to be 81 ± 0.8 VHN at 83.2% RD, where the hardness of pure copper is reported to be 61.2 ± 0.5 VHN at 82% RD. In

comparison to that of 75 min. of sintering duration, the hardness of 10-20 nm diameter CNT composites having 0.5 to 1wt.% of CNT is found to be within the limit of experimental deviation, whereas the same in case of 20-40 nm and 40-60 nm diameter CNT composites is noted to have significant influence on sintering duration irrespective of CNT concentration. It is noticed that the enhancement of hardness of composites having 0.25wt.% CNT is noted to be 12, 25 and 32% for 10-20 nm, 20-40 nm and 40-60 nm diameter CNT, respectively, in comparison to that of pure copper. Beyond 0.25wt.% CNT, the enhancement of hardness of the composites is observed to be in the same range in case of 10-20 nm and 20-40 nm diameter CNT and the results are converged at 1wt.% CNT concentration. It is also observed that the lowest hardness and its enhancement are noted to be 62.3 ± 0.8 VHN and 2% at 78.5% RD, respectively, at 1wt.% CNT of 10-20 nm diameter CNT composites in comparison to that of pure copper.

From the above observation, it is summarised that the diameter of CNT is noted to be an important variable to improve the hardness of the composites only at 0.25wt.% CNT. Beyond which, the same effect is not noticed. In addition, the enhancement of hardness of 40-60 nm diameter CNT composites is noted to be very much significant in comparison to that of 10-20 nm and 20-40 nm diameter CNT composites irrespective of CNT concentration and sintering time. It is observed from the results that the 40-60 nm CNT reinforced composites at 0.25wt.% showed the highest hardness in comparison to that of 20-40 nm and 10-20 nm diameter CNT composites irrespective of sintering time. It is due to the fact that the strong presence of chemical bonding between the matrix and reinforcement is expected to increase the structural stability of a bulk material. As the Young's modulus of CNT is noted to be about 8 times more than that of copper, as reported by Deng *et al*. (2011), the transfer of resisting force to the reinforcement from the matrix led to increase the hardness of composites. The stiffness of 40-60 nm diameter CNT composites is increased due to the fact that the probability of filling the copper in CNT is increased by 1.67 and 3 times in comparison to that of 20-40 nm and 10-20 nm diameter CNT, respectively, and it is expected to increase the hardness of composites. It is inferred that the 40-60 nm CNT had the lowest aspect ratio, increased surface area and higher volume among the rest of the CNT size used in the present study and these parameters assisted to increase the stiffness and hardness of composites in comparison to that of pure copper. As the inner volume of CNT is filled and the outer surface of CNT is coated with copper, the rigidity of composite powder is increased significantly and the intensity of the same is increased with CNT concentration and its

diameter. As the interaction between CNT and copper is increased with its concentration, the hardness of composites is observed to be decreased due to the restriction of the grain movement during the compaction process. Thus, it is expected to limit the grain rearrangement among themselves leading to have the reduced hardness of composites at higher concentration of CNT. It is also noted that the hardness of composites at 1wt.% of CNT is converged to a value at par with the hardness of copper irrespective of diameter of CNT and sintering duration. Deng *et al*. (2014) reported that the difference between coefficient of thermal expansion of CNT (21×10^{-6} m/mK) and copper (16.5×10^{-6} m/mK) is expected to induce the thermal stresses in the composites due to significant temperature gradient after the sintering process, and thus, it could also lead to reduce the hardness of the composites.

4.7.2 Hardness of uniaxial compaction and microwave sintering (UA-MW) processed Cu/CNT composite samples

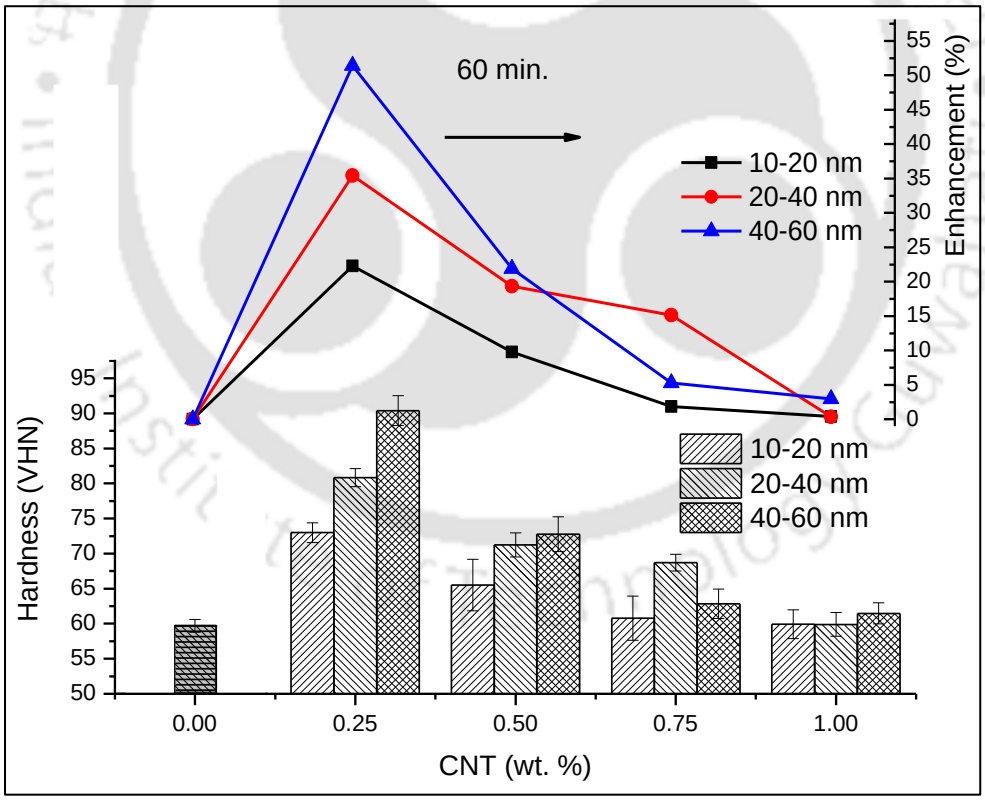

Figure 4.25 Hardness and its enhancement of UA-MW processed Cu/CNT composites having 10-20 nm, 20-40 nm and 40-60 nm size CNT sintered at 600 ℃ for 60 min.

Figure 4.25 shows the hardness and its enhancement of different types of Cu/CNT composites obtained after 60 min. of microwave sintering, where the maximum hardness is

observed to be 73 ± 1.4 VHN at 86.8% RD, 80.8 ± 1.3 VHN at 89.2% RD and 90.4 ± 2.1 VHN at 87.5% RD for 0.25 wt.% CNT of 10-20 nm, 20-40 nm and 40-60 nm diameter CNT reinforced composites, respectively. It is also observed that the hardness of the composites is reduced with an increase of CNT concentration beyond 0.25 wt.%. The CNT diameter is not found to be an influencing parameter on the hardness of the composites beyond 0.5 wt.% CNT and it is converged at 1 wt.% of CNT irrespective of the diameter of CNT. It is also observed that maximum enhancement of hardness of the composites with respect to pure copper is observed to be 22, 35 and 51% for 10-20 nm, 20-40 nm and 40-60 nm diameter CNT based composites, respectively, at 0.25wt.% concentration.

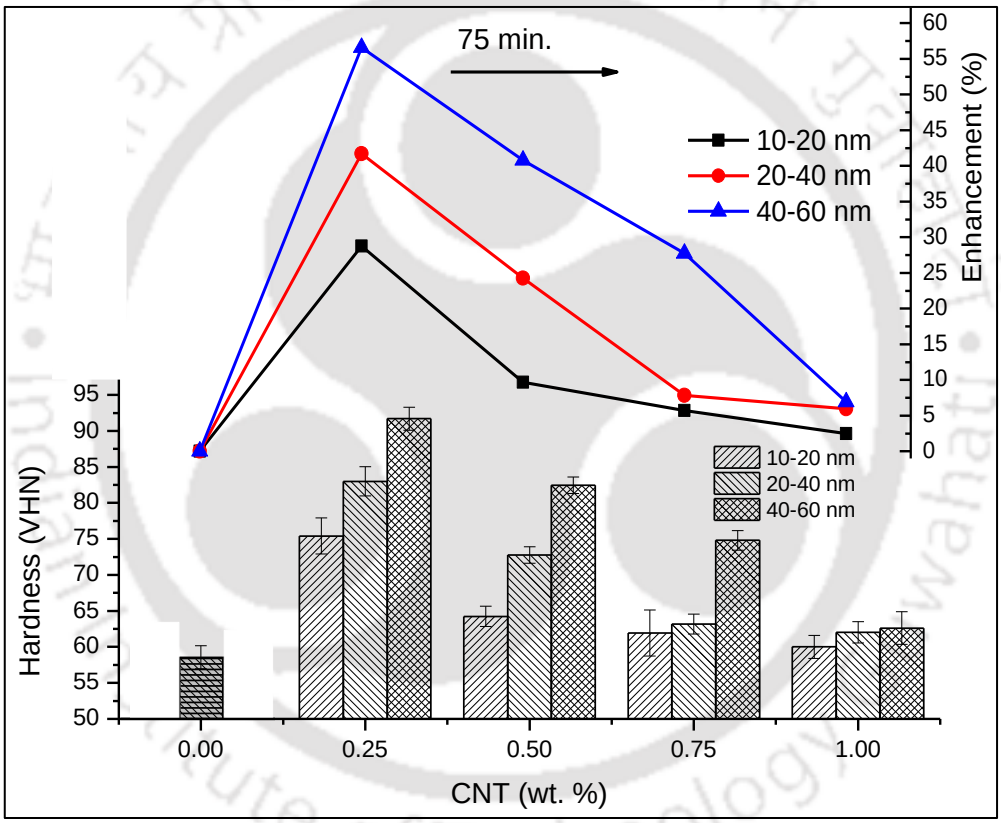

Figure 4.26 Hardness and its enhancement of UA-MW processed Cu/CNT composites having 10-20 nm, 20-40 nm and 40-60 nm size CNT sintered at 600 ℃ for 75 min.

Figure 4.26 shows the hardness and its enhancement of Cu/CNT composites obtained after 75 min. of sintering, where the maximum hardness is observed to be 75.4 ± 2.52 VHN at 87.1% RD, 82.9 ± 2.03 VHN at 90.9% RD and 91.7 ± 1.59 VHN at 87.9% RD for the composites having 10-20 nm, 20-40 nm and 40-60 nm diameter CNT, respectively, at 0.25 wt.% CNT. It is observed that the hardness of 40-60 nm diameter CNT reinforced composites is very much significant till 0.75wt.% in comparison to that of pure copper and

other composites. In case of 1wt.% CNT, the effect of reinforcement is insignificant irrespective of its diameter and converged to the value of hardness of pure copper within the limit of experimental deviation. It is also observed from **Figure 4.26** that the maximum enhancement of hardness is observed to be 29, 42 and 57% for 10-20 nm, 20-40 nm and 40-60 nm diameter CNT based composites, respectively, at 0.25wt.% CNT and 75 min. sintering in comparison to that of unreinforced copper. It is noted that the enhancement of hardness of 40-60 nm diameter composites is very much significant as compared to that of 20-40 nm and 10-20 nm diameter CNT composites, where the maximum hardness of all types of Cu/CNT composites is observed at 75 min. of sintering.

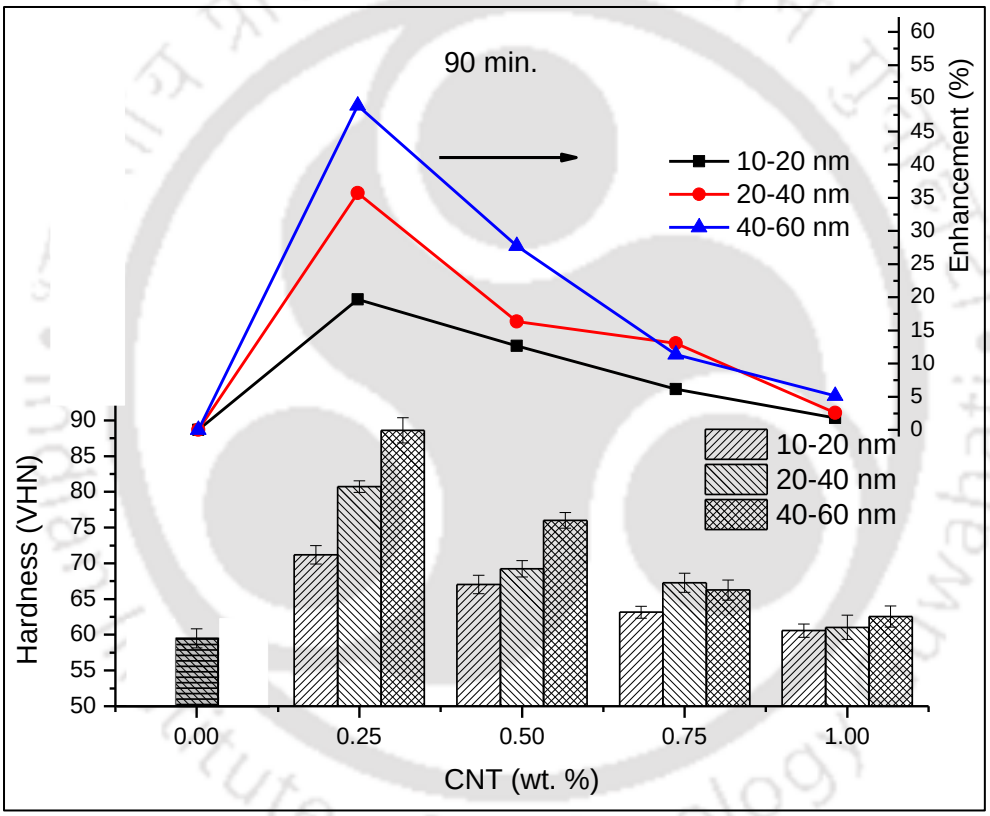

Figure 4.27 Hardness and its enhancement of UA-MW processed Cu/CNT composites having 10-20 nm, 20-40 nm and 40-60 nm size CNT sintered at 600 ℃ for 90 min.

Figure 4.27 shows the hardness of all types of Cu/CNT composites obtained after 90 min. of sintering at 600 °C and the maximum hardness of the composites is observed to be 71.2 ± 1.3 VHN at 84.9% RD, 80.7 ± 0.8 VHN at 86.9% RD and 88.6 ± 1.75 VHN at 86.4% RD for 0.25wt.% of 10-20 nm, 20-40 nm and 40-60 nm diameter CNT reinforced composites, respectively. The hardness of composites is significantly improved at 0.25wt.% for all types of CNT. But, the same is not observed at 0.75 and 1wt.%. It is also observed

from **Figure 4.27** that the maximum enhancement of the hardness of composites is limited to 16, 36 and 49% at 0.25wt.% of 10-20 nm, 20-40 nm and 40-60 nm diameter CNT composites, respectively, in comparison to that of pure copper. It is also noticed that the enhancement of hardness of the composites against CNT diameter is observed to be decreased with an increase of CNT concentration and converging to a specific value from 0.75wt.% CNT onwards, where the results are observed to be at par with that of pure copper within the limit of experimental variation.

It is observed from the above observation that the hardness of Cu/CNT composites processed through UA-MW and UA-CS technique is not found to be significantly influenced by the different sintering duration for a specific concentration of CNT. The variation noticed for the hardness of composites against 60, 75 and 90 min. of sintering is found to be well within the experimental deviation for a specific CNT diameter and its concentration irrespective of processing techniques. It is inferred that there is insignificant influence of sintering time and sintering technique on the hardness of Cu/CNT composites for a particular diameter of CNT and its concentration.

4.7.3 Hardness of cold isostatic pressing and microwave sintering (CIP-MW) processed Cu/CNT composite samples

As the hardness of the composites processed through CIP followed by microwave sintering at 60, 75 and 90 min. is not found to vary significantly irrespective of diameter of CNT, the hardness value obtained from different sintering time is averaged and the same is reported in **Figure 4.28**, which shows the hardness and its enhancement of Cu-CNT composites having different diameter of CNT. It is observed from **Figure 4.28** that the hardness of pure copper is reported to be 57.6 ± 0.8 VHN and the maximum hardness of the composites is observed to be 74.5 ± 0.6 at 92.3% RD, 79.1 ± 1.47 at 93.% RD and 83.2 ± 2.1 VHN at 91.6% RD, respectively, for 10-20 nm, 20-40 nm and 40-60 nm diameter CNT composites at 0.25wt.% CNT and their corresponding enhancement is noted to be 29.2, 37.2 and 44.2% in comparison to that of pure copper. Beyond 0.25wt.%, the hardness of composites is noted to be decreased with an increase of CNT concentration irrespective of its diameter. It is also observed that the hardness of composites having 40-60 nm diameter CNT composites showed significant enhancement irrespective of CNT concentration in comparison to that of pure copper, 10-20 nm and 20-40 nm diameter CNT reinforced composites. The hardness of composites having 0.5 to 1wt.% CNT concentration at 10-20

nm and 20-40 nm diameter CNT is found to vary within the limit of experimental deviation. The maximum enhancement of hardness of 40-60 nm diameter CNT composites is observed to be 15 and 7% higher in comparison to that of 10-20 nm and 20-40 nm diameter CNT composites at 0.25wt.%. The lowest value of hardness of 10-20 nm CNT composites is observed to be 65.8 ± 0.9 VHN at 1wt.%, which is 14% higher than that of pure copper and the enhancement is increased to 21% at 1wt.% of 40-60 nm CNT composites. It is inferred that the increase of CNT diameter showed significant enhancement of the hardness of composites irrespective of concentration of reinforcement and sintering duration followed to prepare the composites.

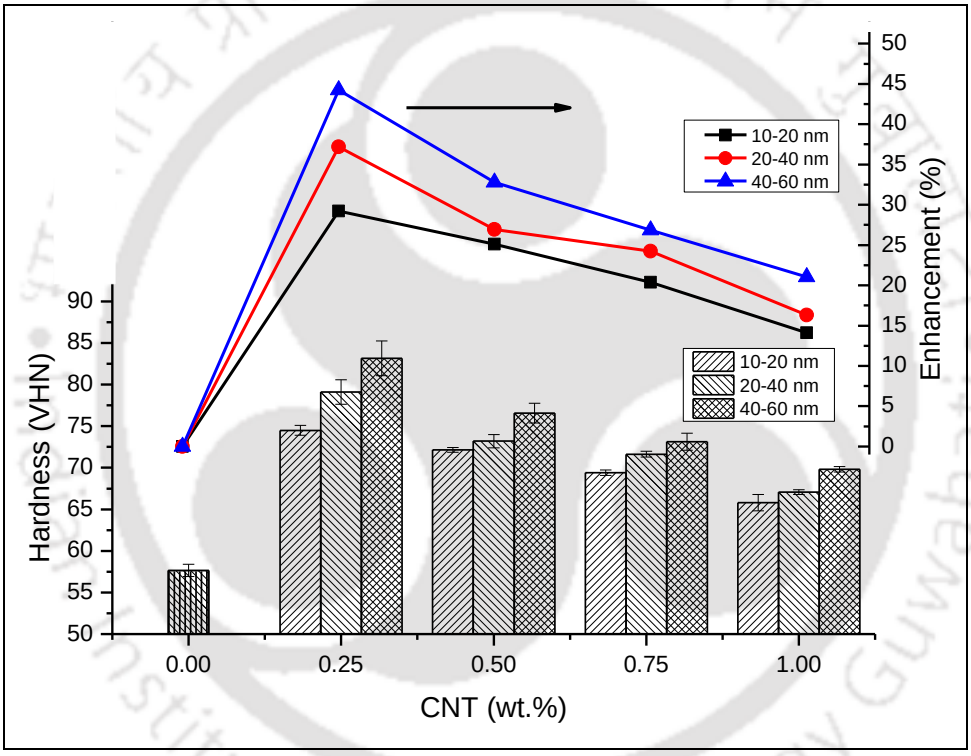

Figure 4.28 Hardness and its enhancement of Cu/CNT composites having 10–20 nm, 20–40 nm and 40–60 nm diameter CNT obtained through CIP compacted and microwave sintered process at 600 °C

The enhancement of hardness of composites is expected due to the involvement of compaction pressure used in UA technique, which is 800 MPa in comparison to that of 300 MPa in CIP, the effect of CIP technique is not effective at lower concentration in comparison to that of UA technique and thus, the improved hardness of composites is observed in later case. Beyond 0.25wt.%, the hardness of composites is found to be decreased irrespective of CNT diameter, compaction and sintering technique followed in the present study. At higher concentration of CNT, the effect of CNT stiffness is dominated in UA compaction technique

in comparison to that of CIP compaction pressure leading to reduce the hardness of the composites.

4.8 Electrical and thermal conductivity of Cu/CNT composites obtained through different processing techniques

This section discusses about the electrical and thermal conductivity of the composites having different CNT diameter and its concentration obtained through different processing techniques namely UA-CS, UA-MW and CIP-MW and the results are discussed below in detail.

4.8.1 Electrical and thermal conductivity of uniaxial compaction and conventional sintering processed Cu/CNT composites

Figure 4.29 shows the electrical and thermal conductivity and their enhancement of Cu/CNT composites having all types of CNT obtained at 600 °C and 60 min. of sintering duration. It is observed that the electrical and thermal conductivity of pure copper are observed to be 35.1 ± 0.7 MS/m and 260 W/mK at 82% RD, respectively, which are correspondingly 39 and 22% lower than that of pure copper obtained from the published literature, and these values are reported to be 57.9 MS/m, Wang *et al*. [2017] at 99.9% RD and 331 W/mK at 99% of RD, Chu *et al*. [2010a] for electrical and thermal conductivity of pure copper, respectively. As the pure copper sample is observed to have a good number of voids and grain boundaries, these are likely to influence scattering of electron conduction. They also act as a thermal barrier for the conduction of electrons leading to reduce its thermal conductivity. At 0.25wt.% CNT, the electrical conductivity of the composites is observed to be 43.2 ± 0.1 MS/m at 84% RD, 44.4 ± 0.1 MS/m at 87.5% RD and 42.5 ± 0.2 MS/m at 84.2% RD for 10-20 nm, 20-40 nm and 40-60 nm diameter CNT composites, respectively and their corresponding enhancement is calculated to be 23, 27 and 22% in comparison to that of pure copper. The thermal conductivity of composites at 0.25wt.% is calculated to be 320 W/mK at 84% RD, 328 W/mK at 87.5% RD, and 314 W/mK at 84.2% RD for 10-20 nm, 20-40 nm and 40-60 nm diameter CNT based composites, respectively. From 0.5wt.% onwards, the electrical and thermal conductivity of the composites are observed to be decreased with an increase of CNT concentration irrespective of its diameter. The average thermal conductivity of 0.5, 0.75 and 1wt.% composites is noted to be about 314 ± 4.5 W/mK at 82.7 % RD, 296 ± 1.5 at 81.4% RD and 292 ± 4.1 W/mK at 80.2% RD, respectively, and their corresponding enhancement in comparison to that of pure copper is observed to be 21,

14 and 12%. In addition, the lowest electrical and thermal conductivity of composites sintered at 60 min. are observed to be 38.84 ± 0.1 MS/m and 287.2 W/mK at 78.9% RD at 1.0wt.% composites having 40-60 nm diameter CNT. It is inferred that the RD has significant influence on the conductivity of the composites.

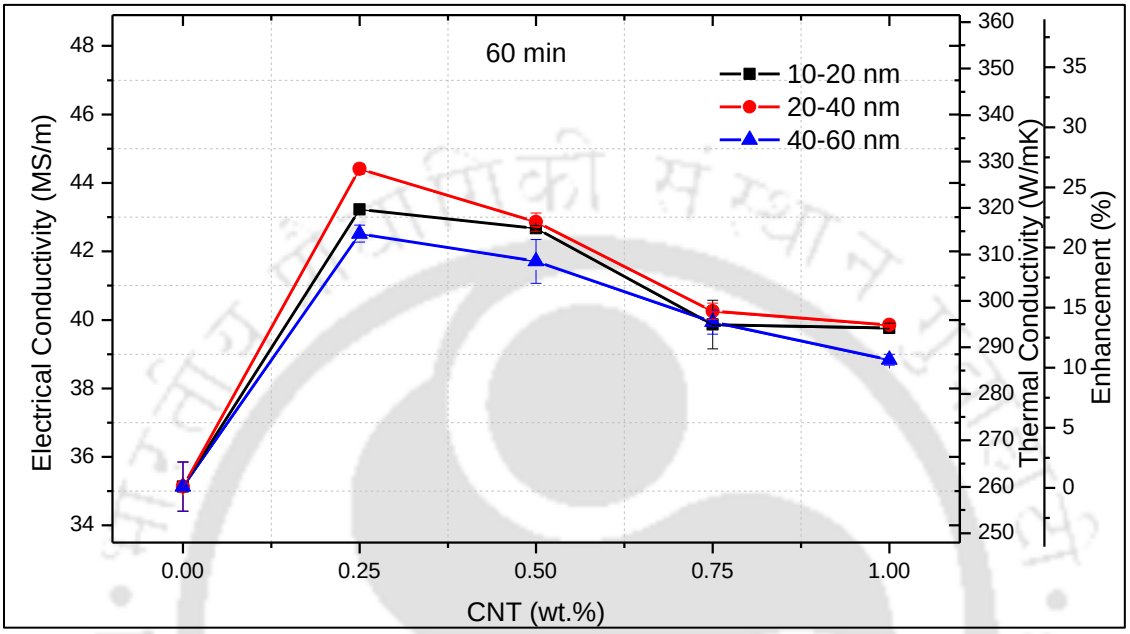

Figure 4.29 Electrical and thermal conductivity and their enhancement of UA-CS processed Cu/CNT composites having all CNT size and the sample sintered at 600 °C for 60 min.

Figure 4.30 shows the electrical and thermal conductivity and their enhancement of Cu and Cu/CNT composites sintered at 600 °C for 75 min. It is observed that the maximum electrical conductivity of the composites is observed to be 46 ± 0.1 MS/m at 85.3% RD, 48 ± 0.5 MS/m at 89.5% RD and 45.3 ± 0.4 MS/m at 85.2% RD for 10-20 nm, 20-40 nm and 40-60 nm CNT size at 0.25wt.%, respectively. It is noted that the thermal conductivity of 0.25wt.% of 20-40 nm diameter CNT composite and its enhancement are found to be maximum, which are noted to be 354 W/mK at 89.5% RD and 33%, respectively. It is noticed that the results of electrical and thermal conductivity of composites having 10-20 nm and 40-60 nm diameter CNT are found to be in the same range irrespective of CNT concentration. In case of 20-40 nm diameter CNT composites, the electrical conductivity of the composites is noted to be significantly improved in comparison to that of respective sample sintered at 60 min. In addition, it is also noted that the trend of electrical and thermal

conductivity of composites is noted to be similar to that of relative density of the composites obtained at 75 min. of sintering duration.

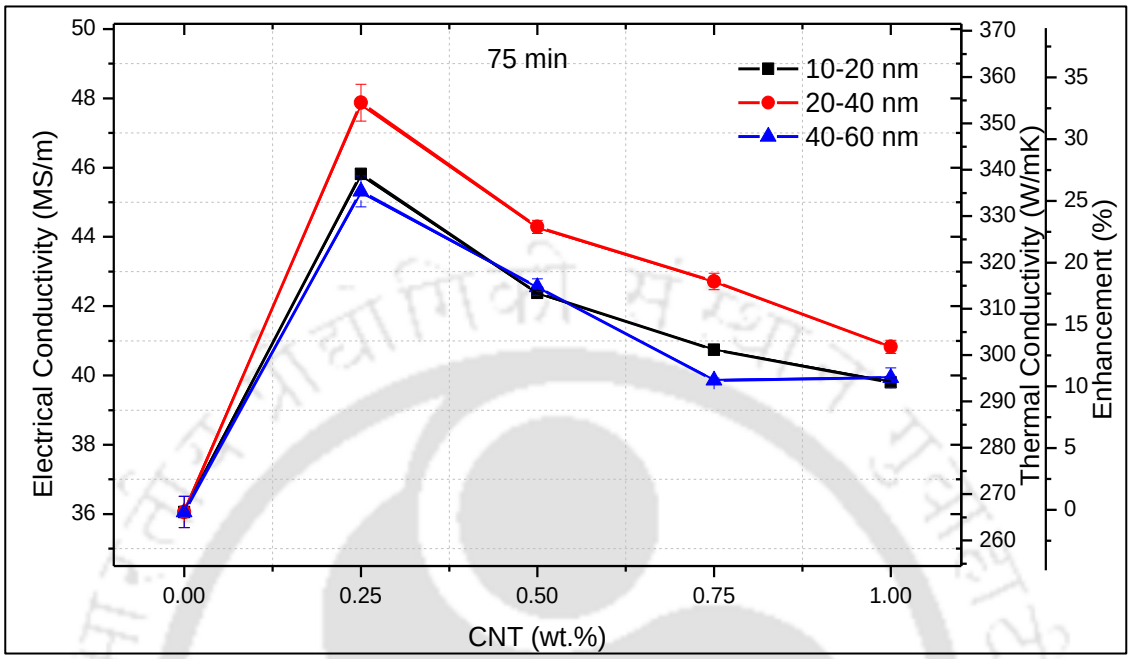

Figure 4.30 Electrical and thermal conductivity and their enhancement of UA-CS processed Cu/CNT composites having all CNT size and the sample sintered at 600 °C for 75 min.

Figure 4.31 shows the electrical conductivity of Cu/CNT composites and corresponding thermal conductivity obtained at 90 min. sintering duration for all CNT diameter. It is observed that the electrical and thermal conductivity of 0.25wt.% of 20-40 nm CNT composites are observed to be 45.2 ± 0.5 MS/m and 334 W/mK at 87% RD, respectively, at 90 min. sintering duration and their enhancement is observed to be 25% in comparison to that of pure copper. It is also observed that the conductivity of composites is observed to be converged at 1wt.% CNT irrespective of CNT size. Beyond 0.25wt.% CNT, the conductivity of the composites is found to be linearly decreased for 20-40 nm diameter CNT composites. Though the enhancement of electrical and thermal conductivity of composites is increased with sintering duration of 60 and 75 min., it is found to be reduced at 90 min. of sintering duration irrespective of CNT diameter and its concentration in comparison to that of pure copper. In case of 40-60 nm diameter CNT composites, the enhancement of electrical and thermal conductivity is observed to be less in comparison to that of 20-40 nm diameter CNT composites irrespective of sintering duration.

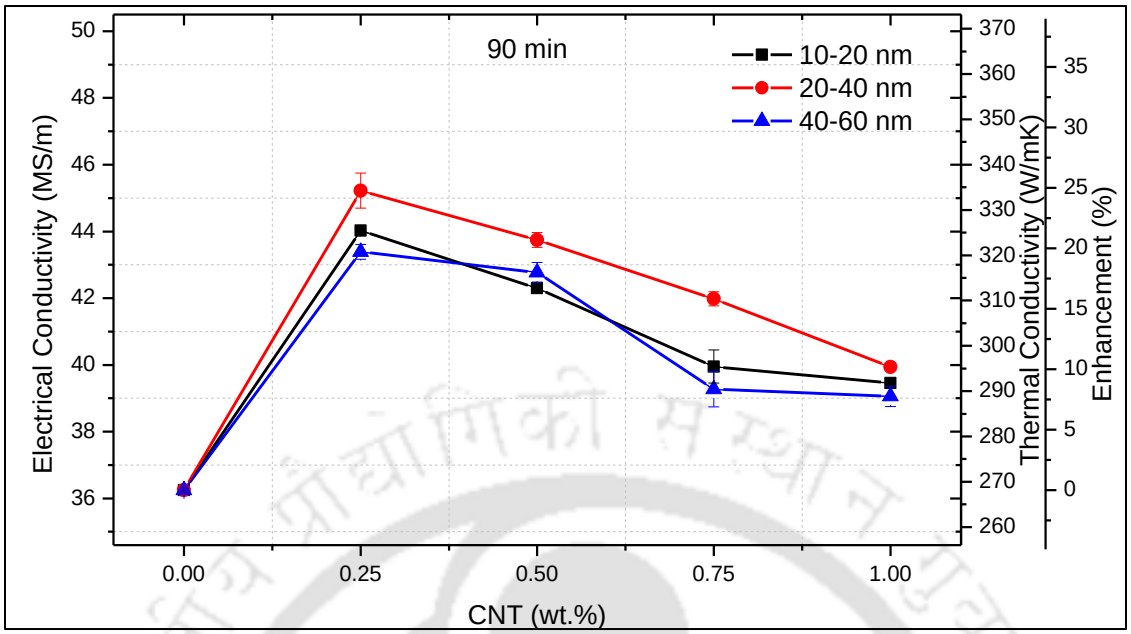

Figure 4.31 Electrical and thermal conductivity and their enhancement of UA-CS processed Cu/CNT composites having all CNT size and the sample sintered at 600 °C for 90 min.

The maximum enhancement of both electrical and thermal conductivity of Cu/CNT composites is observed under the following conditions: (i) 20-40 nm diameter CNT composites irrespective of sintering duration and CNT concentration; (ii) Samples sintered for 75 min. irrespective of CNT diameter and its concentration; (iii) 0.25wt.% CNT composites irrespective of CNT type and sintering duration. In all cases, the results are found to be improved in comparison to that of pure copper irrespective of CNT diameter, concentration and sintering duration. It is inferred from the above observation that the maximum electrical and thermal conductivity of composites are obtained at 0.25 wt.% of 20-40 nm diameter CNT composites sintered at 75 min. duration. As the trend noticed on the conductivity of the composites is found to be similar to that of RD of the composites, it is expected to play a major role to influence the conductivity of the test sample.

An increase of electrical conductivity of Cu/CNT composites is observed till 0.25 wt.% CNT irrespective of sintering duration and diameter of CNT, which could be due to free electron conduction of copper and phonon conduction of CNT, and the same is also supported by Cho *et al*. [2010]. It is expected that the pairing effect of above two mechanisms is expected to increase the electrical conductivity of composites. At 0.25wt.%, the interaction between CNT with copper is expected to be higher due to their chemical bonding, which accelerated the electrons to conduct either current or heat in any possible direction. Thus,

the Cu/CNT composites at 0.25 wt.% have the highest electrical conductivity in comparison to that of other composites. When the CNT concentration is increased beyond 0.25 wt.%, the mobility of free electrons is expected to be restricted due to severity of CNT interaction between themselves and copper leading to reduce the electrical conductivity of the composites. In addition, the random orientation of CNT and its defects are expected to generate large scattering of phonons within the grain boundaries leading to reduce the conductivity of the composites, which is observed to be the lowest in case of 90 min. sintering in comparison to that of 75 min. sintered samples irrespective of diameter of CNT and its concentration. Though the size of grain is expected to increase with sintering time and reduce the number of grain boundaries at 90 min. of sintering, the presence of large number of voids is expected to hinder the effective free electron and phonon conduction in the composites leading to reduce the enhancement of electrical and thermal conductivity.

As the grain size of Cu/CNT composites is increased with CNT diameter, and its concentration, the 40-60 nm diameter CNT composites are observed to have the highest grain size of 6.35 ± 0.12 µm in comparison to that of other composites. It is expected to have a less number of grain boundaries, which reduced the interfacial resistance among them leading to increase the electrical and thermal conductivity of composites. However, the presence of large number of voids with different sizes in 40-60 nm diameter CNT composites, which is also confirmed with reduced relative density, assisted to increase the interfacial thermal and electrical resistance and it further leads to restrict the conductivity of composite materials. As shown in **Figure 4.3**, the strain present in the 40-60 nm diameter CNT composite powder is about 1.5 times higher at 1wt.% in comparison to that of 10-20 nm and 20-40 nm diameter CNT composite. These effects are expected to induce more phonon and electron scattering leading to reduce the enhancement of electrical and thermal conductivity of the composites. Koppad *et al*. [2013] reported that the lattice strain present in the composites contributed to electron scattering leading to reduce its electrical conductivity.

Due to high aspect ratio of 10-20 nm diameter CNT composites, 666 in this case, the CNT is expected to have significant level of random orientation, non-straightness, entanglement, kinks and more defects, which are also confirmed from TEM studies**,** and the same is also supported by Chu *et al*. [2010a]. The observed defects on the CNT led to restrict the effective phonon conduction among the different grain boundaries leading to reduce the conductivity of composites. In addition, many physical defects, including entanglement

noted from TEM studies in case of 10-20 nm diameter CNT composites and reported in **Figure 4.5a-d**, are very much influencing the scattering phenomenon of phonon and thus it led to reduce the electrical and thermal conductivity of 10-20 nm diameter CNT composites. However, the composites having 20-40 nm diameter CNT are expected to have reduced defects in comparison to that of 10-20 nm diameter CNT leading to induce good coupling effect between electron and phonon conduction and increase the electrical and thermal conductivity of the composites. Due to the presence of large number of structural defects and the random orientation of CNT, as reported in FESEM studies, the overall electrical and thermal conductivity of the composites are reduced beyond 0.25 wt.% CNT due to electron and phonon scattering. Koppad *et al*. [2013] also reported that the random orientation of CNT reduced its thermal conductivity by two-order of magnitude.

4.8.2 Electrical and thermal conductivity of uniaxial compaction and microwave sintering processed Cu/CNT composites

Figure 4.32 shows the electrical and thermal conductivity of composites having different diameter of CNT and its concentrations after 60 min. of sintering at 600°C and their enhancement with respect to pure copper obtained by the same synthesis technique. It is observed that the electrical and thermal conductivity of pure copper are observed to be 35.1 ± 0.5 MS/m and 260 W/mK at 83.9% RD, respectively, and their corresponding values are reported as 49 MS/m at 96% RD, Varo and Canakci [2015] and 331 W/mK at 99% RD, Chu *et al*. [2010b]. The significant difference between the reported values of electrical and thermal conductivity of copper and that of the values observed from the present experiments might be due to the fact that the presence of large number of voids and grain boundaries are expected to reduce their electrical and thermal conductivity by obstructing the movement of free electrons. The maximum electrical and thermal conductivity of 10-20 nm, 20-40 nm and 40-60 nm diameter CNT composites are observed to be 44.1 ± 0.3 MS/m and 326 W/mK at 86.8% RD, 46.3 ± 0.1 MS/m and 345 W/mK at 89.1% RD and 43.9 ± 0.3 MS/m and 325 W/mK at 87.5% RD, respectively at 0.25wt.% CNT concentration. It is also noted that the electrical and thermal conductivity of 10-20 nm and 40-60 nm diameter CNT composites are observed to be within the limit of experimental deviation irrespective of CNT concentration, where the maximum enhancement of conductivity is observed to be 25.5% at 0.25 wt. % and it is reduced to 11.4% at 1wt.% CNT concentration. In case of 20-40 nm diameter CNT composites, a significant influence and distinction among other types of CNT based

composites on electrical and thermal conductivity are observed, where the maximum and minimum enhancement are observed to be 32% and 16.1% at 0.25wt.% and 1wt.% CNT, respectively.

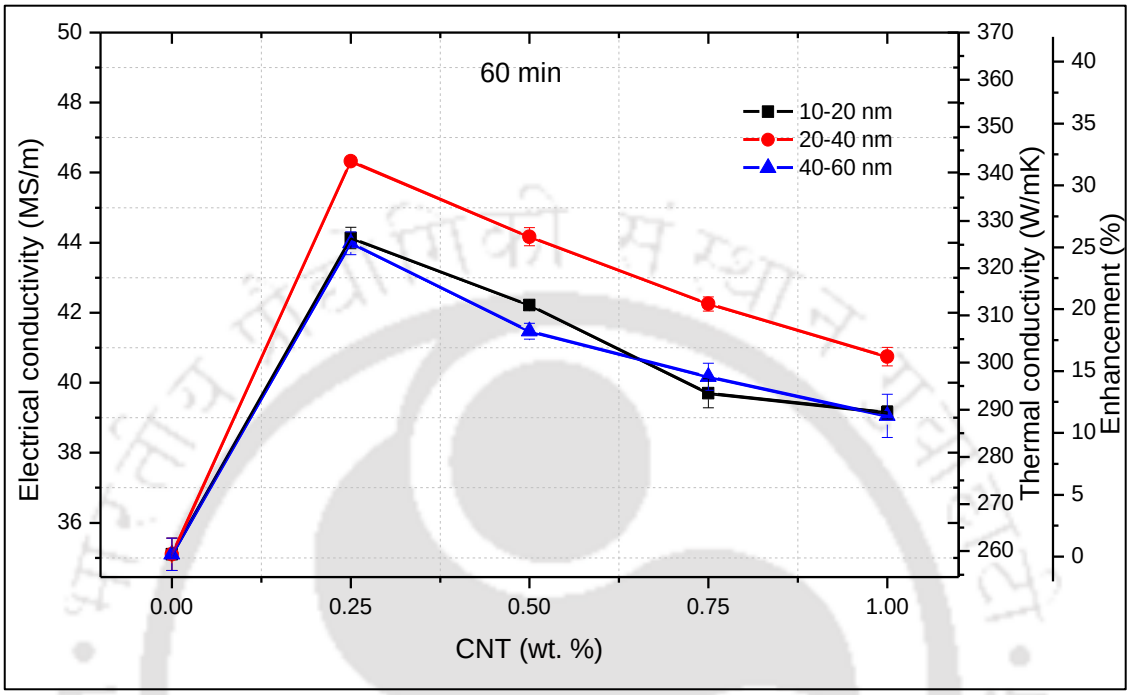

Figure 4.32 Electrical and thermal conductivity and their enhancement of UA-MW processed Cu/CNT composites having all CNT size and the sample sintered at 600 °C for 60 min.

Figure 4.33 shows the electrical and thermal conductivity of copper and Cu/CNT composites having all diameter of CNT after 75 min. of sintering, where the copper having the RD of 83.8% is observed to have the electrical and thermal conductivity of 37.1 ± 0.2 MS/m and 274.3 W/mK, respectively and these results are observed to be 24.3 and 17.1% lower than that of the data reported by Varo and Canakci [2015] and Chu *et al*. [2010a], respectively. Due to the reinforcement of 20-40 nm diameter CNT at 0.25wt.%, the maximum value of electrical and thermal conductivity of the composites is observed to be 49.3 ± 0.1 MS/m and 364.5 W/mK, respectively at 90.9% RD, which showed about 33% enhancement in comparison to that of copper. The results observed for 10-20 nm and 40-60 nm diameter CNT composites sintered at 75 min. at any CNT concentration are found to be approximately the same.

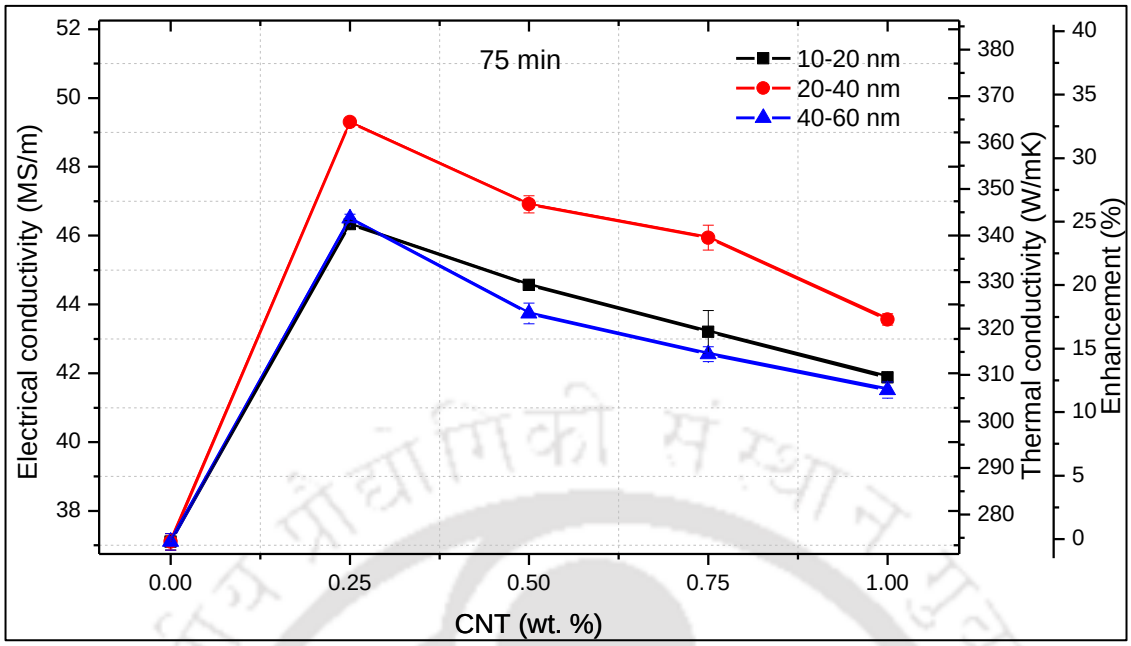

Figure 4.33 Electrical and thermal conductivity and their enhancement of UA-MW processed Cu/CNT composites having all CNT size and the sample sintered at 600 °C for 75 min.

Figure 4.34 shows the electrical and thermal conductivity of Cu/CNT composites having all diameter of CNT at 90 min. of sintering, which are observed to be 36.5 ± 0.2 MS/m and 271 W/mK, respectively at 83.9% RD for pure copper. The maximum electrical and thermal conductivity are observed to be 47.8 ± 0.3 MS/m and 353 W/mK, respectively at 0.25wt.% of 20-40 nm diameter CNT composites having the RD of 86.9% and it is about 30.2% enhancement in comparison to that of pure copper. The lowest electrical and thermal conductivity of the composite are observed to be 39.1 ± 0.4 MS/m and 289.1 W/mK at 79% RD and 1wt.% CNT of 40-60 nm composites, respectively. In addition, the enhancement reported on electrical and thermal conductivity of 0.25 wt.% composites is reduced to 50% at 1 wt.% composites, irrespective of diameter of CNT and sintering duration. In case of 10-20 nm and 40-60 nm diameter CNT, the conductivity of composites is found to be within the experimental variation.

Apart from earlier discussion on the UA-CS processed samples, it is noted from the above observation that the electrical and thermal conductivity of the composites are noted to be improved significantly, which is due to the increased relative density of the composites leading to reduce the scattering of phonon and electron and thus, the conductivity of the UA-MW processed composites for all type of CNT diameter and its concentration is observed to be improved in comparison to that of UA-CS processed Cu and Cu/CNT composites.

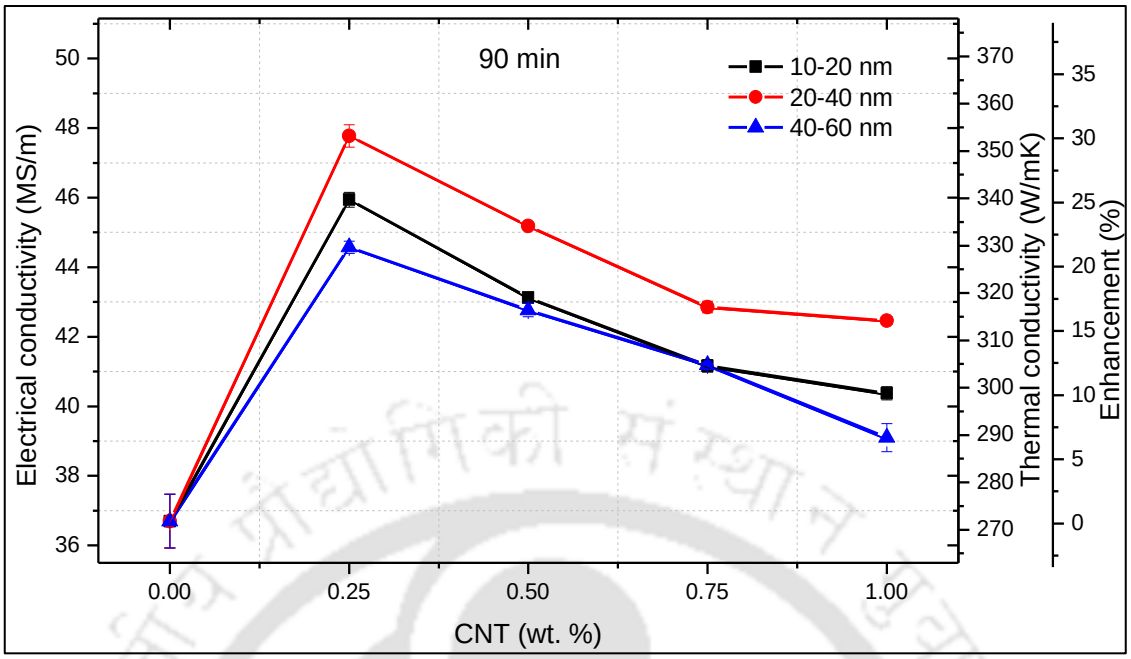

Figure 4.34 Electrical and thermal conductivity and their enhancement of UA-MW processed Cu/CNT composites having all CNT size and the sample sintered at 600 °C for 90 min.

4.8.3 Electrical and thermal conductivity of cold isostatic pressing and microwave sintering processed Cu/CNT composites

Figure 4.35 shows the thermal and electrical conductivity of Cu-CNT composites sintered at 600 °C for 60 min. of sintering duration, where the samples are processed through CIP and microwave sintering. It is observed that the electrical conductivity of pure copper is observed to be 41.9 ± 0.2 MS/m at 86.1% RD and the corresponding thermal conductivity is noted to be 310 W/mK. In general, the maximum enhancement of conductivity of composites is observed at 0.25wt.% irrespective of CNT diameter. It is also observed that the electrical and thermal conductivity of the composites are observed to be 46.9 ± 0.1 MS/m and 347 W/mK at 91.9% RD, 47.9 ± 0.1 MS/m and 355 W/mK at 92.1% RD, and 46.5 ± 0.1 MS/m and 344 W/mK at 91.2% RD, respectively, for 10-20 nm, 20-40 nm and 40-60 nm diameter CNT composites at 0.25wt.% and the corresponding enhancement is noted to be 12, 14 and 11% in comparison to that of pure copper. The electrical and thermal conductivity of the composites having 10-20 nm and 40-60 nm diameter CNT are found to be within the limit of experimental deviation in the range of 0.5 to 1wt.% CNT concentration, which are reported to be 45.5 ± 0.6 MS/m and 336.8 ± 4.1 W/mK, respectively. The conductivity of the composites having 10-20 nm and 20-40 nm CNT is observed to be converged at

0.75wt.% and follows the same decreasing trend upto 1wt.%. In case of 0.75wt.% of 40-60 nm diameter CNT composites, the results are observed to be within the experimental deviation of 1wt.%. In addition, the trend noticed on electrical and thermal conductivity of composites is found to be similar to that of RD of the composites, which is inferred to be one of the major influencing factors on these characteristics.

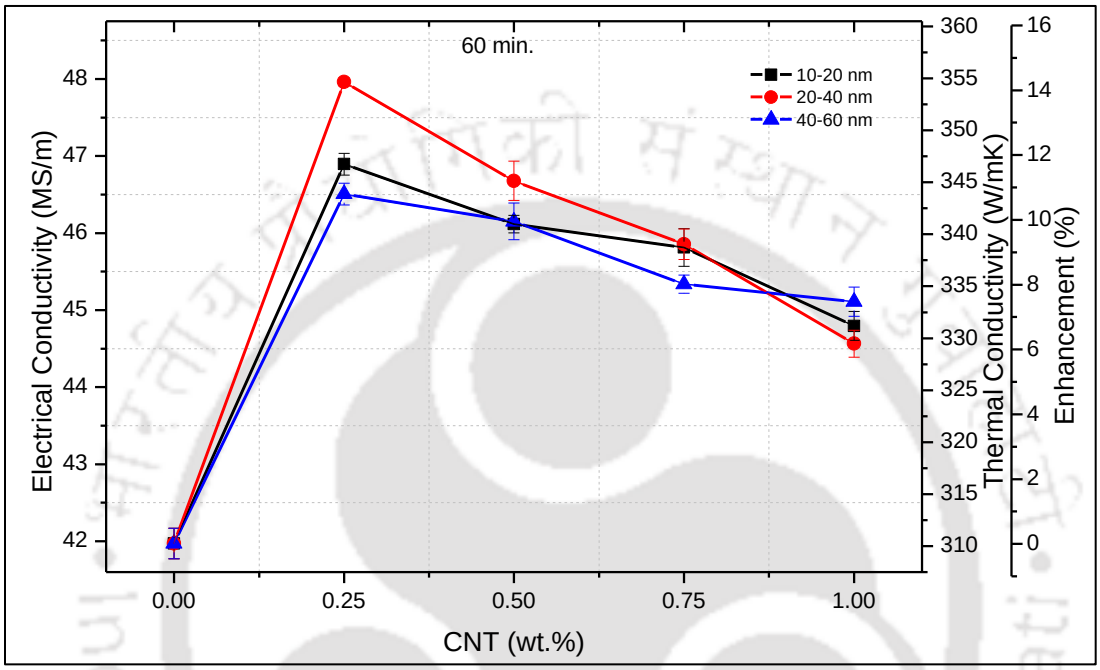

Figure 4.35 Electrical and thermal conductivity and their enhancement of CIP-MW processed Cu/CNT composites having all CNT size and the sample sintered at 600 °C for 60 min.

Figure 4.36 shows the electrical and thermal conductivity of Cu/CNT composites having 10-20 nm, 20-40 nm and 40-60 nm diameter CNT with different concentrations, which are sintered for 75 min. at 600 °C and their corresponding enhancement in comparison to that of pure copper. It is observed that the electrical conductivity of pure copper is observed to be 42.2 ± 0.1 MS/m at 87.5% RD and its thermal conductivity is noted to be 312 W/mK. It is also observed that the maximum electrical conductivity of the composites is observed to be 48.4 ± 0.1 MS/m at 92.9% RD, 50.4 ± 0.2 MS/m at 93.8% RD and 47.7 ± 0.2 MS/m at 92.5% RD, respectively, at 0.25wt.% for 10-20 nm, 20-40 nm and 40-60 nm diameter CNT composites and their corresponding thermal conductivity and enhancement are noted to be 358 W/mK and 15%, 373 W/mK and 20%, and 353 W/mK and 13%. The conductivity of 40-60 nm diameter CNT composites is observed to be saturated beyond 0.75wt.% CNT concentration, whereas the same trend is noticed from 0.5wt.% of CNT

onwards in case of 10-20 nm diameter CNT composites. It is observed that the 20-40 nm diameter CNT based composites showed a decreasing trend beyond 0.25wt.% concentration. The lowest value of electrical and thermal conductivity of the composites is observed to be 44.9 ± 0.2 MS/m and 333 W/mK at 88.2% RD, respectively, at 1wt.% of 40-60 nm diameter CNT and the corresponding enhancement is observed to be 6.7% in comparison to that of pure copper. The conductivity of 40-60 nm diameter CNT composites is noted to be the lowest in comparison to that of 10-20 nm and 20-40 nm diameter CNT irrespective of their concentration. It is inferred that the increase in sintering time is significantly influenced the results in comparison to that of 60 min. sintered composites irrespective of CNT size and it concentration.

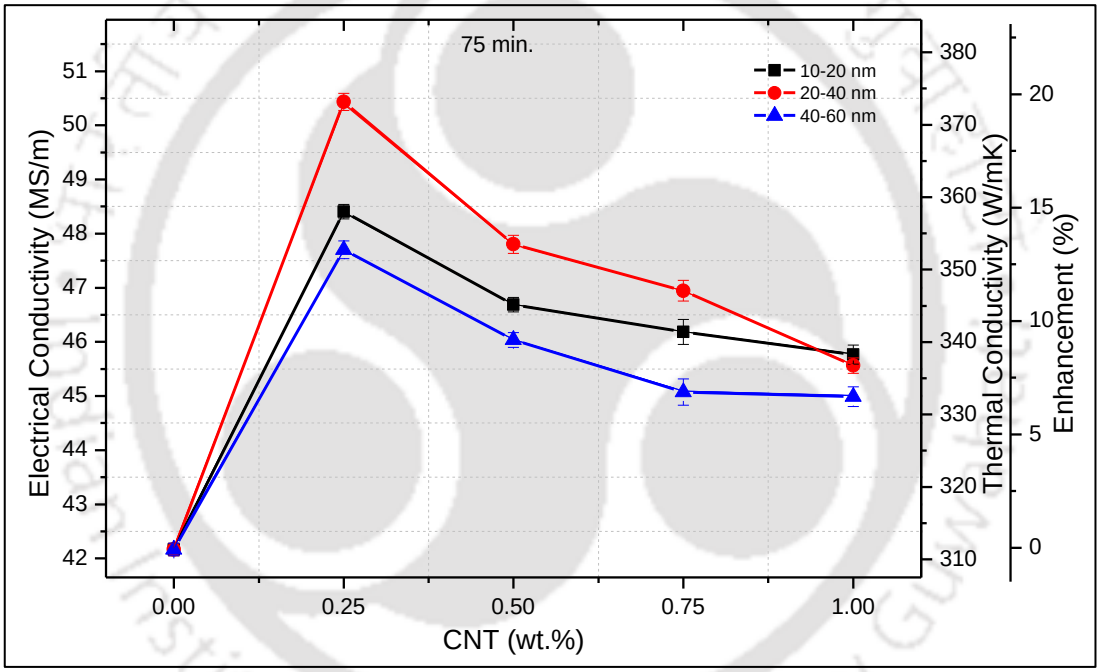

Figure 4.36 Electrical and thermal conductivity and their enhancement of CIP-MW processed Cu/CNT composites having all CNT size and the sample sintered at 600 °C for 75 min.

Figure 4.37 shows the electrical and thermal conductivity of the Cu/CNT composites sintered at 600 °C for 90 min. sintering duration for all CNT diameter against its concentration. It is observed that the maximum electrical and thermal conductivity of the composites are observed to be 47.5 ± 0.2 MS/m and 352 W/mK at 91.9% RD, 48.7 ± 0.1 and 360 W/mK at 93.1% RD and 46.5 ± 0.1 MS/m and 344 W/mK at 91.3% RD at 0.25wt.% CNT, respectively, for 10-20 nm, 20-40 nm and 40-60 nm diameter CNT and their corresponding enhancement is noted to be 13, 16 and 11% in comparison to that of pure

copper. It is also noted that the conductivity of the composites for all types of CNT diameter followed a similar trend irrespective of CNT concentration. The 40-60 nm diameter CNT composites observed to show the lowest value of conductivity similar to that of other sintering duration irrespective of CNT concentration in comparison to that of 10-20 nm and 20-40 nm CNT diameter. It is also observed that the average enhancement of conductivity of the composites is noted to be 7.6% irrespective of CNT concentration except at 0.25wt.%. It is inferred that the CNT diameter, its concentration and sintering duration are found to influence the conductivity of the composites.

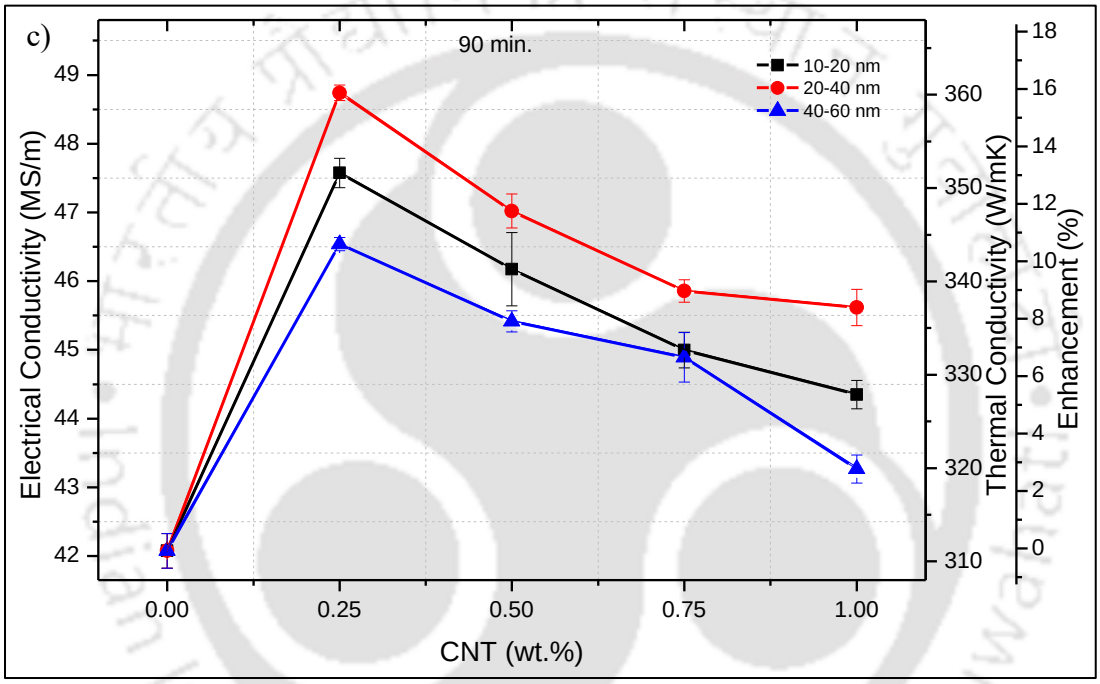

Figure 4.37 Electrical and thermal conductivity and their enhancement of CIP-MW processed Cu/CNT composites having all CNT size and the sample sintered at 600 °C for 90 min.

In general, the value of electrical and thermal conductivity of the composites having 10-20 nm and 40-60 nm diameter CNT are found to be within 5% deviation irrespective of sintering duration and CNT concentration, whereas the 20-40 nm diameter CNT reinforced composites showed a significant improvement in all types of composites. The maximum conductivity of the composites and its enhancement are noted at 0.25wt.% of all types of CNT diameter irrespective of sintering duration. In all cases of sintering duration, the electrical and thermal conductivity of composites are increased up to 0.25wt% CNT and then linearly decreased against the concentration till 1 wt.% CNT.

In addition to earlier discussion, the electrical and thermal conductivity of CIP-MW processed composites are found to be significant in comparison to that of UA-CS and UA-MW processed composites due to improved relative density of the composites. It is also found that the conductivity of composites having 20-40 nm diameter CNT is observed to be the highest irrespective of processing technique in comparison to that of 10-20 nm and 40-60 nm diameter CNT composites. It is also noted that the conductivity of the copper and Cu/CNT composites irrespective of CNT type and its concentration is found to be influenced by the compaction technique and sintering process followed to prepare the composites.

4.9 Comparison of best characteristics of Cu/CNT composites obtained from the different processing techniques

4.9.1 Relative density of Cu/CNT composites

In order to study the influence of different processing techniques on the RD of composites, the best results of RD obtained from CIP-MW, UA-MW and UA-CS processed samples are compared and shown in **Figure 4.38**. Based on earlier discussion made in **section 4.4**, it is noted that the samples sintered at 75 min. irrespective of CNT size and its concentration observed to show the best results among other samples. Thus, the results obtained for these samples are considered in this study. **Figures 4.38** shows the RD of composites reinforced with 10-20 nm, 20-40 nm and 40-60 nm diameter CNT, obtained at 75 min. of sintering duration for all kind of processing techniques reported in the present study. It is observed from **Figure 4.38a** that the RD of 10-20 nm diameter CNT composites is observed to be maximum at 0.25wt.% and then it is decreased irrespective of compaction and sintering technique. The maximum RD of copper is observed to be 87.6% for CIP-MW processed sample, whereas the same for CIP-MW, UA-MW and UA-CS processed composites having 0.25wt.% of 10-20 nm diameter CNT is observed to be 92.9, 87.1 and 85.3%, respectively. The RD of composites obtained through UA-MW and UA-CS technique at 0.5wt.% is at par with that of pure copper obtained by the respective technique and the same for the samples having 0.75 and 1wt.% is observed to be converged at 81.2 ± 1.2%, which confirmed the insignificant influence of these processing techniques on the RD of composites. In addition, these results are observed to be lower than that of pure copper samples. In case of CIP-MW processing technique, the RD of composites showed superior performance in comparison to that of samples processed by other techniques, where the RD of copper is observed to be 87.6% and it is increased to 92.9% with the addition of 0.25wt.%.

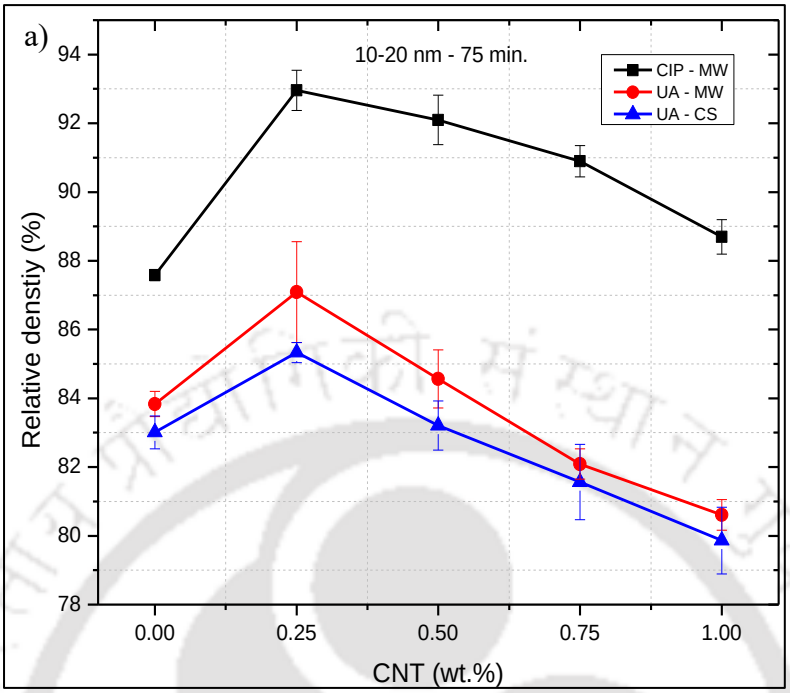

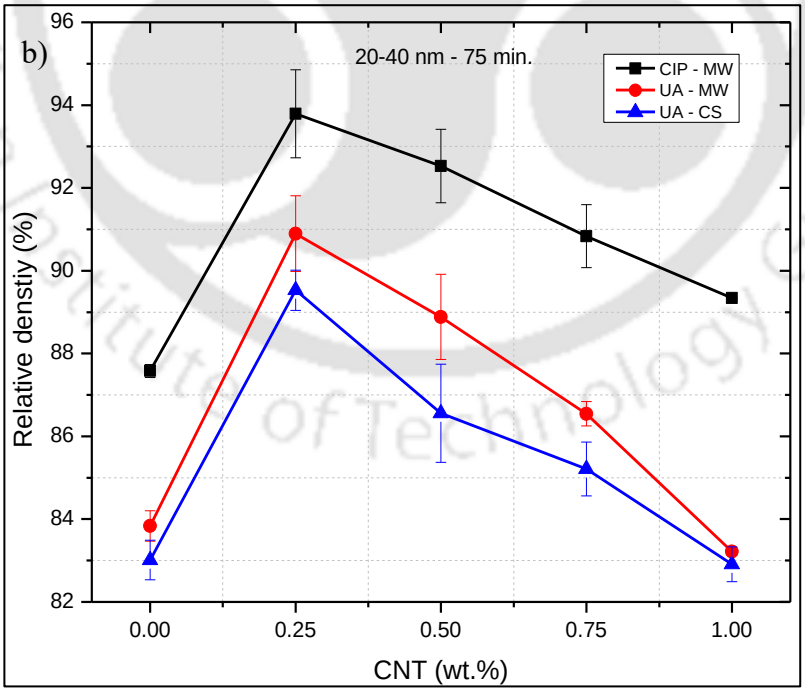

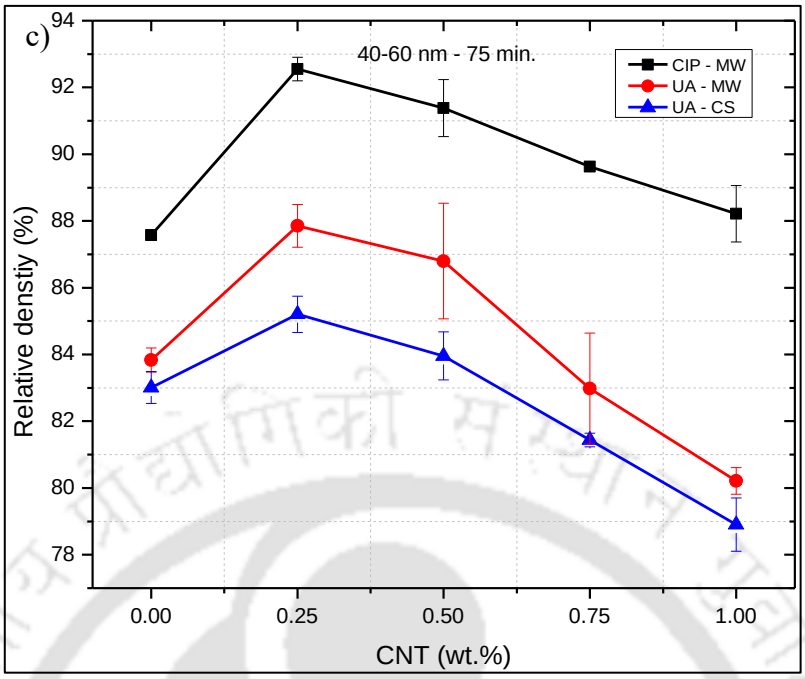

Figure 4.38 Comparison of relative density of Cu/CNT composites processed through CIP-MW, UA-MW and UA-CS sintered at 600 °C for 75 min. and having a) 10-20 nm, b) 20-40 nm, and c) 40-60 nm diameter CNT

Figures 4.38b and **4.38c** show the RD of 20-40 nm and 40-60 nm diameter CNT based composites obtained through CIP-MW, UA-MW and UA-CS sintered at 600 °C for 75 min., respectively. It is noted from **Figure 4.38b** that the RD of copper is observed to be 83.4 ± 0.4 % for UA-MW and UA-CS processed sample. The highest RD of composites is observed to be 93.8, 90.9 and 89.5% for CIP-MW, UA-MW and UA-CS processed 0.25wt.% CNT, 600 °C and 75 min. sintered samples, respectively. Though the RD of composites obtained from UA-MW and UA-CS processing technique has shown significant difference between 0.25 to 0.75wt.% of CNT, no influence is observed at 0 and 1wt.% CNT. The RD of 1wt.% composites obtained by these two techniques is observed to be converged and at par with that of pure copper. However, the RD of 20-40 nm diameter CNT reinforced composites obtained from CIP-MW processing technique is noted to be superior in comparison to that of other composites irrespective of CNT concentration, which is not observed in other processing techniques and other CNT size.

It is observed from **Figure 4.38c** that the maximum RD of composites is observed to be 92.6% for the sample obtained through CIP-MW, whereas the sample processed through UA-MW and UA-CS technique showed the RD in the range of 86.6 ± 1.9%. In addition, the trend observed in case of RD of 40-60 nm and 10-20 nm diameter CNT based composites is

observed to very similar. In case of CIP-MW processed samples, the RD of composites showed the average enhancement of 5, 7, 9 and 11% in comparison to that of UA-MW and UA-CS processed sample having 0.25, 0.5, 0.75 and 1.0 wt.% CNT, respectively.

Overall, it is observed from **Figure 4.38** that the RD of 20-40 nm diameter CNT composites is reported to be maximum at 0.25wt.% CNT in comparison to that of 10-20 nm and 40-60 nm diameter CNT reinforced composites irrespective of processing techniques followed to prepare the composites. Though the trend followed on the RD of composites is observed to be the same irrespective of processing techniques, the RD of UA-CS sample is observed to be the lowest and it is increased when the sintering technique is changed from conventional sintering to microwave sintering technique. Further, the RD of test samples is increased when the sample is processed through CIP-MW technique. These observations are noticed irrespective of sintering duration, CNT size and its concentration. In case of UA-MW and UA-CS compacted samples, the RD of the composites, except 20-40 nm diameter CNT composites, having 0.75 and 1.0wt.% CNT is observed to be lower than that of pure copper and it is approximately the same at 0.5wt.% CNT concentration. The RD of CIP-MW processed samples showed improved performance in comparison to that of UA-MW and UA-CS processed samples irrespective of CNT diameter and its concentration. It is inferred that the selection of a suitable consolidation and sintering technique played an important role to obtain the desired RD of the composites irrespective of sintering duration, CNT diameter and its concentration.

4.9.2 Grain size of copper and Cu/CNT composites

Table 4.4 reports the comparison of average grain size of pure copper and 0.25 and 1.0 wt.% CNT reinforced Cu composites having all diameter of CNT processed through CIP-MW, UA-MW and UA-CS at 75 min. of sintering duration. The obtained grain size of Cu/CNT composites at any CNT type and its concentration is found to be within the experimental deviation irrespective of processing techniques. It is noticed that the grain size of composites is increased with CNT concentration and its diameter in all processing techniques. In comparison with pure copper, the enhancement of average grain size of Cu-0.25wt.% CNT composites is observed to be 4.1 ± 2.5, 9.2 ± 2.8 and 13.4 ± 3.5% for 10-20 nm, 20-40 nm and 40-60 nm diameter CNT reinforced composites, respectively, and the corresponding enhancement at Cu- 1wt.% CNT composites is noted to be 37 ± 1.1, 41.8 ± 1.7 and 52.6 ± 3.4% irrespective of sintering time and processed technique.

Table 4.4 Comparison of grain size of Cu and Cu-CNT composite samples obtained at 60, 75 and 90 min. sintering duration through CIP-MW, UA-MW and UA-CS processing techniques

CNT size (nm)	Grain size (μm)						Sintering duration (min.)
	UA-CS		UA-MW		CIP-MW		
	0.25wt.% CNT	1.0wt.% CNT	0.25wt.% CNT	1.0wt.% CNT	0.25wt.% CNT	1.0wt.% CNT	
Cu	4.02 ± 0.02						60
10-20	4.29 ± 0.12	5.56 ± 0.09	4.15 ± 0.12	5.51 ± 0.09	4.06 ± 0.05	5.45 ± 0.07	
20-40	4.47 ± 0.10	5.71 ± 0.30	4.30 ± 0.08	5.65 ± 0.05	4.26 ± 0.11	5.61 ± 0.13	
40-60	4.70 ± 0.07	6.25 ± 0.10	4.45 ± 0.06	6.05 ± 0.08	4.47 ± 0.09	5.95 ± 0.04	
Cu	4.05 ± 0.11						75
10-20	4.32 ± 0.08	5.59 ± 0.13	4.21 ± 0.07	5.56 ± 0.11	4.11 ± 0.05	5.51 ± 0.09	
20-40	4.56 ± 0.16	5.78 ± 0.02	4.40 ± 0.13	5.78 ± 0.05	4.33 ± 0.09	5.69 ± 0.03	
40-60	4.75 ± 0.07	6.32 ± 0.05	4.55 ± 0.06	6.11 ± 0.07	4.49 ± 0.10	6.05 ± 0.02	
Cu	4.11 ± 0.07						90
10-20	4.39 ± 0.10	5.74 ± 0.07	4.30 ± 0.10	5.65 ± 0.11	4.19 ± 0.07	5.60 ± 0.10	
20-40	4.65 ± 0.11	5.98 ± 0.10	4.52 ± 0.04	5.88 ± 0.08	4.42 ± 0.10	5.75 ± 0.06	
40-60	4.84 ± 0.10	6.49 ± 0.06	4.62 ± 0.07	6.31 ± 0.12	4.55 ± 0.08	6.25 ± 0.05	

The grain size at 1wt.% composites is observed to be about 32.1 ± 1.7% larger than that of 0.25wt.% composites for all diameter of CNT irrespective of processing techniques followed to prepare the composites. The highest grain size of composites is noted at 1wt.% of 40-60 nm diameter CNT composites obtained through UA-CS and it showed about 60% higher in comparison to that of pure copper at 90 min. of sintering and the corresponding enhancement of grain size is limited to 54.5% in case of UA-MW and CIP-MW processed samples. It is also noted that the grain size of CIP-MW processed samples is observed to be the least for the same concentration in comparison to that of the samples obtained through UA-CS and UA-MW techniques. It is inferred that the processing technique followed to prepare the composites is found to play a significant role on the grain size of composites in addition to sintering duration irrespective of CNT size and its concentration.

4.9.3 Hardness of copper and Cu/CNT composites

As the hardness of the composites is observed to be maximum at 75 min. of sintering duration irrespective of processing techniques, a comparison is made among the results obtained through UA-MW, UA-CS and CIP-MW and it is shown in **Figure 4.39**. The test sample having 0.25wt.% CNT concentration at a specific CNT size showed the hardness within 5% deviation irrespective of processing techniques. In addition, the maximum hardness of the composites is noted at 0.25wt.% for 40-60 nm diameter CNT irrespective of processing techniques used to develop the composites. It is also noted that the average hardness of 40-60 nm diameter CNT composites is noted to be about 13 and 7% higher in comparison to that of 10-20 nm and 20-40 nm diameter CNT composites, respectively, at any CNT concentration and consolidation technique. At 1.0wt.% CNT, the hardness of composites obtained through CIP-MW, UA-MW and UA-CS is observed to be 68.3 ± 0.8, 61.6 ± 0.8 and 65.1 ± 1.4 VHN, respectively, irrespective of CNT diameter. In case of CIP-MW technique, the hardness of composites having 0.5 to 1wt.% is noted to be significantly increased in comparison to that of UA-MW and UA-CS processed composites. It is inferred that the compaction technique, sintering technique and selection of CNT diameter are found to play a significant role to enhance the hardness of the composites.

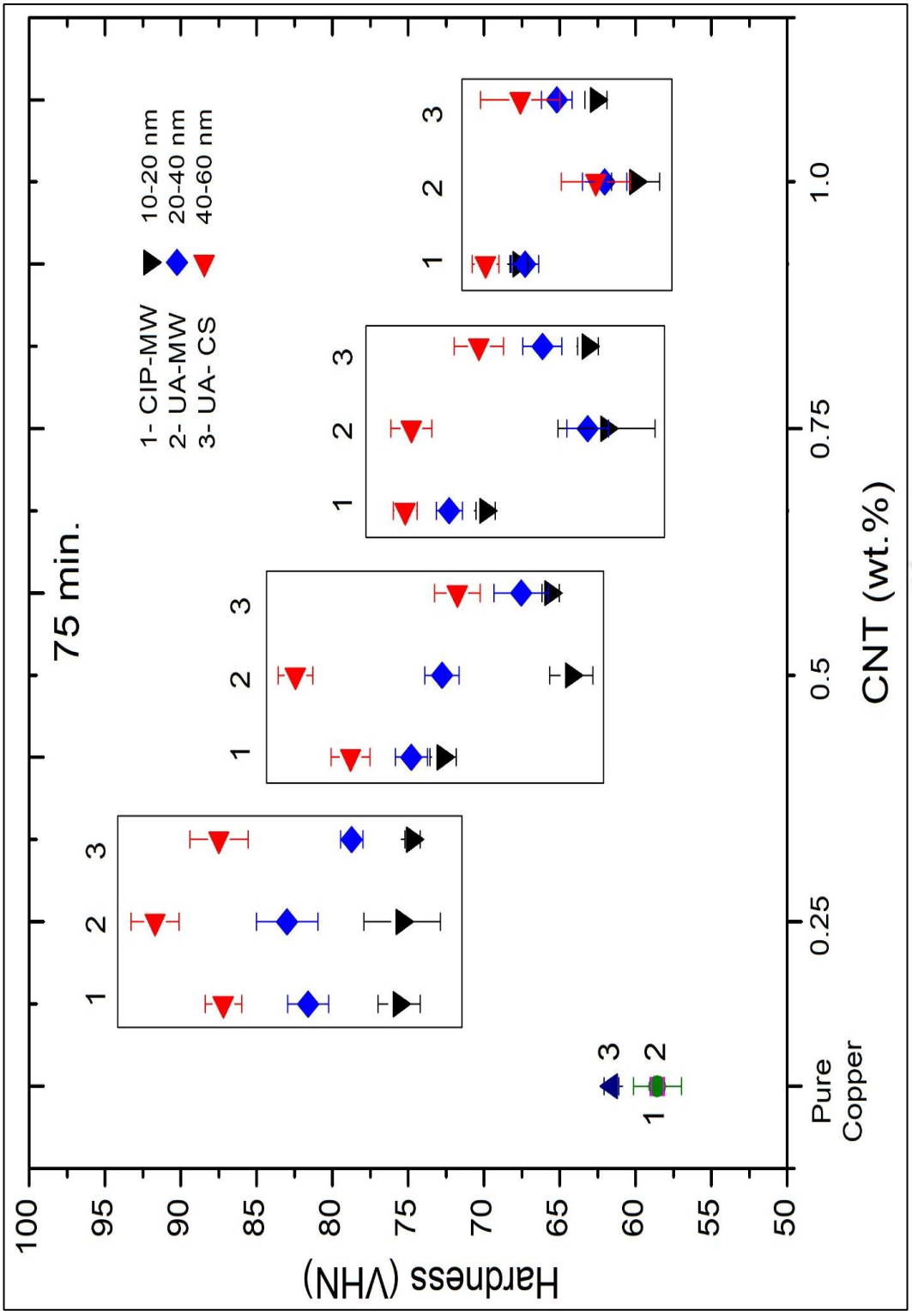

Figure 4.39 Comparison of hardness of Cu and Cu/CNT composite samples obtained through CIP-MW, UA-MW and UA-CS processing techniques at 75 min. sintering duration

4.9.4 Hardness and grain size of copper and Cu/CNT composites

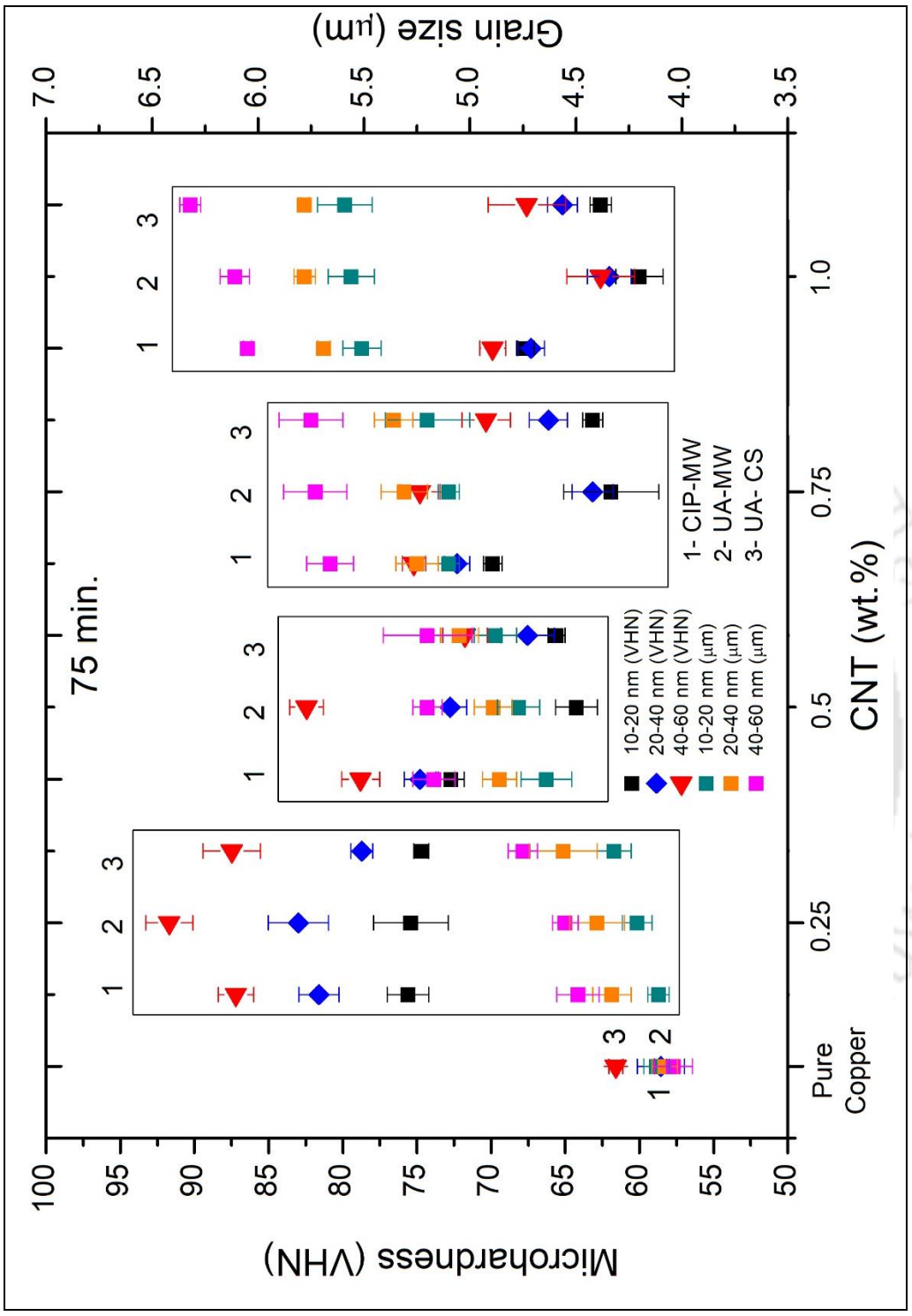

Figure 4.40 Relationship between hardness and grain size of Cu/CNT composites samples obtained through CIP-MW, UA-MW and UA-CS processing techniques at 75 min. sintering duration

Figure 4.40 shows the hardness and grain size of the composites for all types of CNT and processing techniques at 75 min. of sintering duration. It is observed that the hardness of the composites at 0.25wt.% is noted to be maximum, where the grain size is noticed to be the least in comparison to that of rest of CNT concentration irrespective of processing

techniques. In addition, the hardness of the composites is also observed to be decreased with an increase of grain size irrespective of CNT type, its concentration and processing techniques. It is noted that the hardness of the composites is noted to be inversely proportional to the grain size and thus, the Hall-Petch relation is found to be valid in all the cases of the composites, Deng *et al*. [2017]. It is also noticed that the grain size of the composites is found to be decreased in the order of UA-CS, UA-MW and CIP-MW.

4.9.5 Thermal conductivity of copper and Cu/CNT composites

The thermal conductivity of Cu-CNT composites obtained through CIP-MW, UA-MW and UA-CS processing technique is compared in order to understand the influence of different compaction and sintering techniques and the results are shown in **Figure 4.41.** The thermal conductivity of pure copper obtained through CIP-MW is observed to be 312 W/mK at 87.5% RD, which is noted to be 14 and 17% more in comparison to that of UA-MW and UA-CS processed sample, respectively, and their corresponding thermal conductivity is noted to be 274 W/mK at 84% RD, Vignesh Babu and Kanagaraj [2018] and 266.6 W/mK at 83% RD. It is also observed that the thermal conductivity of pure copper obtained through SPS technique is reported to be 331 W/mK at 99% RD, Chu *et al*. [2010a], which is about 6% higher than that the results obtained from the present study. It is inferred that the presence of a good number of grain boundaries and voids in the sintered product played a significant role on reducing the thermal conductivity of pure copper irrespective of processing techniques. The maximum thermal conductivity of Cu-1 vol.% CNT composites is reported to be 359.2 W/mK, Cho *et al*. [2010] and 327.9 W/mK, Nie *et al*. [2012] for 20-70 nm and 20-30 nm diameter CNT reinforced composites, respectively at 99% RD, whereas the thermal conductivity of 1 vol.% of 9.5 nm CNT reinforced composites is noted to be 273 W/mK, Sule *et al*. [2014]. It is observed from our studies that the thermal conductivity of composites obtained from CIP-MW at 1.23 vol.% is found to have the maximum enhancement of 5.6% irrespective of CNT diameter in comparison to that of UA-MW and UA-CS processed samples. The maximum thermal conductivity of CIP-MW processed Cu/CNT composites having 1.23 vol.% is noted to be 357.8, 372.8, 352.6 W/mK, respectively, for 10-20 nm, 20-40 nm and 40-60 nm diameter CNT composites, whereas the corresponding results obtained from UA-MW technique are noted to be 342.5, 364.5 and 343.8 W/mK, Vignesh Babu and Kanagaraj [2018] and the UA-CS technique showed the results of 338.7, 353.9 and 335 W/mK, respectively.

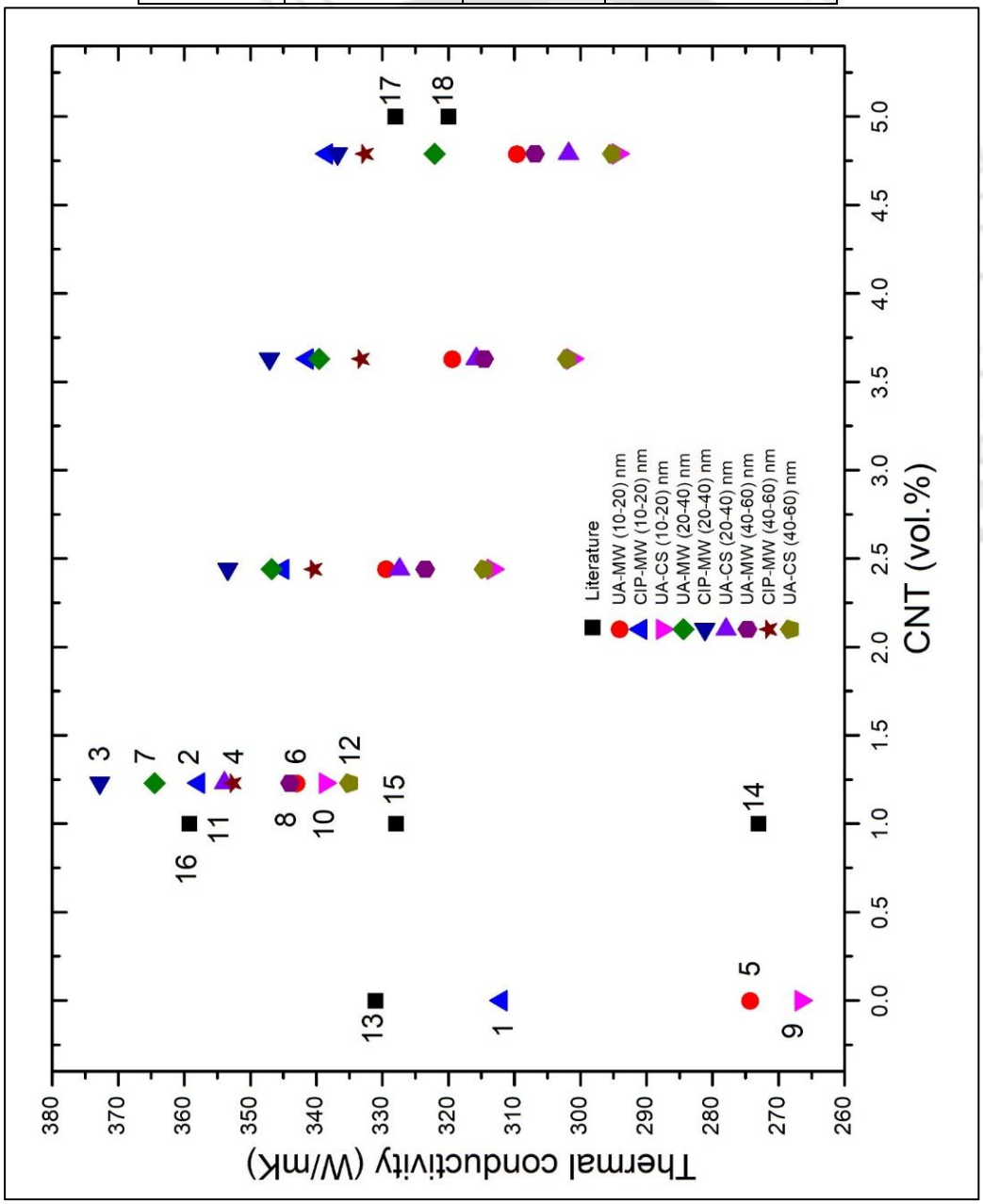

1. Pure Cu - 87.5 % RD 2.10-20 nm - 92.9 % RD 3. 20-40 nm - 93.8 % RD 4. 40-60 nm - 92.5 % RD	Experimental data CIP 300 MPa MW @ 600 °C
5. Pure Cu - 84 % RD 6. 10-20 nm - 87.1 % RD 7. 20-40 nm - 91 % RD 8. 40-60 nm - 87.9 % RD	Experimental data Vignesh Babu et.al (2018) UA 800 MPa MW @ 600 °C
9. Pure Cu - 83 % RD 10. 10-20 nm - 85.3 % RD 11. 20-40 nm - 89.5 % RD 12. 40-60 nm - 85.2 % RD	Experimental data UA 800 MPa CS @ 600 °C
13. (Chu *et al.* 2010a) – 99 % RD- SPS 40-60 MPa. 14. (Sule *et al.* 2014) - 10 nm- 96.8-99 % RD- SPS 15. (Nie *et al.* 2012) - 20-30 nm- 99 % RD- SPS. 16. (Cho *et al.* 2010) - 20-70 nm- 96.8-99% RD- SPS 17. (Chu *et al.* 2010a) - 10-30 nm- 99 % RD- SPS. 18. (Chu *et al.* 2010b) - 10-20 nm- 98.8 % RD- SPS	

Figure 4.41 Comparison of thermal conductivity of Cu/CNT composites obtained through different processing techniques along with literature

It is also observed that the thermal conductivity of CIP-MW composites having 4.79 vol.% CNT showed about 10% improvement in comparison to that of UA-MW and UA-CS processed samples at the same concentration. It is noted from the literature that the composites having 5 vol.% showed the thermal conductivity of 320 W/mK, Chu *et al*. [2010b] and 328 W/mK, Chu *et al*. [2010a] at 99% RD for 10-30 nm and 10-20 nm diameter CNT reinforced composites, respectively, where the samples are obtained through SPS technique.It is inferred from the above discussion that an increase of CNT concentration beyond an optimum value is found to reduce the thermal conductivity of composites irrespective of CNT diameter and processing technique followed to prepare the composites. It is also noted that the obtained results irrespective of processing techniques are at par with highly expensive and high end consolidation process i.e. SPS technique.

4.9.6 Overall comparison of best characteristics of Cu/CNT composites

Figure 4.42 shows the comparison best results obtained from the present study on the RD, hardness, electrical conductivity and thermal conductivity of the composites having 0.25wt.% CNT sintered at 600 °C for 75 min. for all types of CNT and processing techniques. The maximum electrical and thermal conductivity of UA-CS, UA-MW and CIP-MW processed 20-40 nm diameter CNT composites are observed to be 47.8 MS/m and 353.9 W/mK at 89.5%, 49.3 MS/m and 364.5 W/mK at 90.9%, and 50.4 MS/m and 372.8 W/mK at 93.8%, respectively, and the corresponding enhancement is noted to be 32.7, 32.8 and 19.6% in comparison to that of pure copper. It is found that the processing techniques followed to prepare the composite samples are observed to significantly influence the electrical and thermal conductivity of the composites irrespective of CNT diameter. In case of 10-20 nm and 40-60 nm diameter CNT composites, these properties are found to be very similar. In case of hardness of the composites, the maximum value is observed to be 87.5, 91.7 and 87.2 VHN for UA-CS, UA-MW and CIP-MW processed composites having 40-60 nm diameter CNT, respectively. The average enhancement of hardness of the composites is noted to be 49.1 ± 7.3%, 36.2 ± 7.4% and 26.3 ± 4.4% for 40-60 nm, 20-40 nm and 10-20 nm diameter CNT composites, respectively, irrespective of processing technique in comparison to that of pure copper. It is also noted that the hardness of 40-60 nm diameter CNT composites showed the maximum enhancement of 57% for UA-MW processed technique, which is noted to be significant in comparison to that of 10-20 nm and 20-40 nm diameter CNT composites. It is inferred that the best characteristics of the composites are

observed at 0.25wt.% and 75 min. of sintering duration irrespective of CNT size and processing techniques.

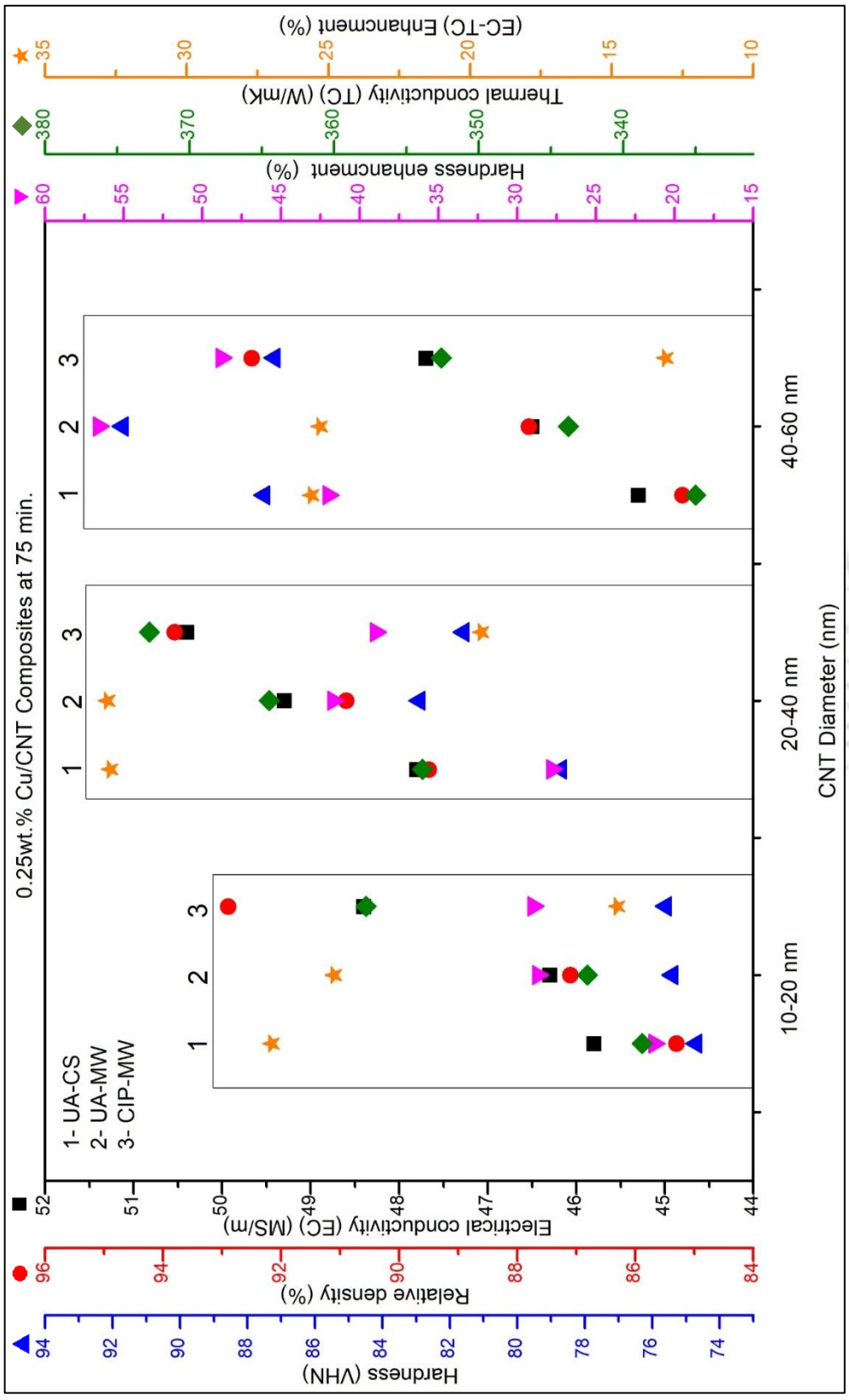

Figure 4.42 Best characteristics obtained for Cu- 0.25wt.% CNT sintered at 75min. against different processed techniques

CHAPTER 5

CONCLUSIONS

The Cu/CNT composite powder having 10-20 nm, 20-40 nm and 40-60 nm diameter CNT with different concentration of reinforcement varying from 0.25 to 1wt.% with an increment of 0.25wt.% is successfully synthesized through molecular level mixing technique and the same is tested using several characterization techniques. The pure copper powder is also synthesized by the same technique and these results are used as reference data. The sintering kinetics of Cu and Cu/CNT composites are studied in order to obtain suitable sintering parameters. The influences of different processing techniques such as uniaxial compaction (UA), and cold isostatic press (CIP), conventional sintering (CS) and microwave sintering (MW) on the characteristics of the composites are studied and the important findings are concluded as follows:

5.1 Powder characterization of Cu/CNT composites

- The Cu/CNT composite powder synthesized through molecular level mixing technique is found to have a good encapsulation of CNT by copper.
- The homogenous dispersion of CNT in Cu matrix and the presence of chemical bonding between the matrix and reinforcement are confirmed.
- As the thermal stability of composite powder is observed from 550 °C onwards, it gives the flexibility of sintering the same at a desired temperature without any degradation or oxidation.
- No structural change in the composite powder is observed due to the reinforcement of CNT in comparison to that of pure copper.

5.2 Sintering kinetics of Cu/CNT composites

- Diffusion time of Cu/CNT composites is reduced with an increase of sintering temperature and CNT size.
- Addition of CNT irrespective of its diameter is found to reduce the diffusion time of composites.

- Due to the presence of CNT, the diffusion process in the composites is accelerated in order to have complete diffusion of grain boundaries in short time in comparison to that of pure copper.
- When the sintering temperature and CNT size are increased, synergic effect of them helped to reduce the diffusion time significantly in comparison to that of pure copper. However, the diffusion time is not found to be varied with an increase of CNT concentration at any CNT size.

5.3 Relative density of Cu/CNT composites

- The samples sintered at 75 min. is observed to show the best results among other samples irrespective of CNT size and its concentration.
- The RD of 20-40 nm diameter CNT composites is found to be the highest in comparison to that of other CNT composites irrespective of concentration of CNT and sintering duration.
- The maximum RD of Cu/CNT composites is achieved at 0.25wt.% of CNT irrespective of diameter of CNT and sintering duration
- The RD of 10-20 nm and 40-60 nm diameter CNT composites is not significantly influenced by sintering time but the results are merged irrespective of CNT concentration.
- The RD of composites obtained through CIP-MW is observed to be superior irrespective of CNT size, its concentration and sintering duration in comparison to that of other processing techniques.
- The RD of the composites is found to be increased in the order of UA-CS, UA-MW and CIP-MW processing techniques.
- The 0.25wt.% CNT composite sample sintered at 600 °C for 75 min. showed the best characteristics of Cu/CNT composites irrespective of processing technique.

5.4 Microstructure of Cu/CNT composites

- The grain size of composites is observed to be increased with CNT diameter, CNT concentration and sintering time in comparison to that of pure copper irrespective of processing technique.
- The CIP-MW processed composites are found to have the least grain size and very less number of defects irrespective of CNT diameter, its concentration and sintering duration in comparison to that of UA-CS and UA-MW processed composites.

5.5 Hardness of Cu/CNT composites

- Irrespective of processing technique,
  - the diameter of CNT is observed to be an important variable to improve the hardness of the composites only at 0.25wt.% CNT irrespective of CNT size.
  - the hardness of the composites is observed to be maximum at 75 min. of sintering duration irrespective of CNT size and its concentration.
  - the hardness of 40-60 nm diameter CNT composites is observed to be superior in comparison to that of 10-20 nm and 20-40 nm diameter CNT composites irrespective of CNT concentration and sintering time.

5.6 Electrical and thermal conductivity of Cu/CNT composites

- The samples sintered at 75 min. showed the maximum electrical and thermal conductivity of the composites irrespective of CNT diameter and its concentration.
- The maximum conductivity is observed at 0.25wt.% CNT composites irrespective of CNT diameter and sintering duration.
- The maximum enhancement of electrical and thermal conductivity of Cu/CNT composites is observed at 20-40 nm diameter CNT composites irrespective of sintering duration and CNT concentration.
- Irrespective of CNT diameter, its concentration and sintering duration,
  - the electrical and thermal conductivity of the composites are found to be improved in comparison to that of pure copper.
  - the conductivity of the composites obtained through CIP-MW process is found to be superior in comparison to that of other processing techniques.
- The conductivity of composites obtained through CIP-MW processing technique is found to be at par with that of the results obtained through the highly expensive spark plasma sintering (SPS) technique.
- Using the proposed methodology, desirable thermal and electrical characteristics of composites can be obtained without using the high end facility, SPS.

5.7 Comparison of results obtained from all processing techniques

- The RD, electrical conductivity and thermal conductivity of 20-40 nm diameter CNT reinforced composites obtained from CIP-MW technique sintered at 600 °C for 75 min. are noted to be superior in comparison to that of pure copper irrespective of CNT concentration.

- Selection of a suitable consolidation and sintering technique is found to play an important role to obtain the desired characteristics such as relative density, dense microstructure, grain size, electrical conductivity and thermal conductivity of the composites irrespective of sintering duration, CNT diameter and its concentration.
- A trend noticed on the RD of the composites is found to be reflected on the conductivity of the composites.
- The maximum hardness of the composites is observed to be 88.8 ± 2.5 VHN at 88.5% RD for 0.25wt.% of 40-60 nm diameter CNT and 75 min. sintered composites irrespective of processing technique, which is about 57% more than that of pure copper.
- The maximum electrical and thermal conductivity of the composites are observed to be 50.4 MS/m and 372.8 W/mK at 93.8% RD, respectively, for the 0.25wt.% of 20-40 nm diameter CNT composites sintered at 600 °C for 75 min. and processed through CIP-MW technique, which is about 20% more than that of pure copper obtained by the same technique.

5.8 Future scope of the work

The findings obtained from the present work gives a foot path for the further development and improving the effectiveness of the composite materials and a product. An outline of the scope of future research is drawn and it is given below:

- The oxidation stability of the composite materials can be studied at higher working temperature in order to explore the same for high temperature applications.
- Quality of sintered products may be improved by the deformation process at different compaction pressure in CIP in order to increase the relative density, hardness and conductivity of the composite materials.
- The presence of CNT may be aligned by suitable technique in order to improve the directional properties of the composites.
- Sintering process may be performed under different pressure either uniaxial or isostatic conditions to increase the quality and the characteristics of test materials.
- An attempt may be made to develop and characterise a prototype model of different products e.g. stave, heat transfer tube and others in order to explore the same for futuristic potential industrial applications.

REFERENCES

An, X., Zhang, Yilei, Zhang, Yuxi, Yang, S., 2015. Finite element modeling on the compaction of copper powder under different conditions. Metallurgical and Materials Transactions A 46, 3744–3752.

Arnaud, C., Lecouturier, F., Mesguich, D., Ferreira, N., Chevallier, G., Estournès, C., Weibel, A., Laurent, C., 2016. High strength - High conductivity double-walled carbon nanotube - Copper composite wires. Carbon 96, 212–215.

Arribas, A.S., Bermejo, E., Chicharro, M., Zapardiel, A., Luque, G.L., Ferreyra, N.F., Rivas, G.A., 2006. Analytical applications of a carbon nanotubes composite modified with copper microparticles as detector in flow systems. Analytica Chimica Acta 577, 183–189.

Ayyappadas, C., Muthuchamy, A., Raja Annamalai, A., Agrawal, D.K., 2017. An investigation on the effect of sintering mode on various properties of copper-graphene metal matrix composite. Advanced Powder Technology. 28, 1760–1768.

Bhat, A., Balla, V.K., Bysakh, S., Basu, D., Bose, S., Bandyopadhyay, A., 2011. Carbon nanotube reinforced Cu-10Sn alloy composites: Mechanical and thermal properties. Materials Science and Engineering A 528, 6727–6732.

Bittencourt, C., Ke, X., Van Tendeloo, G., Thiess, S., Drube, W., Ghijsen, J., Ewels, C.P., 2012. Study of the interaction between copper and carbon nanotubes. Chemical Physics Letters 535, 80–83.

Burke, J.T., 1997. IR spectroscopy or hooke's law at the molecular level - A Joint freshman physics-chemistry experience. Journal of Chemical Education 74, 1213.

Cha, S.I., Kim, K.T., Arshad, S.N., Mo, C.B., Hong, S.H., 2005a. Extraordinary strengthening effect of carbon nanotubes in metal-matrix nanocomposites processed by molecular-level mixing. Advanced Materials 17, 1377–1381.

Cha, S.I., Kim, K.T., Lee, K.H., Mo, C.B., Hong, S.H., 2005b. Strengthening and toughening of carbon nanotube reinforced alumina nanocomposite fabricated by molecular level mixing process. Scripta Materialia 53, 793–797.

Chai, G., Chen, Q., 2010. Characterization study of the thermal conductivity of carbon nanotube copper nanocomposites. Journal of Composite Materials 44, 2863–2873.

Chen, P., Zhang, J., Shen, Q., Luo, G., Dai, Y., Wang, C., Li, M., Zhang, L., 2017. Microstructure and thermal conductivity of carbon nanotube reinforced Cu composites. Journal of Nanoscience and Nanotechnology 17, 2447–2452.

Cheng, B., Bao, R., Yi, J., Li, C., Tao, J., Liu, Y., Tan, S., You, X., 2017. Interface optimization of CNT/Cu composite by forming TiC nanoprecipitation and low interface energy structure via spark plasma sintering. Journal of Alloys and Compounds 722, 852–858.

Cho, S., Kikuchi, K., Miyazaki, T., Takagi, K., Kawasaki, A., Tsukada, T., 2010. Multiwalled carbon nanotubes as a contributing reinforcement phase for the improvement of thermal conductivity in copper matrix composites. Scripta Materialia 63, 375–378.

Cho, S., Takagi, K., Kwon, H., Seo, D., Ogawa, K., Kikuchi, K., Kawasaki, A., 2012. Multi-walled carbon nanotube-reinforced copper nanocomposite coating fabricated by low-pressure cold spray process. Surface and Coatings Technology 206, 3488–3494.

Chu, K., Guo, H., Jia, C., Yin, F., Zhang, X., Liang, X., Chen, H., 2010a. Thermal properties of carbon nanotube-copper composites for thermal management applications. Nanoscale Research Letters 5, 868–874.

Chu, K., Wu, Q., Jia, C., Liang, X., Nie, J., Tian, W., Gai, G., Guo, H., 2010b. Fabrication and effective thermal conductivity of multi-walled carbon nanotubes reinforced Cu matrix composites for heat sink applications. Composites Science and Technology 70, 298–304.

Ci, L., Ryu, Z., Jin-Phillipp, N.Y., Ruhle, M., 2006. Investigation of the interfacial reaction between multi-walled carbon nanotubes and aluminum. Acta Materialia 54, 5367–5375.

Colla, V., Matino, I., Branca, T.A., Fornai, B., Romaniello, L., Rosito, F., 2017. Efficient use of water resources in the steel industry. Water 9, 1–15.

Daoush, W.M., 2008. Processing and characterization of CNT / Cu Nanocomposites by powder technology. Powder Metallurgy and Metal Ceramics 47, 531–537.

Daoush, W.M., Lim, B.K., Mo, C.B., Nam, D.H., Hong, S.H., 2009. Electrical and mechanical properties of carbon nanotube reinforced copper nanocomposites

fabricated by electroless deposition process. Materials Science and Engineering A 513–514, 247–253.

Deng, H., Yi, J., Xia, C., Yi, Y., 2017. Mechanical properties and microstructure characterization of well-dispersed carbon nanotubes reinforced copper matrix composites. Journal of Alloys and Compounds 727, 260–268.

Deng, L., Eichhorn, S.J., Kao, C.-C., Young, R.J., 2011. The effective young's modulus of carbon nanotubes in composites. ACS Applied Materials & Interfaces 3, 433–440.

Deng, L., Young, R.J., Kinloch, I.A., Sun, R., Zhang, G., Noé, L., Monthioux, M., 2014. Coefficient of thermal expansion of carbon nanotubes measured by Raman spectroscopy. Applied Physics Letters 104, 051907–4.

Eksi, A.K., Varol, R., Saritas, S., 2004. Hardness and densification behaviour of cold isostatically pressed powders. Metalurgija 58, 633–636.

Esumi, K., Ishigami, M., Nakajima, A., Sawada, K., Honda, H., 1996. Chemical treatment of carbon nanotubes. Carbon 34, 279–281.

Feng, Y., Yuan, H.L., Zhang, M., 2005. Fabrication and properties of silver-matrix composites reinforced by carbon nanotubes. Materials Characterization 55, 211–218.

Gao, X., Yue, H., Guo, E., Zhang, H., Lin, X., Yao, L., Wang, B., 2016. Mechanical properties and thermal conductivity of graphene reinforced copper matrix composites. Powder Technology 301, 601–607.

Gill, P., Munroe, N., 2012. Study of carbon nanotubes in Cu-Cr metal matrix composites. Journal of Materials Engineering and Performance 21, 2467–2471.

Goudah, G., Ahmad, F., Mamat, O., 2010. Microstructural studies of sintered carbon nanotubes reinforced copper matrix composite. Journal of Engineering Science and Technology 5, 272–283.

Guiderdoni, C., Estournès, C., Peigney, A., Weibel, A., Turq, V., Laurent, C., 2011. The preparation of double-walled carbon nanotube/Cu composites by spark plasma sintering, and their hardness and friction properties. Carbon 49, 4535–4543.

He, J., Zhao, N., Shi, C., Du, X., Li, J., Nash, P., 2008. Reinforcing copper matrix composites through molecular-level mixing of functionalized nanodiamond by co-deposition route. Materials Science and Engineering A 490, 293–299.

Hippmann, S., Li, Q., Addinal, R., Volk, W., 2013. Carbon nanotubes-reinforced copper matrix composites produced by melt stirring. Proceedings of the Institution of Mechanical Engineers, Part N: Journal of Nanoengineering and Nanosystems 227, 63–66.

Huang, K., Yang, Y., Qin, Y., Yang, G., Yin, D., 2015. A new densification mechanism of copper powder sintered under an electrical field. Scripta Materialia 99, 85–88.

Huang, Z., Zheng, Z., Zhao, S., Dong, S., Luo, P., Chen, L., 2017. Copper matrix composites reinforced by aligned carbon nanotubes: Mechanical and tribological properties. Materials and Design 133, 570–578.

Iijima, S., 1991. Helical microtubules of graphitic carbon. Letters to Nature 354, 56–58.

Iron & Steel sec, 2013. Technology compendium on energy saving opportunities Iron & Steel Sector, 1–82.

Jafari, J., Givi, M.K.B., Barmouz, M., 2015. Mechanical and microstructural characterization of Cu/CNT nanocomposite layers fabricated via friction stir processing. International Journal of Advanced Manufacturing Technology 78, 199–209.

Jenei, P., Gubicza, J., Yoon, E.Y., Kim, H.S., Lábár, J.L., 2013. High temperature thermal stability of pure copper and copper-carbon nanotube composites consolidated by High Pressure Torsion. Composites Part A: Applied Science and Manufacturing 51, 71–79.

Jenei, P., Yoon, E.Y., Gubicza, J., Kim, H.S., Lábár, J.L., Ungár, T., 2011. Microstructure and hardness of copper-carbon nanotube composites consolidated by High Pressure Torsion. Materials Science and Engineering A 528, 4690–4695.

Kang, S.-J.L., 2005. Sintering densification, graingrowth and microstructure. Elsevier Butterworth-Heinemann, 3-65.

Khaleghi, E., Torikachvili, M., Meyers, M.A., Olevsky, E.A., 2012. Magnetic enhancement of thermal conductivity in copper-carbon nanotube composites produced by electroless plating, freeze drying, and spark plasma sintering. Materials Letters 79, 256–258.

Kim, K.T., Cha, S. Il, Hong, S.H., 2007. Hardness and wear resistance of carbon nanotube reinforced Cu matrix nanocomposites. Materials Science and Engineering A 448–451, 46–50.

Kim, K.T., Cha, S. Il, Hong, Seong Hyeon, Hong, Soon Hyung, 2006. Microstructures and tensile behavior of carbon nanotube reinforced Cu matrix nanocomposites. Materials Science and Engineering A 430, 27–33.

Kim, K.T., Eckert, J., Liu, G., Park, J.M., Limd, B.K., Hong, S.H., 2011. Influence of embedded-carbon nanotubes on the thermal properties of copper matrix nanocomposites processed by molecular-level mixing. Scripta Materialia 64, 181–184.

Kim, K.T., Eckert, J., Menzel, S.B., Gemming, T., Hong, S.H., 2008. Grain refinement assisted strengthening of carbon nanotube reinforced copper matrix nanocomposites. Applied Physics Letters 92, 121901–3.

Kittel, C., 2005. Introduction to solid state physics. JohnWiley & Sons, Inc. 157.

Koppad, P.G., Rama, H.R.A., Ramesh, C.S., Kashyap, K.T., Koppad, R.G., 2013. On thermal and electrical properties of multiwalled carbon nanotubes/copper matrix nanocomposites. Journal of Alloys and Compounds 580, 527–532.

Korzhavyi, P.A., Soroka, I.L., Isaev, E.I., Lilja, C., Johansson, B., 2012. Exploring monovalent copper compounds with oxygen and hydrogen. Proceedings of the National Academy of Sciences 109, 686–689.

Kretsis, G., Johnson, A.F., 2018. Conceptual design of composite structures, Comprehensive Composite Materials II. Elsevier Ltd.

Kumar, G.S., Prasad, G., Pohl, R.O., 1993. Experimental determinations of the Lorenz number. Journal of Materials Science 28, 4261–4272.

Laha, T., Chen, Y., Lahiri, D., Agarwal, A., 2009. Tensile properties of carbon nanotube reinforced aluminum nanocomposite fabricated by plasma spray forming. Composites Part A: Applied Science and Manufacturing 40, 589–594.

Lahiri, D., Bakshi, S.R., Keshri, A.K., Liu, Y., Agarwal, A., 2009. Dual strengthening mechanisms induced by carbon nanotubes in roll bonded aluminum composites. Materials Science and Engineering A 523, 263–270.

Lal, M., Singhal, S.K., Sharma, I., Mathur, R.B., 2013. An alternative improved method for the homogeneous dispersion of CNTs in Cu matrix for the fabrication of Cu/CNTs composites. Applied Nanoscience 3, 29–35.

Lim, B.K., Hwang, J.W., Lee, D.J., Suh, S.H., Hong, S.H., 2012. Fabrication processes and

multi-functional applications of carbon nanotube nanocomposites. Journal of Composite Materials 46, 1731–1737.

Lim, D.K., Shibayanagi, T., Gerlich, A.P., 2009. Synthesis of multi-walled CNT reinforced aluminium alloy composite via friction stir processing. Materials Science and Engineering A 507, 194–199.

Long, X., Bai, Y., Algarni, M., Choi, Y., Chen, Q., 2015. Study on the strengthening mechanisms of Cu/CNT nano-composites. Materials Science and Engineering A 645, 347–356.

Madavali, B., Lee, J.H., Lee, J.K., Cho, K.Y., Challapalli, S., Hong, S.J., 2014. Effects of atmosphere and milling time on the coarsening of copper powders during mechanical milling. Powder Technology 256, 251–256.

Ministry of steel, India 2018. Annual Report- Ministry of Steel, Government of India, 1–153.

Ministry of steel, India 2012. National Steel Policy 2012, Government of India, 1–25.

Mohanty, T.R., Sahoo, S.K., Moharana, M.K., 2016. Study on blast furnace cooling stave for various refractory linings based on numerical modeling. IOP Conference Series: Materials Science and Engineering 115.

Nam, D.H., Kim, Y.K., Cha, S.I., Hong, S.H., 2012. Effect of CNTs on precipitation hardening behavior of CNT/Al-Cu composites. Carbon 50, 4809–4814.

Nie, J.H., Jia, C.C., Jia, X., Li, Y., Zhang, Y.F., Liang, X.B., 2012. Fabrication and thermal conductivity of copper matrix composites reinforced by tungsten-coated carbon nanotubes. International Journal of Minerals, Metallurgy and Materials 19, 446–452.

Noguchi, T., Magario, A., Fukazawa, S., Shimizu, S., Beppu, J., Seki, M., 2004. Carbon Nanotube/Aluminium composites with uniform dispersion. Materials Transactions 45, 602–604.

Peng, Y., Chen, Q., 2009. Ultrasonic-assisted fabrication of highly dispersed copper/multi-walled carbon nanotube nanowires. Colloids and Surfaces A: Physicochemical and Engineering Aspects 342, 132–135.

Pham, V.T., Bui, H.T., Tran, B.T., Van Tu, N., Le, D.Q., Than, X.T., Van Chuc, N., Doan, D.P., Phan, N.M., 2011. The effect of sintering temperature on the mechanical

properties of a Cu/CNT nanocomposite prepared via a powder metallurgy method. Advances in Natural Sciences: Nanoscience and Nanotechnology 2, 015006.

Pialago, E.J.T., Park, C.W., 2014. Cold spray deposition characteristics of mechanically alloyed Cu-CNT composite powders. Applied Surface Science 308, 63–74.

Qian, D., Wagner, G.J., Liu, W.K., Yu, M.-F., Ruoff, R.S., 2002. Mechanics of carbon nanotubes. Applied Mechanics Reviews 55, 495–533.

Rajkumar, K., Aravindan, S., 2011. Tribological studies on microwave sintered copper-carbon nanotube composites. Wear 270, 613–621.

Rajkumar, K., Aravindan, S., 2009. Microwave sintering of copper-graphite composites. Journal of Materials Processing Technology 209, 5601–5605.

Raza, K., Khalid, F.A., 2014. Optimization of sintering parameters for diamond-copper composites in conventional sintering and their thermal conductivity. Journal of Alloys and Compounds 615, 111–118.

Shukla, A.K., Nayan, N., Murty, S.V.S.N., Mondal, K., Sharma, S.C., George, K.M., Bakshi, S.R., 2013a. Processing copper-carbon nanotube composite powders by high energy milling. Materials Characterization 84, 58–66.

Shukla, A.K., Nayan, N., Murty, S.V.S.N., Sharma, S.C., Chandran, P., Bakshi, S.R., George, K.M., 2013b. Processing of copper-carbon nanotube composites by vacuum hot pressing technique. Materials Science and Engineering A 560, 365–371.

Steel, 2018. World Steel in Figures 2018, 1–30.

Subramaniam, C., Yamada, T., Kobashi, K., Sekiguchi, A., Futaba, D.N., Yumura, M., Hata, K., 2013. One hundred fold increase in current carrying capacity in a carbon nanotube-copper composite. Nature Communications 4, 2202.

Subramaniam, C., Yasuda, Y., Takeya, S., Ata, S., Nishizawa, A., Futaba, D., Yamada, T., Hata, K., 2014. Carbon nanotube-copper exhibiting metal-like thermal conductivity and silicon-like thermal expansion for efficient cooling of electronics. Nanoscale 6, 2669–2674.

Sule, R., Olubambi, P.A., Sigalas, I., Asante, J.K.O., Garrett, J.C., 2014. Effect of SPS consolidation parameters on submicron Cu and Cu-CNT composites for thermal management. Powder Technology 258, 198–205.

Sule, R., Olubambi, P.A., Sigalas, I., Asante, J.K.O., Garrett, J.C., Roos, W.D., 2015. Spark plasma sintering of sub-micron copper reinforced with ruthenium-carbon nanotube composites for thermal management applications. Synthetic Metals 202, 123–132.

Sun, X.-K., Kim, K.-T., 1997. Simulation of cold die compaction densification behaviour of iron and copper powders by cam–clay model. Powder Metallurgy 40, 193–195.

Tsai, P.C., Jeng, Y.R., 2013. Experimental and numerical investigation into the effect of carbon nanotube buckling on the reinforcement of CNT/Cu composites. Composites Science and Technology 79, 28–34.

Uddin, S.M., Mahmud, T., Wolf, C., Glanz, C., Kolaric, I., Volkmer, C., Höller, H., Wienecke, U., Roth, S., Fecht, H.J., 2010. Effect of size and shape of metal particles to improve hardness and electrical properties of carbon nanotube reinforced copper and copper alloy composites. Composites Science and Technology 70, 2253–2257.

Ullbrand, J.M., Córdoba, J.M., Tamayo-Ariztondo, J., Elizalde, M.R., Nygren, M., Molina-Aldareguia, J.M., Odén, M., 2010. Thermomechanical properties of copper-carbon nanofibre composites prepared by spark plasma sintering and hot pressing. Composites Science and Technology 70, 2263–2268.

Varo, T., Canakci, A., 2015. Effect of the CNT content on microstructure, physical and mechanical properties of Cu-based electrical contact materials produced by flake powder metallurgy. Arabian journal for science and engineering 40, 2711–2720.

Vignesh Babu, R., Kanagaraj, S., 2018. Thermal, electrical and mechanical characterization of microwave sintered Copper/carbon nanotubes (CNT) composites against sintering duration, CNT diameter and its concentration. Journal of Materials Processing Technology 258, 296–309.

Wang, H., Zhang, Z.H., Hu, Z.Y., Song, Q., Yin, S.P., Kang, Z., Li, S.L., 2018. Improvement of interfacial interaction and mechanical properties in copper matrix composites reinforced with copper coated carbon nanotubes. Materials Science and Engineering A 715, 163–173.

Wang, H., Zhang, Z.H., Zhang, H.M., Hu, Z.Y., Li, S.L., Cheng, X.W., 2017. Novel synthesizing and characterization of copper matrix composites reinforced with carbon nanotubes. Materials Science and Engineering A 696, 80–89.

Wang, Z., Cai, X., Yang, C., Zhou, L., Hu, C., 2018. An electrodeposition approach to obtaining carbon nanotubes embedded copper powders for the synthesis of copper matrix composites. Journal of Alloys and Compounds 735, 1357–1362.

Xu, L.S., Chen, X.H., Liu, X.J., Yu, Y., Wu, Y.R., 2011. Thermal Conductivity and microhardness of MWCNTs / Copper nanocomposites. International symposium on advanced packaging materials 26–30.

Xue, Z.W., Wang, L.D., Zhao, P.T., Xu, S.C., Qi, J.L., Fei, W.D., 2012. Microstructures and tensile behavior of carbon nanotubes reinforced Cu matrix composites with molecular-level dispersion. Materials and Design 34, 298–301.

Yadoji, P., Peelamedu, R., Agrawal, D., Roy, R., 2003. Microwave sintering of Ni-Zn ferrites: Comparison with conventional sintering. Materials Science and Engineering B 98, 269–278.

Yang, P., You, X., Yi, J., Fang, D., Bao, R., Shen, T., Liu, Y., Tao, J., Li, C., Tan, S., Guo, S., 2018. Simultaneous achievement of high strength, excellent ductility, and good electrical conductivity in carbon nanotube/copper composites. Journal of Alloys and Compounds 752, 431–439.

Zak Fang, Z., 2010. Sintering of Advanced Materials. Woodhead Publishing Limited,33-36.

Zhang, X., Shi, C., Liu, E., He, F., Ma, L., Li, Q., Li, J., Zhao, N., He, C., 2017. In-situ space-confined synthesis of well-dispersed three-dimensional graphene/carbon nanotube hybrid reinforced copper nanocomposites with balanced strength and ductility. Composites Part A: Applied Science and Manufacturing 103, 178–187.

Zhang, Y., Zhang, Q., Li, Y., Wang, N., Zhu, J., 2000. Coating of carbon nanotubes with tungsten by physical vapor deposition. Solid State Communications 115, 51–55.

Zhang, Y.X., Huang, M., Li, F., Wen, Z.Q., 2013. Controlled synthesis of hierarchical CuO nanostructures for electrochemical capacitor electrodes. International Journal of Electrochemical Science 8, 8645–8661.

Zhou, S. ming, Zhang, X. bin, Ding, Z. peng, Min, C. yan, Xu, G. liang, Zhu, W. ming, 2007. Fabrication and tribological properties of carbon nanotubes reinforced Al composites prepared by pressureless infiltration technique. Composites Part A: Applied Science and Manufacturing 38, 301–306.

OUTCOME OF THE THESIS WORK

PAPERS PUBLISHED SO FAR:

- **R. Vignesh Babu** and S. Kanagaraj. "Thermal, electrical and mechanical characterization of microwave sintered Copper/carbon nanotubes (CNT) composites against sintering duration, CNT diameter and its concentration", Journal of materials processing technology. 258 (2018) 296–309. doi:10.1016/j.jmatprotec.2018.04.010. (Impact factor: 4.178)

- **R. Vignesh Babu**, K. A. Verma, M. Charan, and S. Kanagaraj. "Tweaking the diameter and concentration of carbon nanotubes and sintering duration in Copper based composites for heat transfer applications". Advanced powder technology. 29 (2018) 2356–2367. doi:10.1016/j.apt.2018.06.015. (Impact factor: 3.25)

- **R. Vignesh Babu** and S. Kanagaraj. "Studies on the sintering behaviour of Copper/Carbon nanotube composites and their characteristics". Advanced powder technology. (2019). doi.org/10.1016/j.apt.2019.06.035. (Impact factor: 3.25) (In press)

PAPER UNDER REVIEW:

- **R. Vignesh Babu** and S. Kanagaraj. Studies on the influence of compaction and sintering technique on the mechanical and thermal properties of Cu/CNT composites having different CNT size and its concentration.

PAPER PRESENTED IN INTERNATIONAL CONFERENCES:

- **R Vignesh Babu** and S Kanagaraj. Copper/Carbon nanotubes composite: A perfect engineering solution to replace the existing heat conducting material in machineries and equipment used in the steel manufacturing industries. **International Conference on Materials Science and Manufacturing Engineering (MSME 2018)**, 8-10 Nov, 2018, Novotel Paris Centre Tour Eiffel, Paris, France. **(SERB-DST, India Funding)**

- **R Vignesh Babu** and S Kanagaraj. Copper/Carbon nanotube composite: An alternate material to improve the performance of electrical and thermal systems. **International Conference on Powder Metallurgy & Particulate Materials (**PM18), 21-23 Feb 2018, **CIDCO Convention & Exhibition Centre**, Navi Mumbai, India.

- **R Vignesh Babu**, Rupjyoti Bhuyan, M Charan and S Kanagaraj. Thermal conductivity enhancement of Copper/carbon nanotube nanocomposites by varying the aspect ratio of CNT. **International Conference and Technology Meet on Military and Marine Applications** (IWCEM 2016), 04-06 June 2016, Jaipur, India.

- **R Vignesh Babu**, M Charan, Kunwar Avanish Verma and S Kanagaraj. Mechanical properties of Cu/CNT nanocomposites synthesized through molecular level mixing with different aspect ratio of CNT. **International Conference on Powder Metallurgy & Particulate Materials (**PM16), 18-20 Jan 2016, Hotel Hyatt Regency Pune, India.

- **R. Vignesh Babu**, Kunwar Avanish Verma, M. Charan, S. Kanagaraj. Effect of molecular level mixing in improving the dispersion of carbon nanotubes in copper matrix. **International Conference on Powder Metallurgy & Particulate Materials (**PM 15), 19-21 Jan 2015, IIT Bombay, India.

- S. Kanagaraj, Susanta Behera and **R. Vignesh Babu**. Preparation and characterization of copper- carbon nanotube nanocomposites via powder metallurgy technique. **International Conference on Powder Metallurgy & Particulate Materials (**PM 15), 19-21 Jan 2015, IIT Bombay, India.